A PARAMETRIC STUDY OF THE STRESS DISTRIBUTION IN A FOUR-CELLED BOX BEAM MODEL OF THE ASR-21 CLASS CATAMARAN CROSS-STRUCTURE

by

PAUL HERBERT FENTON

Lieutenant, United States Navy

B.S., United States Naval Academy
(1964)

SUBMITTED IN PARTIAL FULFILLMENT OF THE

REQUIREMENTS FOR THE DEGREE OF

MASTER OF SCIENCE IN NAVAL ARCHITECTURE

AND MARINE ENGINEERING

AND THE PROFESSIONAL DEGREE OF

OCEAN ENGINEER

at the

MASSACHUSETTS INSTITUTE OF TECHNOLOGY

June, 1972

Signature of Author Signature redacted
Department of Ocean Engineering
May 12, 1972

Certified by Signature redacted
Thesis Supervisor

Accepted by Signature redacted
Chairman, Departmental Committee
on Graduate Students

A PARAMETRIC STUDY OF THE STRESS DISTRIBUTION IN A FOUR-CELLED BOX BEAM MODEL OF THE ASR-21 CATAMARAN CROSS STRUCTURE

by

Paul Herbert Fenton
Lieutenant, United States Navy

Submitted to the Department of Ocean Engineering on May 12, 1972, in partial fulfillment of the requirements for the degree of Master of Science in Naval Architecture and Marine Engineering, and the Professional Degree, Ocean Engineer.

ABSTRACT

The objectives of this thesis are:

(a) to attempt to analyze the stress distribution in the cross structure of the ASR-21 Class Catamaran by finite element analysis utilizing the ICES STRUDL-II Program of the Massachusetts Institute of Technology, Department of Civil Engineering.

(b) to develop a set of plating effectiveness curves for a doubly symmetrical model of the catamaran cross structure based on output from a finite element analysis, and to compare the values obtained from the actual cross structures to these curves.

(c) to attempt to draw some basic conclusions concerning the design of the actual cross structures.

This study is three dimensional in nature. Various geometric parameters are varied for the model to analyze what effect they produce on the resultant stresses in the cross structure. The breadth to depth (B/D), the length to breadth (L/B), and the flange area to web area (A_f/A_w) ratios are the primary variables considered. A total of twenty-one (21) geometric variations are performed.

The catamaran cross structure and models are assumed to be cut at the inboard side of each hull and removed for proper loading. The three loadings used are symmetric bending moment, antisymmetric bending moment and shear, and torsional moment.

The stress distribution obtained from the model indicates that there is very little variation in the effectiveness at various B/D or A_f/A_w ratios for a given L/B ratio. There is a slight increase in average stress across a set of elements as A_f/A_w increases. The effectiveness of the various element sections of the actual ASR-21 catamaran cross structures is generally higher than that predicted by the model effectiveness curves. The effective breadth used for the design of the ASR-21 Class catamaran cross structures is very conservative when compared to the actual effective breadths determined in the thesis. Linearity in the stress distribution response to various loading conditions was observed.

An effort should be made to study additional structural cross sections planned for use in future catamaran cross structures, and to examine the plating effectiveness at the higher L/B ratios proposed for them. A satisfactory analytical solution of the cross structure using the stress function should be conducted.

Thesis Supervisor: Alaa Mansour
Title: Assistant Professor of Naval Architecture

ACKNOWLEDGEMENTS

The author is sincerely grateful for the suggestions and guidance received from Assistant Professor Alaa Mansour, Department of Ocean Engineering. A debt of gratitude is extended to Mrs. Robert Audet who labored through the typing of this thesis when eight months pregnant.

TABLE OF CONTENTS

LIST OF FIGURES

LIST OF FIGURES
(Cont'd.)

LIST OF FIGURES
(Cont'd.)

LIST OF TABLES

LIST OF TABLES
(Cont'd.)

INTRODUCTION

Since 1965 there has been a great surge of interest in the catamaran ship. The large deck area and favorable stability of this ocean vehicle make it ideal for numerous ocean engineering tasks. Serious efforts have been channeled towards two areas in the analysis of the catamaran: the hydrodynamics of the hulls, and the statistical response of the ship to limiting sea conditions that allows one to determine the maximum loads on the ship's structural members.

References (1) through (8) have dealt almost exclusively with the problem of predicting the maximum loads that the new catamaran submarine rescue ship (ASR-21 Class) will experience throughout its life cycle. Of particular interest has been the analysis of the loadings on the cross structures which connect the demi-hulls, and the fabrication problems associated with joining the cross structures to the demi-hulls.

The variations in the predicted loadings which have resulted from the analyses are interesting. This is not because of their absolute values but rather because of the variations evidenced in the calculations of these quantities. This indicates that some degree of uncertainty still exists in the selection of the most proper procedural method for analysis.

It is generally accepted by all the authors that three distinct conditions of maximum loading exist. Lankford (3) describes these conditions for the catamaran when it is at zero speed in beam seas, when it is at zero speed in quartering seas, and finally when it is in a condition of either grounding or docking. The beam seas-zero speed case produces vertical bending moments, a smaller torsional moment and slight vertical shear forces. The vertical bending moments tend to roll the hulls, and the vertical shear forces tend to heave the hulls differentially. The quartering seas-zero speed case produces a twisting moment on the hulls about the center of torsion and a slightly lower bending moment. The grounding-docking case considered primarily by Lankford illustrates the most severe torsional loading to which the cross structure could be subjected. It is assumed for this case that one hull is supported forward and one hull is supported aft. Table 1 is a summary of the loadings that various researchers have determined for the ASR-21 catamaran. These figures do not include the catamaran cross structure weight.

These variations in loading point to the difficulty associated with an analysis of the stress and displacement distribution which are produced by these loads on the cross structures. When an analysis is performed on the structures, the results are a direct function of the applied loads. Calculations for a range of loadings could be costly, cumbersome and time consuming.

As long as the loads are assumed to give results that correspond to the linear elastic range of the utilized construction materials, then the use of finite element analysis appears to be the most versatile method to use. Because of the linearity that exists between the applied loadings and the

TABLE 1

PREDICTED CATAMARAN SEA

LOADINGS (FOOT-TONS)

	Lankford (3)	Scott (8)	Schade (4)	Dinsenbacher (4)
1. Beam Seas (Maximum Bending Moment)	55,000	26,572	60,900	53,400
2. Quartering Seas (Maximum Torsional Moment)	27,120	23,495	73,500	16,500
3. Grounding-Docking (Torsional Moment)	102,790	--	--	--

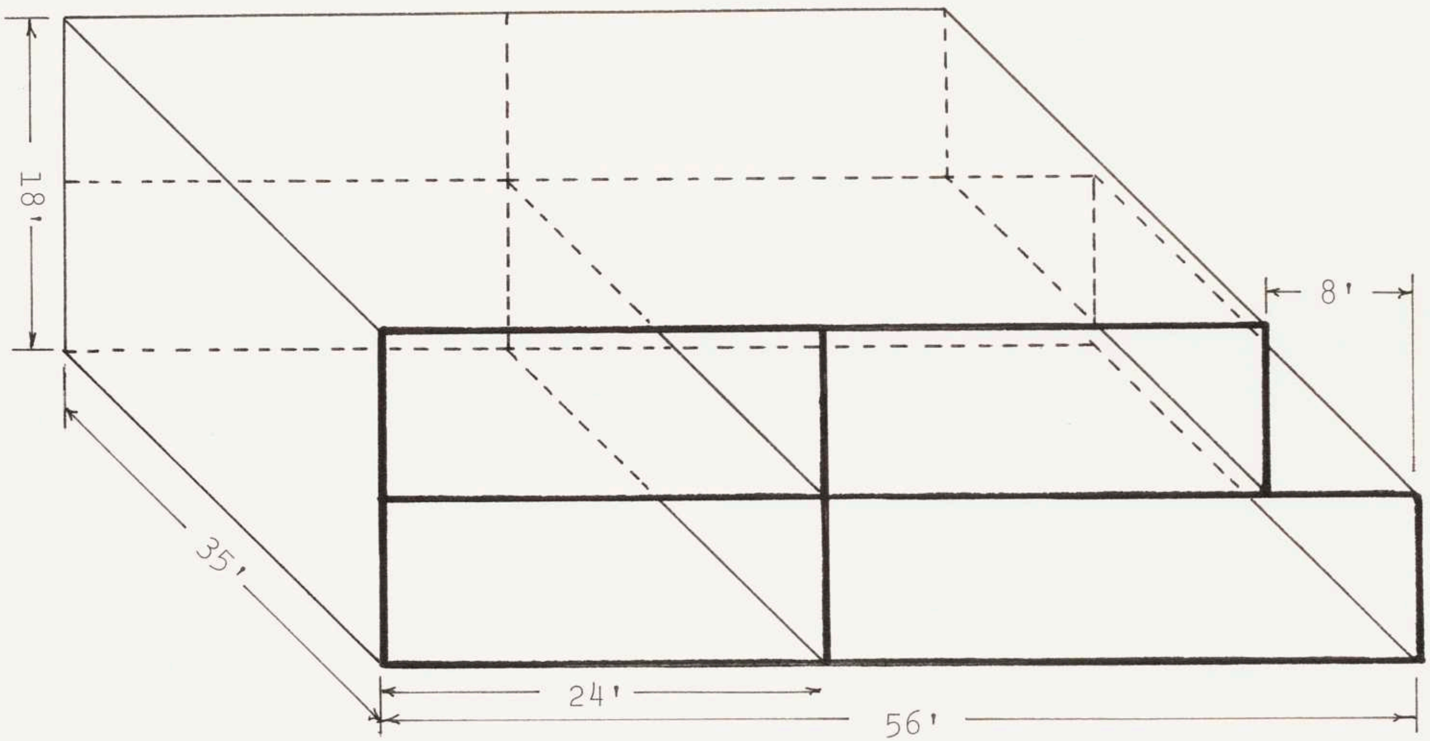

FIGURE I
FORWARD CROSS STRUCTURE OF ASR-21 CATAMARAN

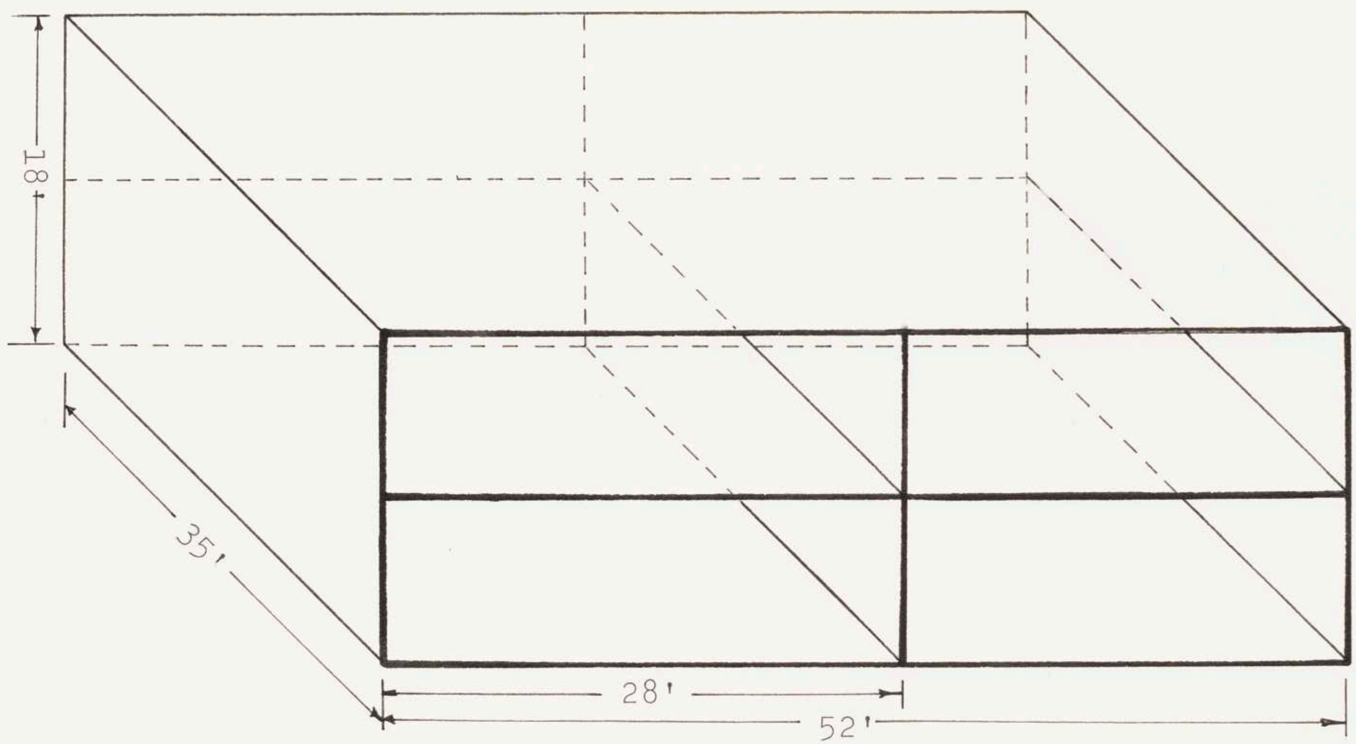

FIGURE II
AFTER CROSS STRUCTURE OF ASR-21 CATAMARAN

TABLE 2

CHARACTERISTICS OF THE ASR-21 CATAMARAN

CROSS STRUCTURES

	Forward		After
Length (feet)	35		35
Breadth (feet	56		52
Depth (feet)	18		18
Flange Thicknesses (inches)			
Main Deck	5/16		5/16
01 Level	9/16		9/16
02 Level	3/8		3/8
Web Thicknesses (inches)			
Frame 21	1/2	Frame 84	3/8
Frame 37	3/8	Frame 96	3/8
Frame 49	3/8	Frame 110	1/2
L/B	.62		.671
B/D	3.11		2.89
A_f/A_w	2.82		3.05

output displacements, structural analysis can be performed for standard loads, and by scaling the results of these loads either up or down, and assuring oneself that he remains within the linear range, results for any reasonable loading can be quickly calculated.

The objectives of this thesis are three-fold. An attempt is made to analyze the stress distribution in the cross structures of the ASR-21 Class Catamaran by finite element analysis utilizing the ICES STRUDL-II program of the Massachusetts Institute of Technology, Department of Civil Engineering (Ref. 9). The forward and after cross structures and their locations relative to the ship itself are indicated in Figures I, II and III. Development of a set of curves for the top plating effectiveness similar to those presented by Schade (Refs. 12, 13) and Mansour (Ref. 11) are calculated for a range of length to breadth, breadth to depth, and flange area to web area ratios. These calculations are based on a finite element analysis of a doubly symmetrical model of the cross structure. By plotting the effectiveness of the top plating of the actual catamaran cross structures on the previously determined effectiveness curves, conclusions are drawn about the design of the actual ASR-21 cross structures.

Loading conditions utilized in this analysis approximate as closely as possible the various loadings deemed most critical by the investigators previously mentioned. The characteristics of the actual ASR-21 cross structures are included here in Table 2.

PROCEDURE

Loading Analysis

In order to apply the desired loads to the cross structure the sections of the cross members between the hulls of the catamaran were cut at the inboard side of each hull and removed. The vertical bending moment, shear and torsional moment were then applied to the cross structure as one would apply them to a free body diagram of a beam (Fig. IVa). The beam in this instance is a closed, thin-walled, multicelled box beam.

Conceivably, the cross structure can be loaded simultaneously to some degree by all of the sea loading conditions specified in the Introduction. By dividing the loads into three separate loading conditions, insuring equilibrium, and analyzing each, the effect of the individual loadings on the cross structure can be examined. Equations (1) to (3) are applicable for determining the relationships between the fully loaded beam and the individual loading cases.

<u>Shear Load</u> $$V_z = \frac{M_{x1}}{L} \qquad (1)$$

(L is the hull to hull spacing)

<u>Antisymmetric Bending Moment</u> $$M_{x3} = \frac{V_z L}{2} = \frac{M_{x1}}{2} \qquad (2)$$

<u>Symmetric Bending Moment</u> $$M_{x2} = M_{x1} + M_{x3} \qquad (3)$$

The beam seas case then becomes the superposition of the symmetric bending moment loading (Fig. IVc), a smaller

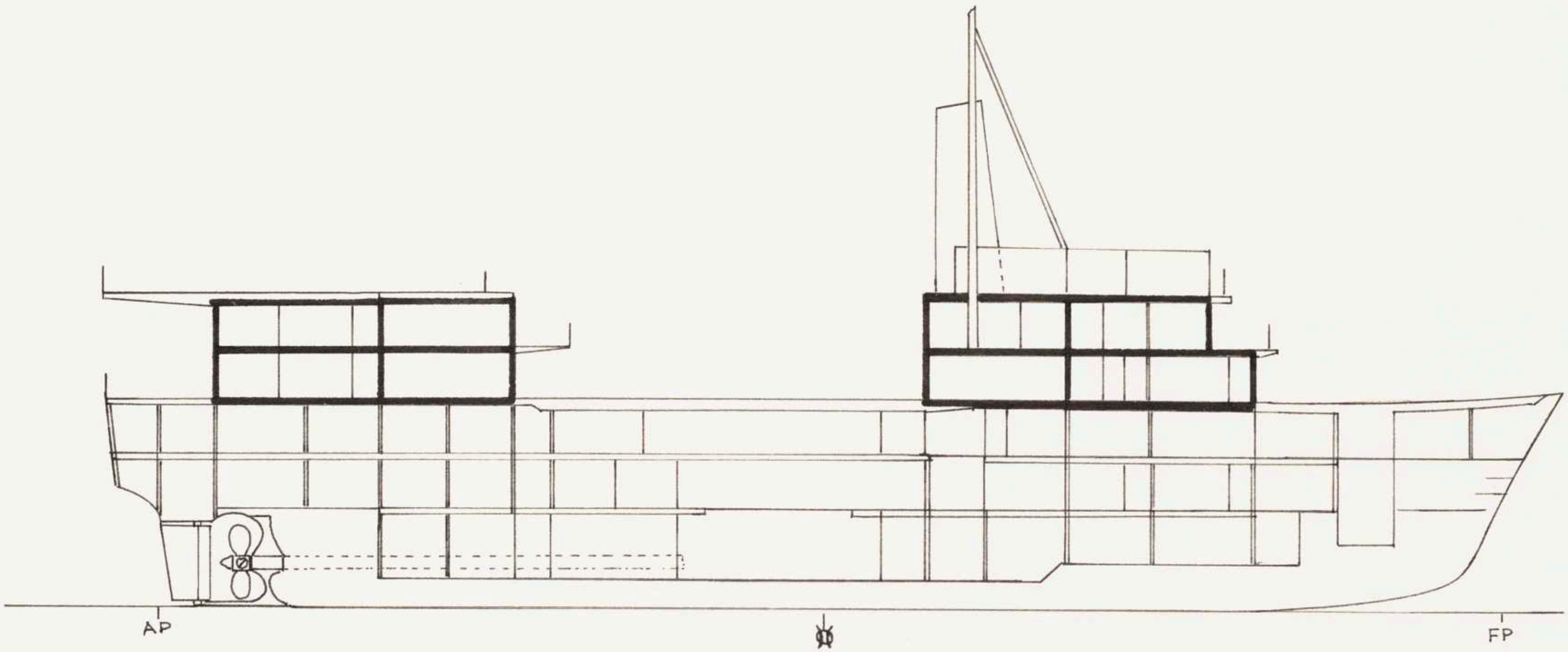

FIGURE III
INBOARD PROFILE, PORT HULL, OF ASR-21
CATAMARAN WITH CROSS STRUCTURES (HEAVILY OUTLINED)

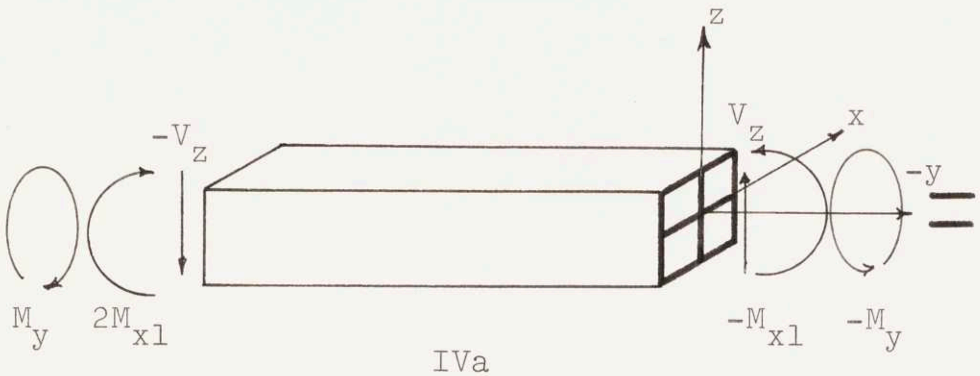

IVa

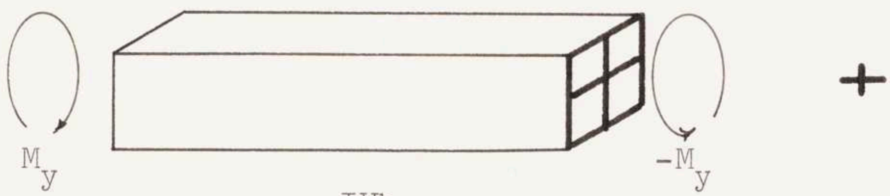

IVb
TORSIONAL MOMENT

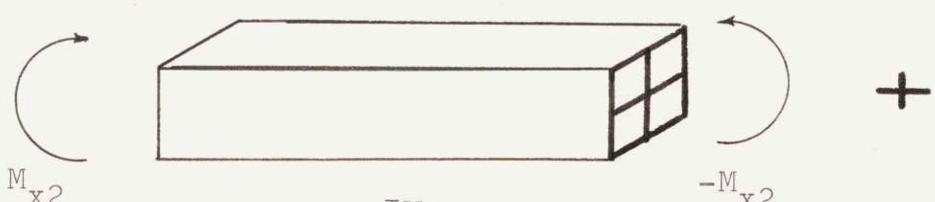

IVc
SYMMETRICAL BENDING MOMENT

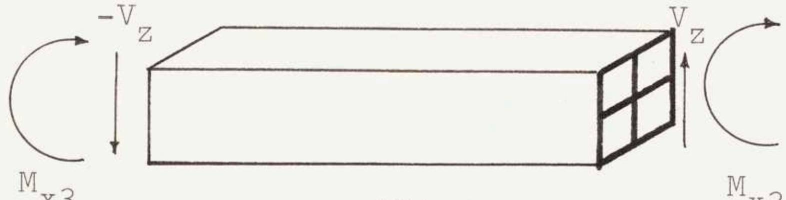

IVd
ANTISYMMETRICAL BENDING MOMENT AND SHEAR

FIGURE IV
THE LOADED BOX BEAM

torsional moment (Fig. IVb) and the antisymmetric bending moment and shear loadings (Fig. IVd). The quarter seas case is primarily the torsional loading (Fig. IVb) with a smaller bending moment also operating on the structure.

Finite Element Modelling

The forward and after cross structures (Figs. I, II) were subdivided into a set of elements and nodes in accordance with reference (9) for use with the ICES-STRUDL II finite element program. As can be observed in Figures (V) and (VI) there are 116 elements/130 nodes and 112 elements/125 nodes for the forward and after structures, respectively. Additionally, the forward cross structure has no planes of symmetry, and the after cross structure has only one plane of symmetry. To run numerous analyses with these two structures with varying L/B, B/D and A_f/A_w ratios would be extremely expensive because of the computer time required to calculate the stiffness matrices. For the two runs made with the actual structures the computer calculation time required to solve the partitioned matrix was 316.76 seconds and 341.47 seconds. Therefore, a doubly symmetrical model was constructed (Fig. VII). With this model it was possible to reduce the computer costs significantly by taking advantage of the double symmetry, and completing the analysis for only one quarter of the structure with 35 elements/45 nodes (Fig. VIII). In fact, only 24.47 seconds of computer time was required to solve the partitioned

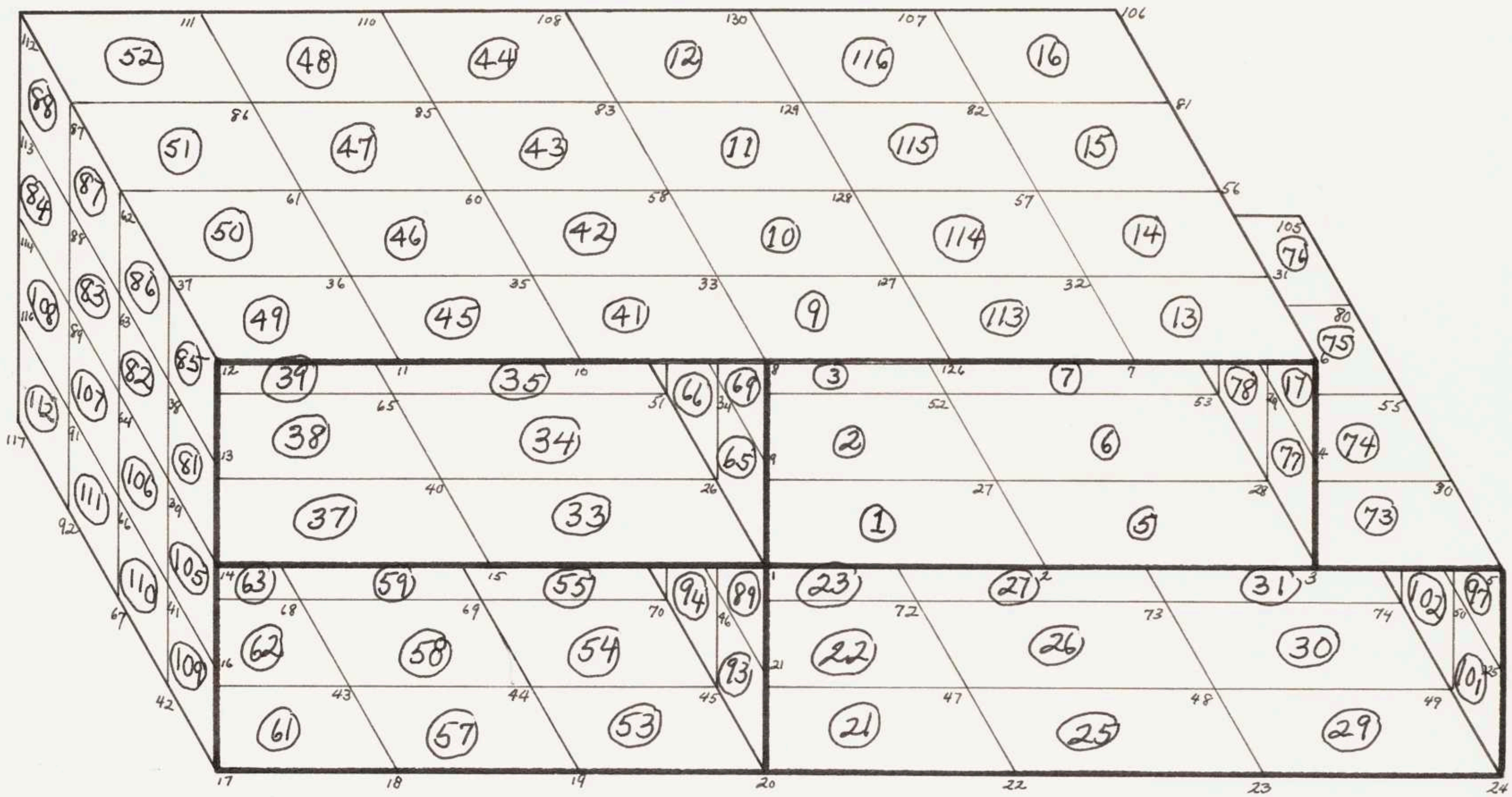

Scale: 1/8" = 1'-0"

FIGURE V
FINITE ELEMENT MODEL OF ASR-21 FORWARD CROSS STRUCTURE

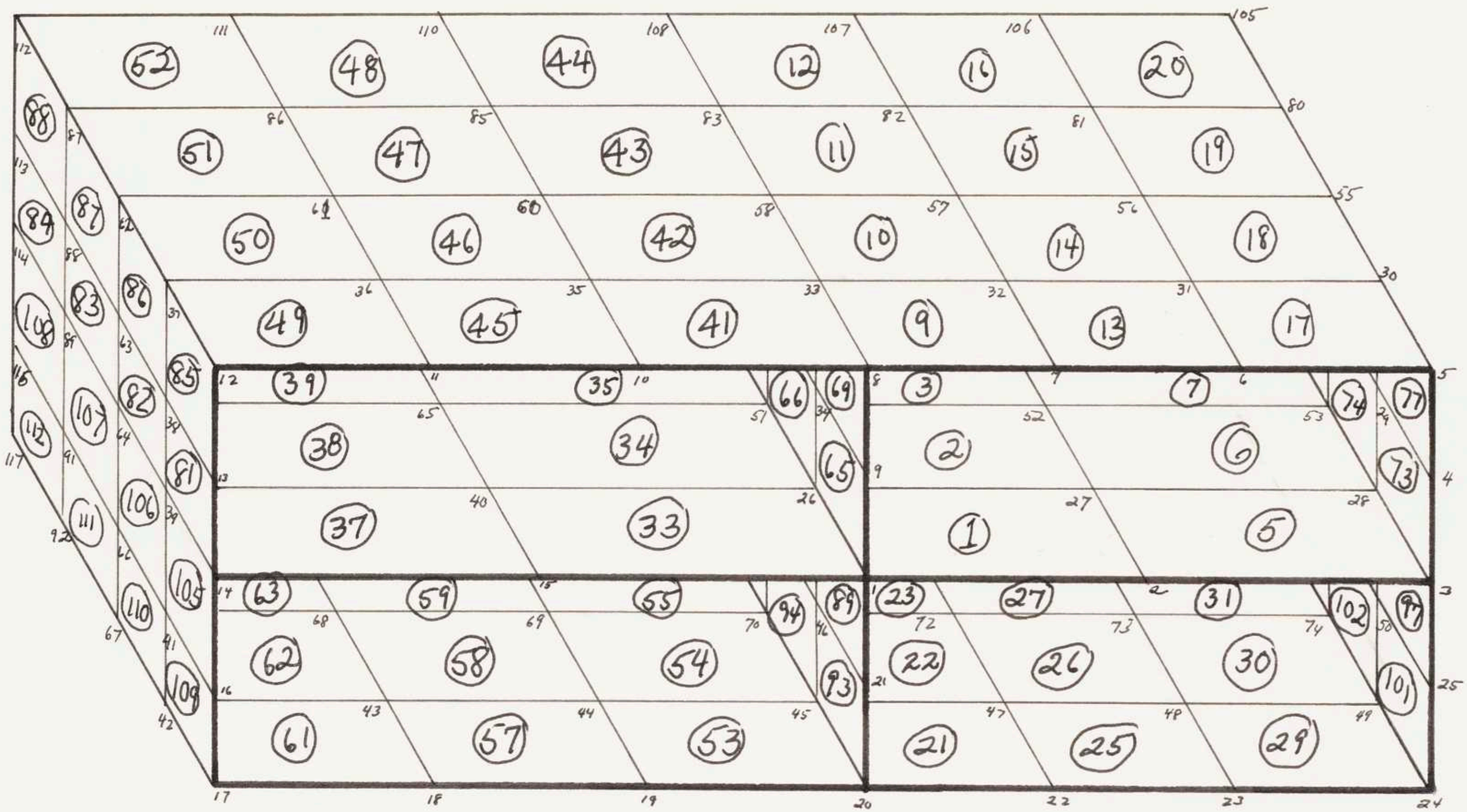

Scale: 1/8" = 1'-0"

FIGURE VI
FINITE ELEMENT MODEL OF ASR-21 AFTER CROSS STRUCTURE

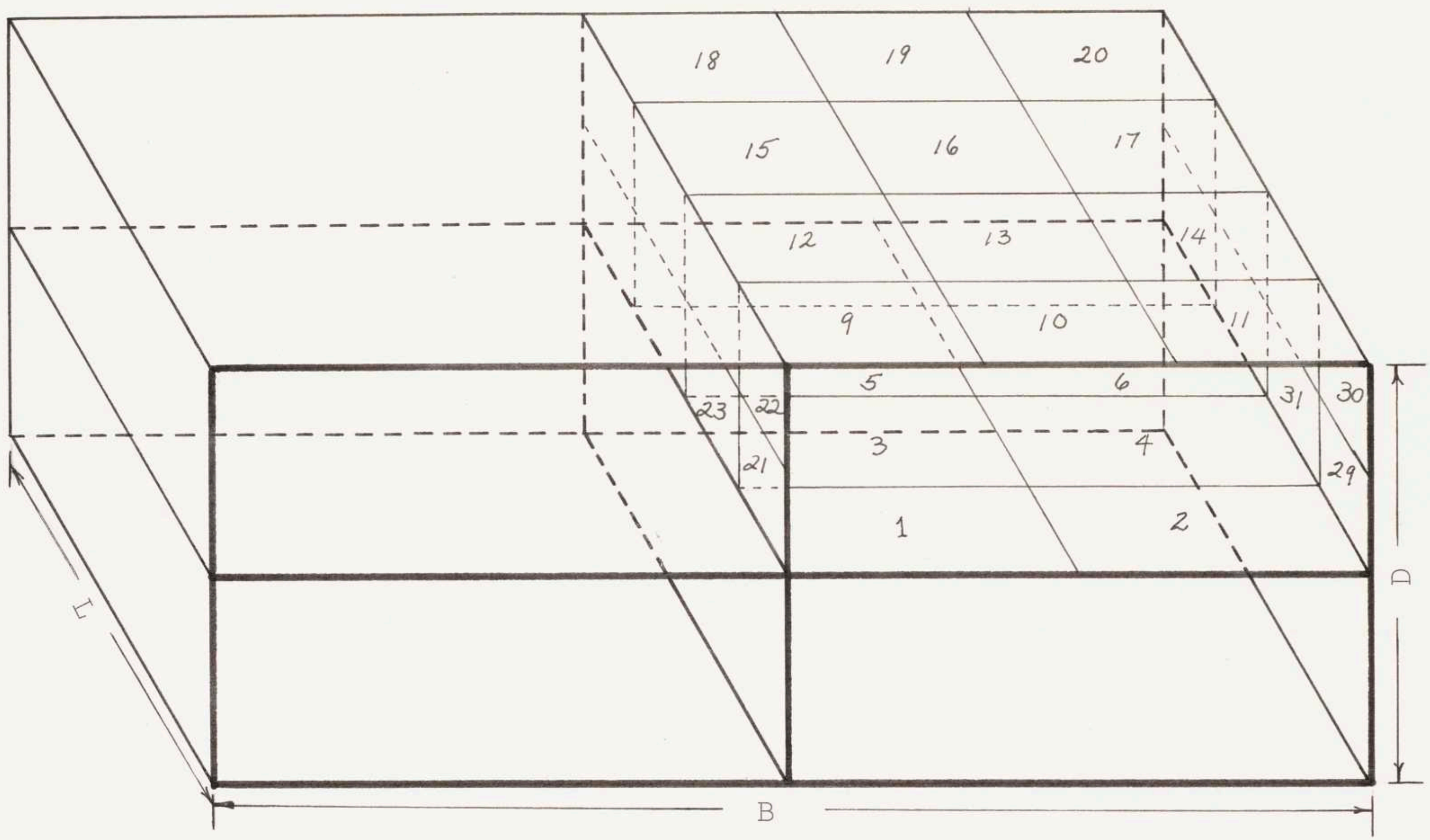

FIGURE VII
CROSS STRUCTURE MODEL WITH QUARTER STRUCTURE DETAILED

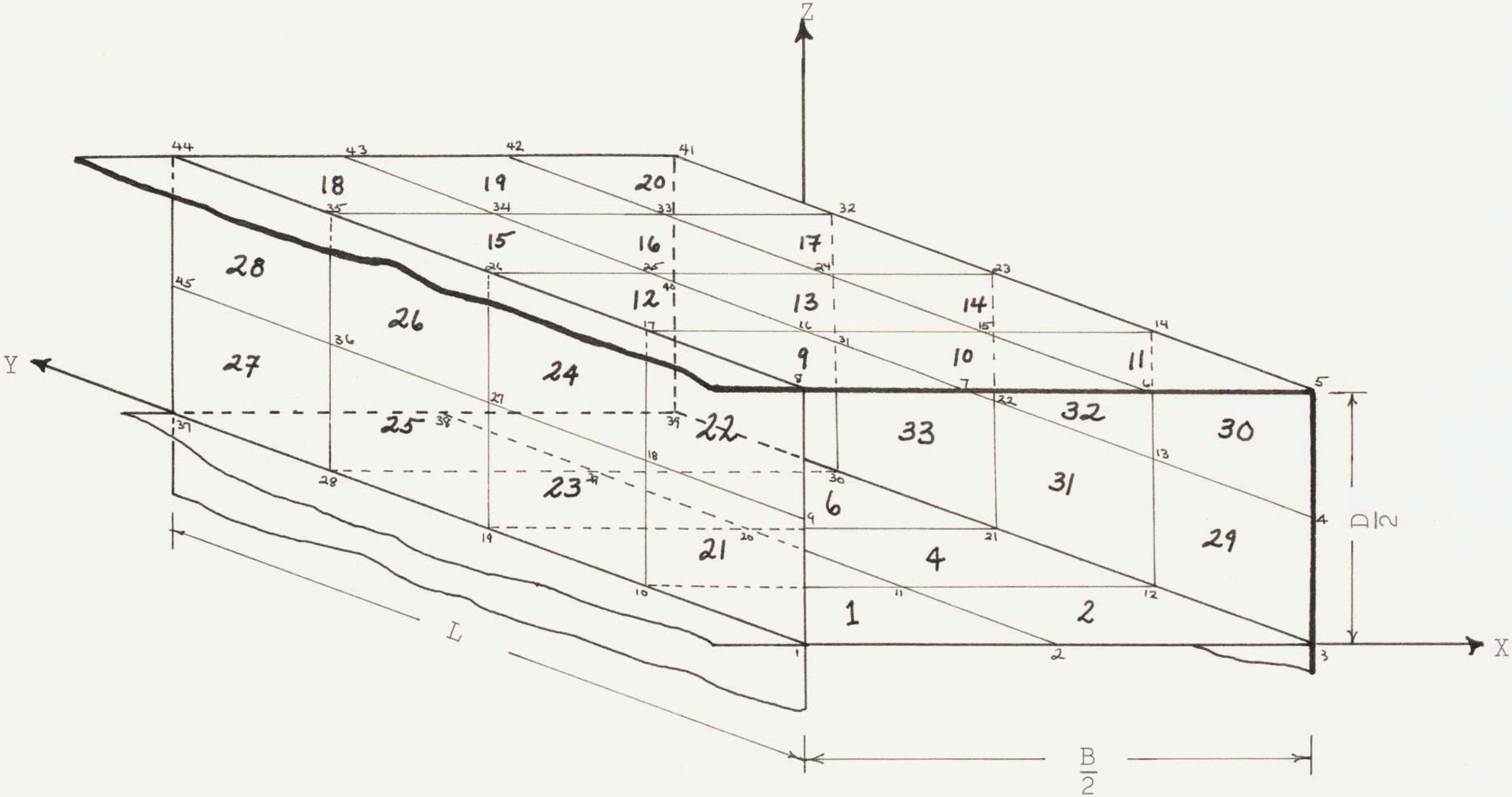

FIGURE VIII
QUARTER STRUCTURE FINITE MODEL ILLUSTRATING NODE, ELEMENT AND COORDINATE LOCATION

matrix for the quarter structure. Hence, all computer analysis involving the variance of length to breadth, breadth to depth, and flange area to web area ratios were performed on the quarter structure. Single runs were made with each of the actual cross structures.

Range of Parameters

The ranges of selected parameter values utilized in this thesis were established by the actual catamaran cross structure parameter values. Table (2) indicates the catamaran's cross structure length to breadth, breadth to depth, and flange area to web area ratios. In order to observe the effect of these ratios on the stress level and the effectiveness of the plating, the parameters were varied both above and below the values of the actual structure. The following ratio ranges were utilized in this thesis:

$$.3 \leq L/B \leq 1.5$$

$$2.5 \leq B/D \leq 3.5$$

$$2.5 \leq A_f/A_w \leq 3.5$$

The last parameter, A_f/A_w, is actually a function of the second parameter, B/D, and the ratio of plating thicknesses, t_f/t_w.

$$A_f/A_w = (B/D)\ (t_f/t_w) \qquad (4)$$

It can be observed from equation (4) that given the specific ranges of the two parameters, a unique set of plating thickness ratios can be obtained. To facilitate the analysis it was assumed that the thickness of the flange, t_f, was held constant at a value of .38 inches. Another goemetric descriptor that was held constant in the thesis was the cross structure breadth, B. A breadth of 50 feet was used. Table (3) lists the values of the plate thicknesses assumed for the analysis.

TABLE 3

FLANGE AND WEB PLATING THICKNESS

A_f/A_w \ B/D	2.5	3.0	3.5
2.5		t_f = .38 t_w = .45	
3.0	t_f = .38 t_w = .3167	t_f = .38 t_w = .38	t_f = .38 t_w = .444
3.5		t_f = .38 t_w = .32	

Model Loading

For this thesis the standard moment, M_{x1}, was arbitrarily set equal to 1000 foot-tons. From equations (1) to (3) this implies that

M_{x3} = 500 foot-tons

M_{x2} = 1500 foot-tons

V_z = 1000/L tons

Results for different loads can be obtained by scaling the stresses obtained from these standard loads provided the yield strength of the material is not exceeded.

Applying the loads to the finite element model is probably the major departure from theoretical analysis. Essentially, this statement can be reduced to the fact that a uniformly applied moment must be approximated by individual concentrated forces which are applied to the nodes. An increase in the number of nodes and elements will produce a better approximation, but only at the expense of time and money.

Division of the applied moment into nodal forces was based on the assumption that each transverse bulkhead will carry the load associated with each flange. Since the center transverse bulkhead has adjacent flange areas on both sides, it was assumed that the center bulkhead carried twice the load that the end transverse bulkheads carried. Nodal forces for the full structure under symmetrical bending moment loading were then determined by equations (5) through (10). The moment distribution was assumed to be linear in the vertical direction: zero load at nodes 1, 3, 14, half the maximum load at nodes 13, 4, 9 and maximum at nodes 5, 8, 12.

$$M_{x2} = 1500 \text{ foot-tons} \tag{5}$$

$$F_{13}(D/4) + F_{12}(D/2) = 375 \text{ foot-tons} \tag{6}$$

$$F_9\ (D/4) + F_8\ (D/2) = 750 \text{ foot-tons} \tag{7}$$

$$F_4\ (D/4) + F_5\ (D/2) = 375 \text{ foot-tons} \tag{8}$$

$$F_4 = F_{13} = 1/2\ F_{12} = 1/2\ F_5 \tag{9}$$

$$F_9 = F_5 = F_{12} \tag{10}$$

To obtain the forces for the quarter structure the forces at the center transverse bulkhead were divided in half (The plate thicknesses are also divided in half where the quarter structure is removed from the full structure). The application of the nodal forces to the full and quarter structures are illustrated in Figure IX. Symmetrical bending moment nodal forces for the various B/D ratios utilized in this thesis are presented in Table 4. Similar results for the antisymmetric bending moment case with M_{x3} = 500 foot-tons are included in Table 5.

TABLE 4

FULL AND QUARTER STRUCTURE NODAL LOADINGS
FOR SYMMETRIC BENDING MOMENT
(M_{x2} - 1500 foot-tons) AND VARIOUS B/D RATIOS

Full Structure

Nodal Forces (tons)

Node Number	B/D = 2.5	B/D = 3.0	B/D = 3.5
8, 120	-60.	-72.	-84.4
5, 9, 12, 117, 121, 124	-30.	-36.	-42.2
4, 13, 116, 125	-15.	-18.	-21.1
20, 108	60.	72.	84.4
17, 21, 24, 105, 109, 112	30.	36.	42.2
16, 25, 104, 113	15.	18.	21.1

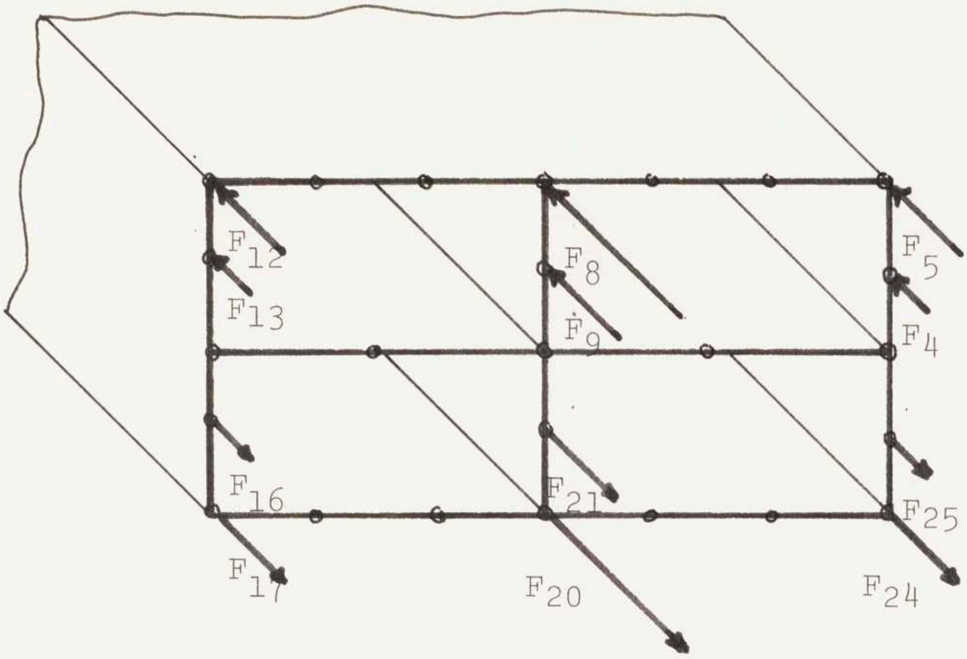

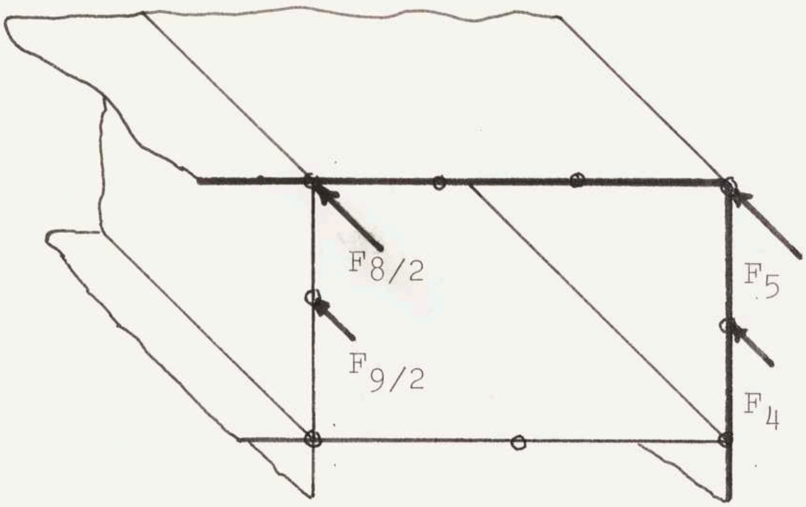

FIGURE IX
FULL AND QUARTER STRUCTURE NODAL FORCES
FOR THE SYMMETRICAL BENDING MOMENT LOADING

TABLE 4 (Cont'd.)

Quarter Structure

Nodal Forces (tons)

Node Number	B/D = 2.5	B/D = 3.0	B/D = 3.5
5, 8	-30.	-36.	-42.2
4, 9	-15.	-18.	-21.1
41, 44	30.	36.	42.2
40, 45	15.	18.	21.1

TABLE 5

FULL AND QUARTER STRUCTURE NODAL LOADINGS

FOR ANTISYMMETRIC BENDING MOMENT

(M_{x3} = 500 foot-tons) AND VARIOUS B/D RATIOS

Full Structure

Nodal Forces (tons)

Node Number	B/D = 2.5	B/D = 3.0	B/D = 3.5
8, 108	20.	24.	28.13
5, 9, 12, 105, 109, 112	10.	12.	14.06
4, 13, 104, 113	5.	6.	7.03
20, 120	-20.	-24.	-28.13
17, 21, 24, 117, 121, 124	-10.	-12.	-14.06
16, 25, 116, 125	-5.	-6.	-7.03

TABLE 5 (Cont'd.)

Quarter Structure

Nodal Forces (tons)

Node Number	B/D = 2.5	B/D = 3.0	B/D = 3.5
5, 8, 41, 44	10.	12.	14.06
4, 9, 40, 45	5.	6.	7.03

The total shear load for the end cross section must be divided in much the same way as the bending moments. In addition to distributing the shear so that one half the total shear is applied to the center transverse bulkhead and one half is distributed equally between the other two transverse bulkheads, the shear must also be divided so that each node carries its share of the load. For this procedure it was assumed that any node having neighboring nodes on both sides would carry a full proportion of the load at that particular bulkhead. Any node that had only one neighboring node (either the top or bottom nodes) would carry one half the load of a node with two neighbors. Figure X shows how the total shear (q) is applied to the nodes of the full cross structure and the quarter structure. A summary of calculations for the nodal shear forces for various lengths of the cross structure, and M_{x1} = 1000 foot-tons is presented in Table 6.

TOTAL SHEAR = q

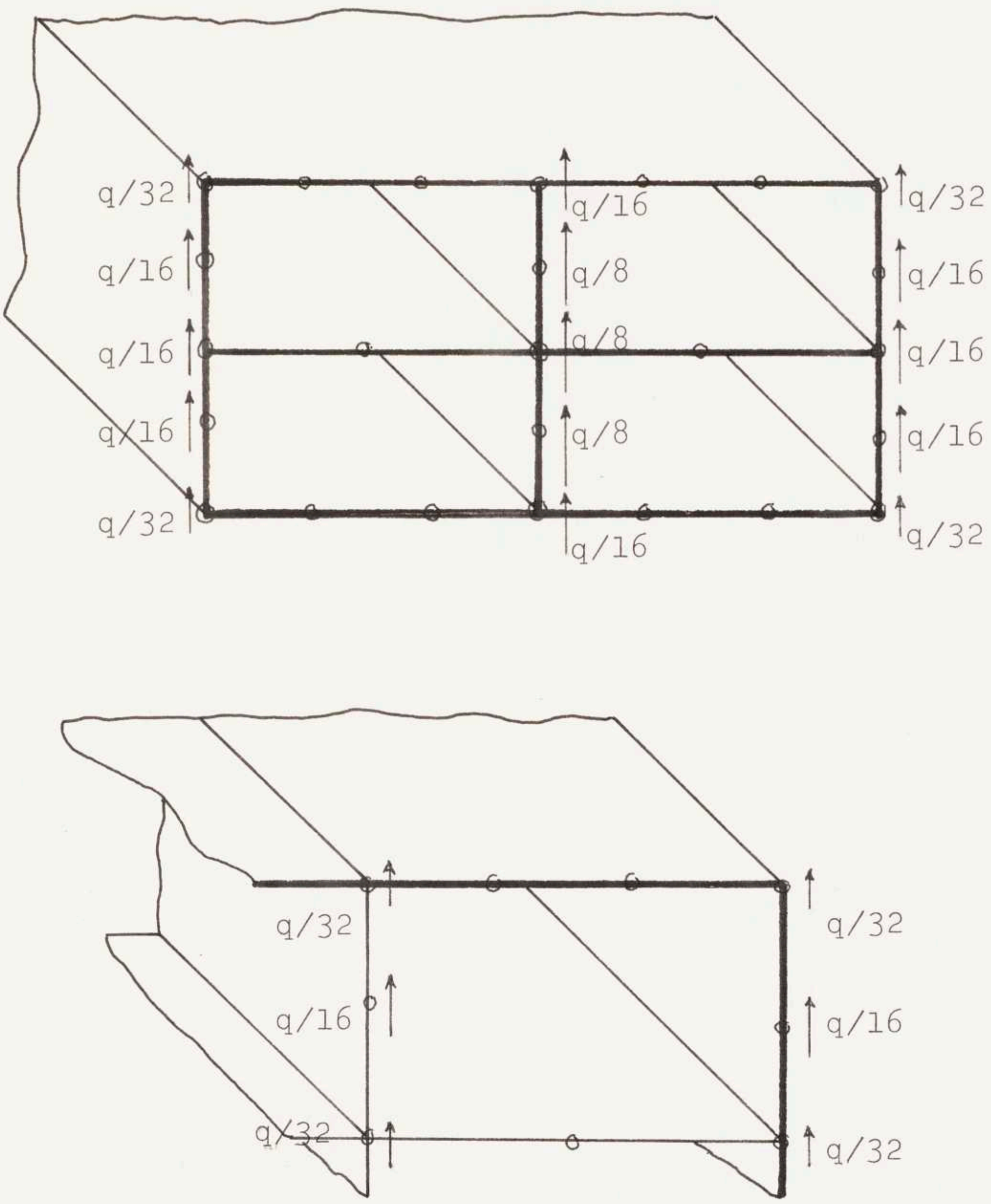

FIGURE X
FULL & QUARTER STRUCTURE NODAL LOADS
FOR SHEAR FORCES

TABLE 6

QUARTER STRUCTURE NODAL SHEAR FORCES

($V_Z = M_{x1}/L = 1000/L$ tons) FOR VARIOUS LENGTHS

Nodal Forces (tons)

Node Number	L=15	L=25	L=35	L=45	L=55	L=65	L=75
Total Shear of Full Struc.	66.67	40.	28.6	22.2	18.2	15.4	13.34
4, 9	4.17	2.5	1.79	1.39	1.14	.96	.835
1, 3, 5, 8	2.08	1.25	.895	.695	.57	.48	.4175
40, 45	-4.17	-2.5	-1.79	-1.39	-1.14	-.96	-.835
37, 39, 41, 44	-2.08	-1.25	- .895	- .695	- .57	-.48	-.4175

The nodal loading due to the torsional moment, M_y, arises from the assumption that the center reinforcing bulkhead and deck do not carry any load, and from the assumptions implied by the use of the well known Bredt Formula (Ref. 19).

$$M_y = 2AQ \tag{11}$$

Q = Shear Flow

A = Area enclosed by the perimeter of the section

The first assumption is verified by the application of the general analytical solution method involving shear flow about the individual cells of the cross structure (See Appendix A). The shear flows in the center bulkhead and deck cancel because of the double symmetry resulting in a zero stress in the center reinforcing membranes. This statement does not hold true for unsymmetrical cases such as the actual ASR-21 cross structures.

Equation (11) can be further modified by defining the shear flow as the force per unit length of cross structure.

$$Q = F/c \tag{12}$$

$$F = M_y c/2A \tag{13}$$

c = The length between node midpoints

F = nodal force

The loading for the quarter structure is shown in Figure (XI), and values for the nodal forces for an applied moment, M_y, of 1000 foot-tons are specified in Table 7.

TABLE 7

QUARTER STRUCTURE NODAL LOADINGS

FOR TORSIONAL MOMENT (M_y = 1000 foot-tons)

AND VARIOUS B/D RATIOS

Nodal Forces (tons)

Node Number	B/D = 2.5	B/D = 3.0	B/D = 3.5
3, 5 (positive z direction)	1.5	1.25	1.07
4	3.0	2.5	2.14
5 (negative y direction)	-2.5	-2.5	-2.5
6, 7	-5.0	-5.0	-5.0
8	-2.5	-2.5	-2.5

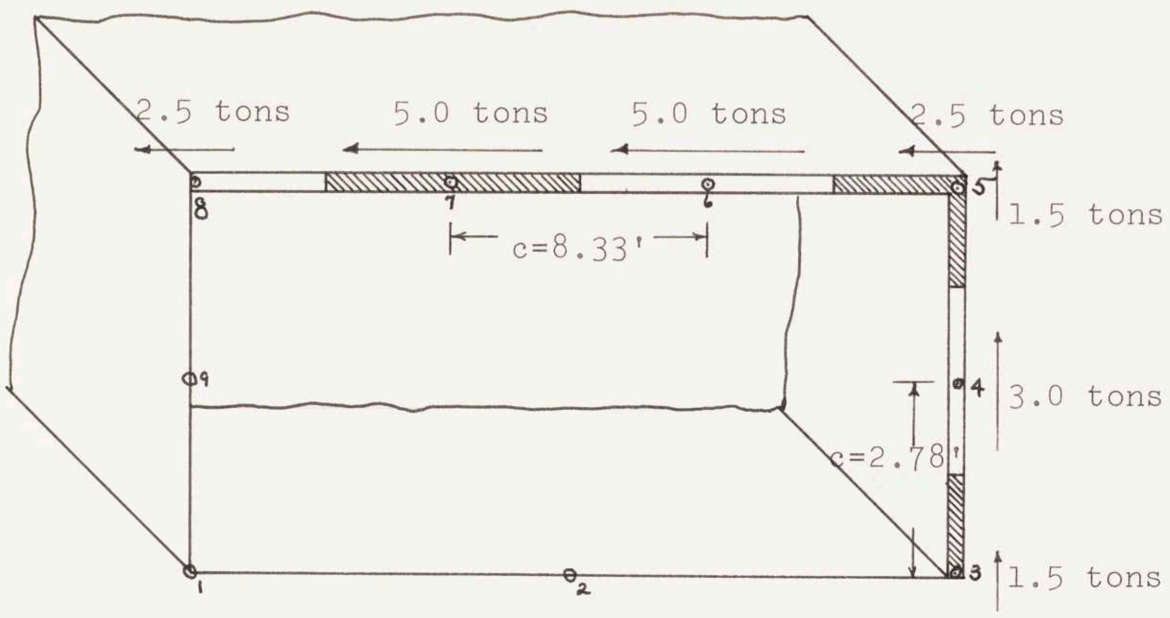

FIGURE XI
QUARTER STRUCTURE NODAL LOADS
FOR TORSIONAL MOMENT (B/D=3.0)

Plating Effectiveness

The concept of effective plating width and breadth resulted from work done by Von Karman and Schnadel in the 1920's. The aircraft industry referred to it as the plating efficiency in the late 1930's. Significant work was performed in this area by Schade (Ref. 12 and 13) in the early 1950's, and most recently by Mansour (Ref. 11). Both terms, effectiveness and efficiency, aid in graphically illustrating the fact that shear lag exists in stiffened plating. Because of the shear lag, stress peaks occur at the stiffening bulkheads, and much lower stresses exist in the remainder of the plating. This phenomenon means that only a small width of the plating is being stressed to any significant degree. Hence, there is some effective width of the plate that is carrying the load.

Equations (14) and (15) define the effectiveness, and Figure XII shows how these definitions are applied to the catamaran cross structure.

$$\rho_1 = \sigma avg/\sigma max1 \qquad (14)$$

$$\rho_2 = \sigma avg/\sigma max2 \qquad (15)$$

Because the finite element solution gives the stress resultant at the center of an element, extrapolation of the data was necessary to obtain the maximum stresses at the plating edges. Reference (28) assumes that the shear lag has a parabolic distribution in the transverse direction for box beams. Since data was obtained for three transverse elements across the top plating, the parabolic assumption was

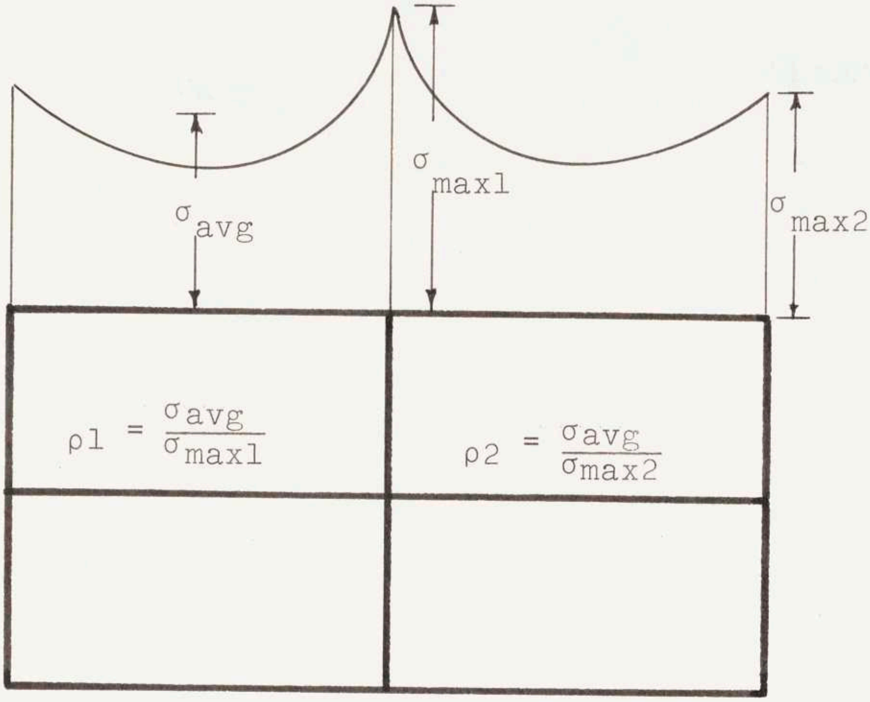

FIGURE XII
TOP PLATE EFFECTIVENESS DEFINITION

used to fit the data, and to calculate the maximum stresses at each edge of the plate. Integration of this distribution over the entire width of the plating was performed to obtain the average value of the stress. (Equation 16)

$$\sigma_{yavg} = 1/x_o \int_o^{x_o} \sigma_y(x)\, dx \qquad (16)$$

x_o = The overall width of plating

$\sigma_y(x)$ = The longitudinal stress in the y direction as a function of plate width

From equation (16) and the extrapolated maximums the effectiveness of the plating can be calculated using equations (14) and (15).

RESULTS

1. Tabulated computer results of the longitudinal, girth and shear stress distribution in the forward and after ASR-21 Catamaran cross structures are presented in Tables C-1 and C-2. Symmetric bending moment, antisymmetric bending moment and shear, and combined loadings are included.

2. The stress results for the cross structure model under symmetric and antisymmetric loadings are included in Tables C-3 through C-9.

3. The computer results for the stresses resulting from the torsional loads are included in Table C-10; the calculated results are in Table C-11.

4. Average longitudinal stresses and plating effectiveness calculations are summarized:

   (a) in Table C-12 for the symmetric and antisymmetric bending moment loadings of the quarter structure model.

   (b) in Table C-13 for the combined loading case of the quarter structure model.

   (c) in Table C-14 for all the loading conditions of the ASR-21 Catamaran cross structures.

5. Typical longitudinal stress distributions for the cross structures are illustrated:

   (a) in Figure XIII for the symmetric bending moment case of the quarter structure.

(b) in Figure XIV for the antisymmetric bending moment case of the quarter structure.

(c) in Figure XV for the combined loading case of the quarter structure.

(d) in Figure XVI and XVII for the combined loading case of the actual forward and after ASR-21 cross structure.

6. Girth stress distributions are plotted:

(a) in Figure XVIII for the symmetric bending moment case of the quarter structure.

(b) in Figure XIX for the antisymmetric bending moment case of the quarter structure.

(c) in Figure XX for the combined loading case of the quarter structure.

(d) in Figures XXI and XXII for the combined loading case of the actual forward and after ASR-21 cross structures.

7. Shear stress distributions are shown:

(a) in Figure XXIII for the symmetric bending moment case of the quarter structure.

(b) in Figure XXIV for the Antisymmetric bending moment case of the quarter structure.

(c) in Figure XXV for the combined loading case of the quarter structure.

(d) in Figures XXVI and XXVII for the combined loading case of the actual ASR-21 cross structures.

(e) in Figure XXVIII for the torsional loading of the quarter structure.

8. Plating effectiveness as a function of the length to breadth ratio (L/B) for all the loading conditions are plotted in Figures XXIX to XXXIV. Table 8 which precedes the graphs shows the numbering sequence one uses to locate the effectiveness of the actual structures.

9. Average stress along the top of the quarter structure is plotted versus the L/B ratio for the combined loading case in Figure XXXIX.

10. The qualitative effect of the various loading conditions on the displacement of the quarter structure is shown in Figures XXXV to XXXVIII.

11. The effective breadths of the model and the actual cross structures at positions along the length of the structures are presented in Table 9 and Figure XL.

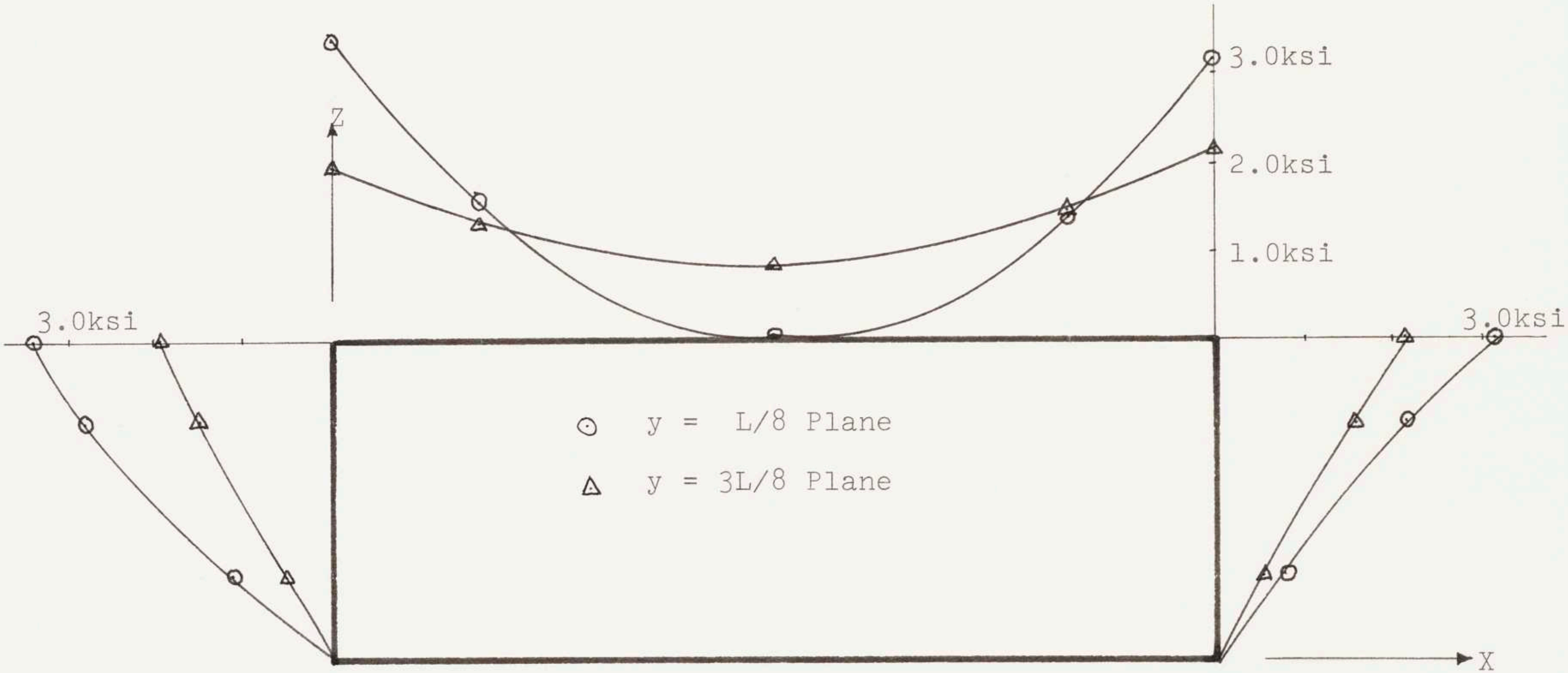

Stress Results for

L/B=.7
B/D=3.0
A_f/A_w=3.0

FIGURE XIII
SYMMETRICAL BENDING MOMENT LONGITUDINAL STRESS DISTRIBUTION OF QUARTER STRUCTURE

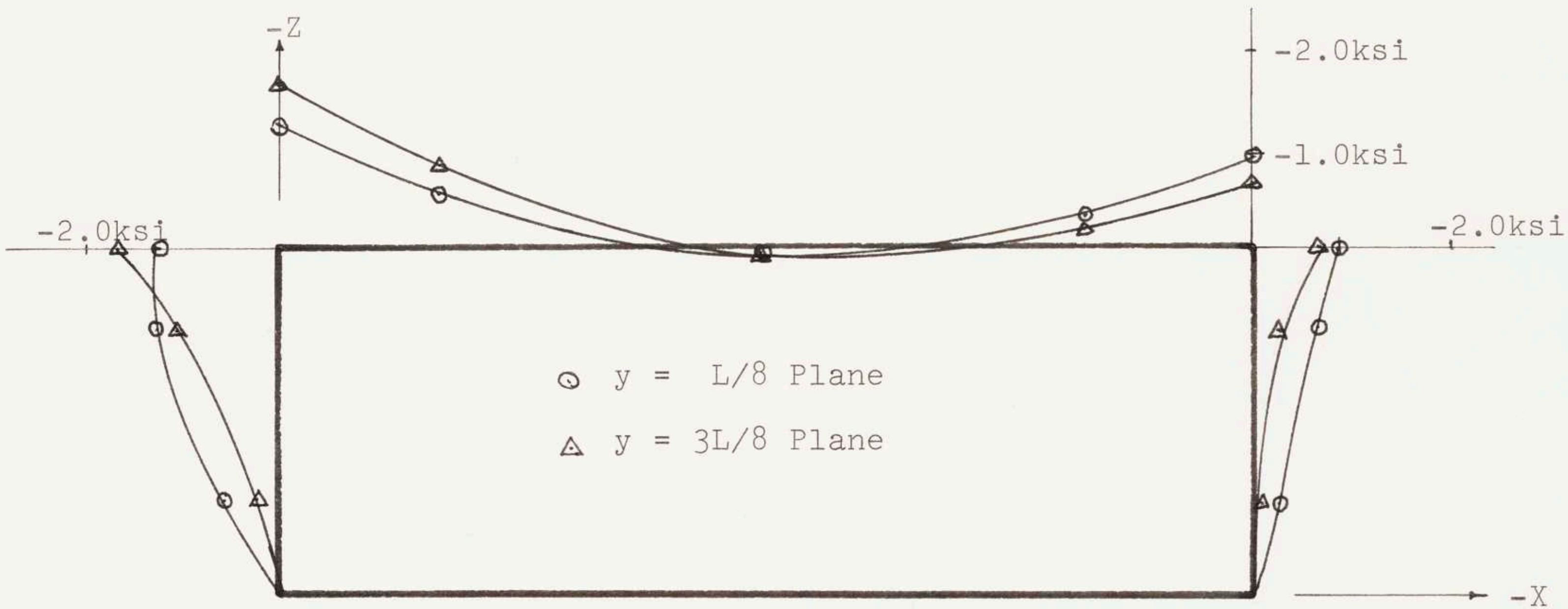

Stress Results For

L/B=.7
B/D=3.0
A_f/A_w=3.0

FIGURE XIV
ANTISYMMETRICAL BENDING MOMENT + SHEAR
LONGITUDINAL STRESS DISTRIBUTION OF QUARTER STRUCTURE

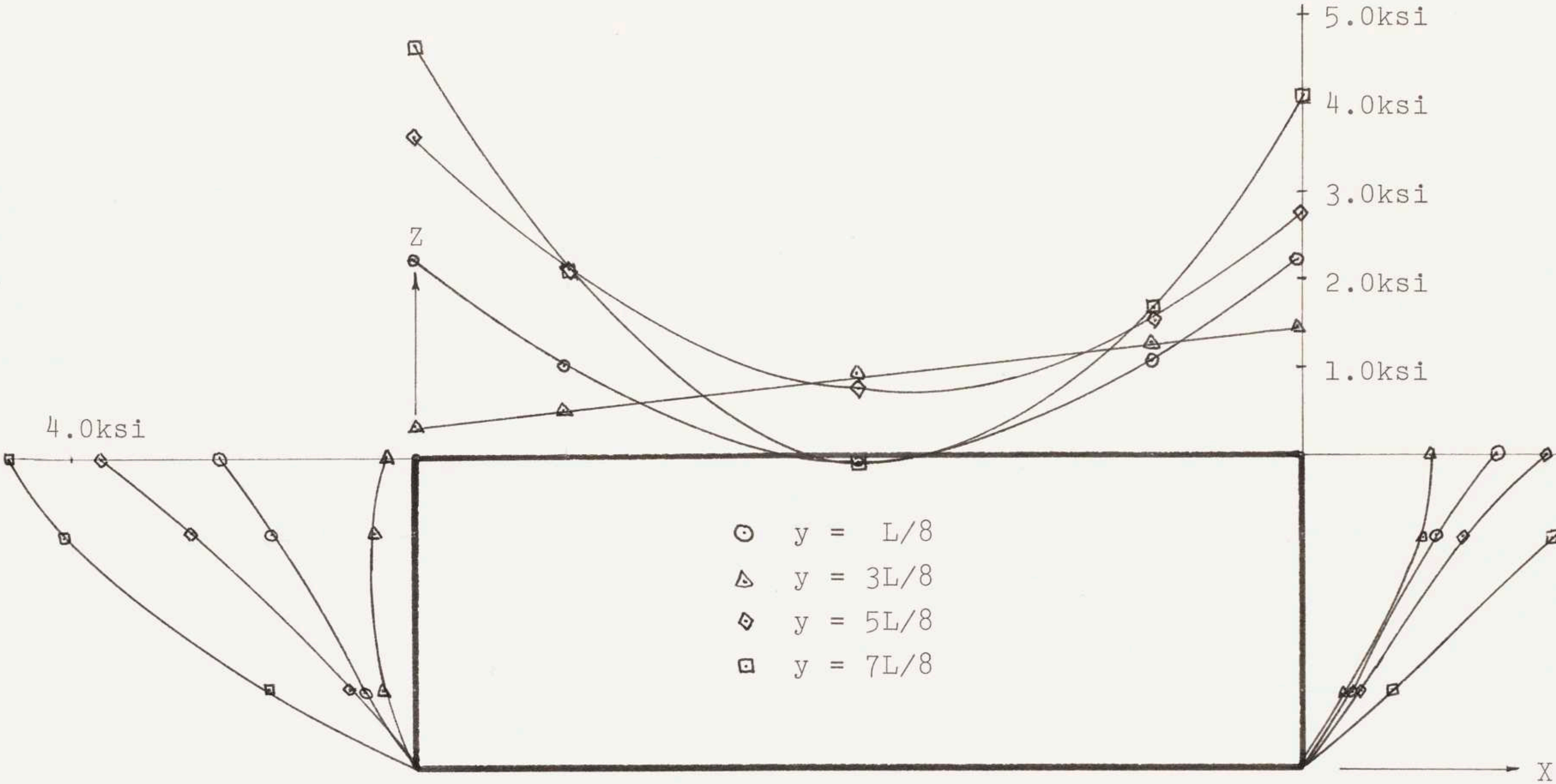

Stress Results For

L/B=.7
B/D=3.0
A_f/A_w=3.0

FIGURE XV
COMBINED LONGITUDINAL STRESS DISTRIBUTION OF QUARTER STRUCTURE

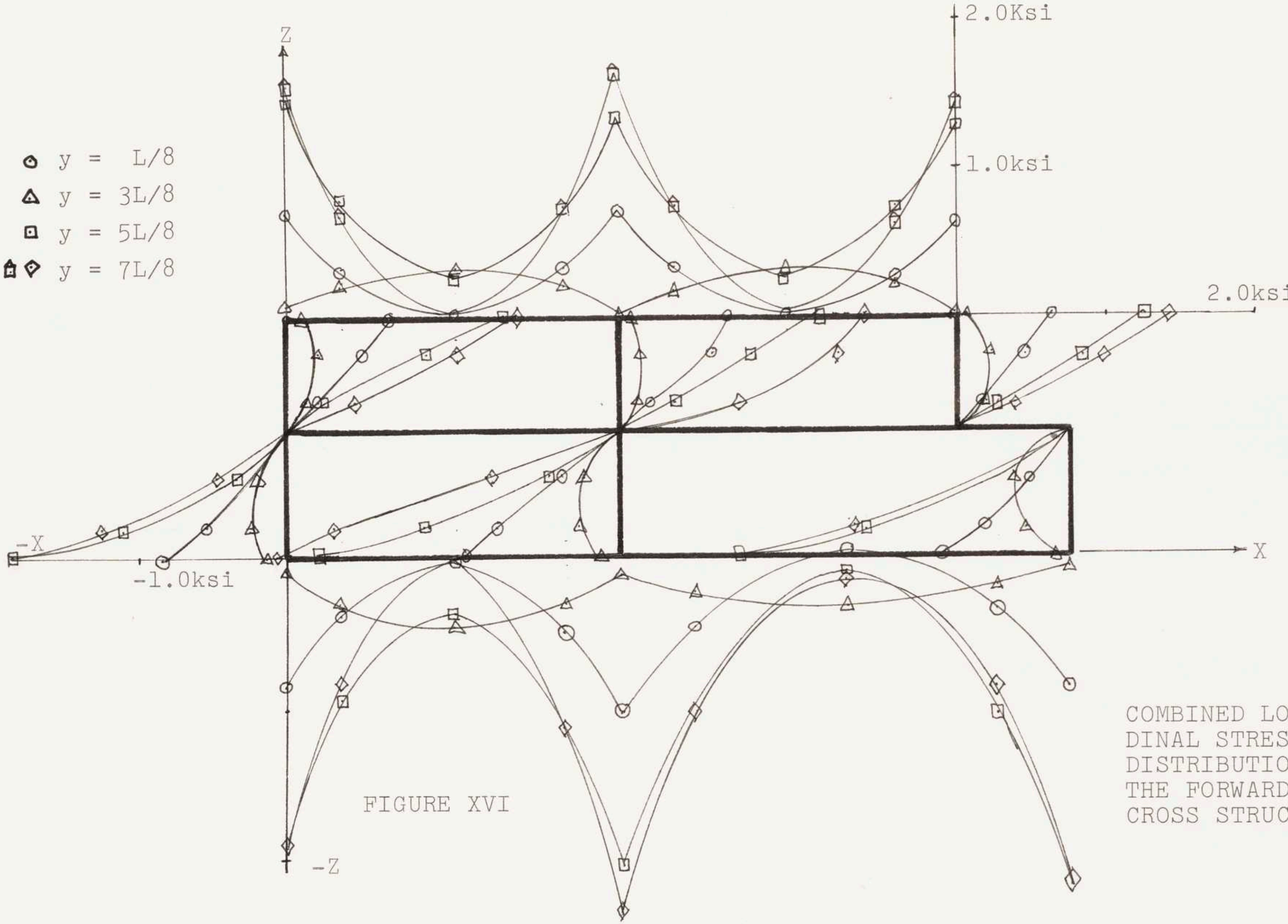

FIGURE XVI

COMBINED LONGITUDINAL STRESS DISTRIBUTION FOR THE FORWARD ASR-21 CROSS STRUCTURE

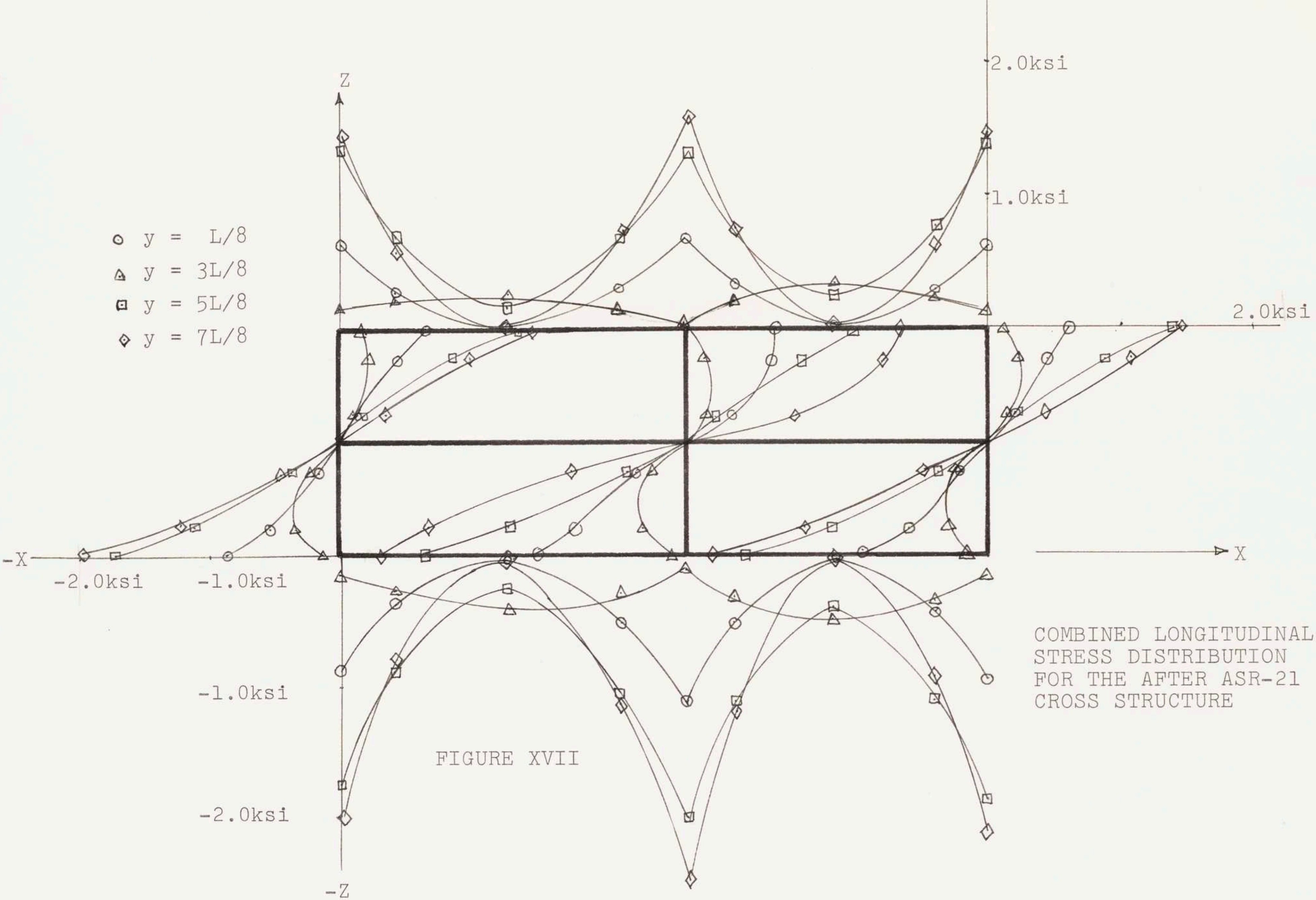

COMBINED LONGITUDINAL STRESS DISTRIBUTION FOR THE AFTER ASR-21 CROSS STRUCTURE

FIGURE XVII

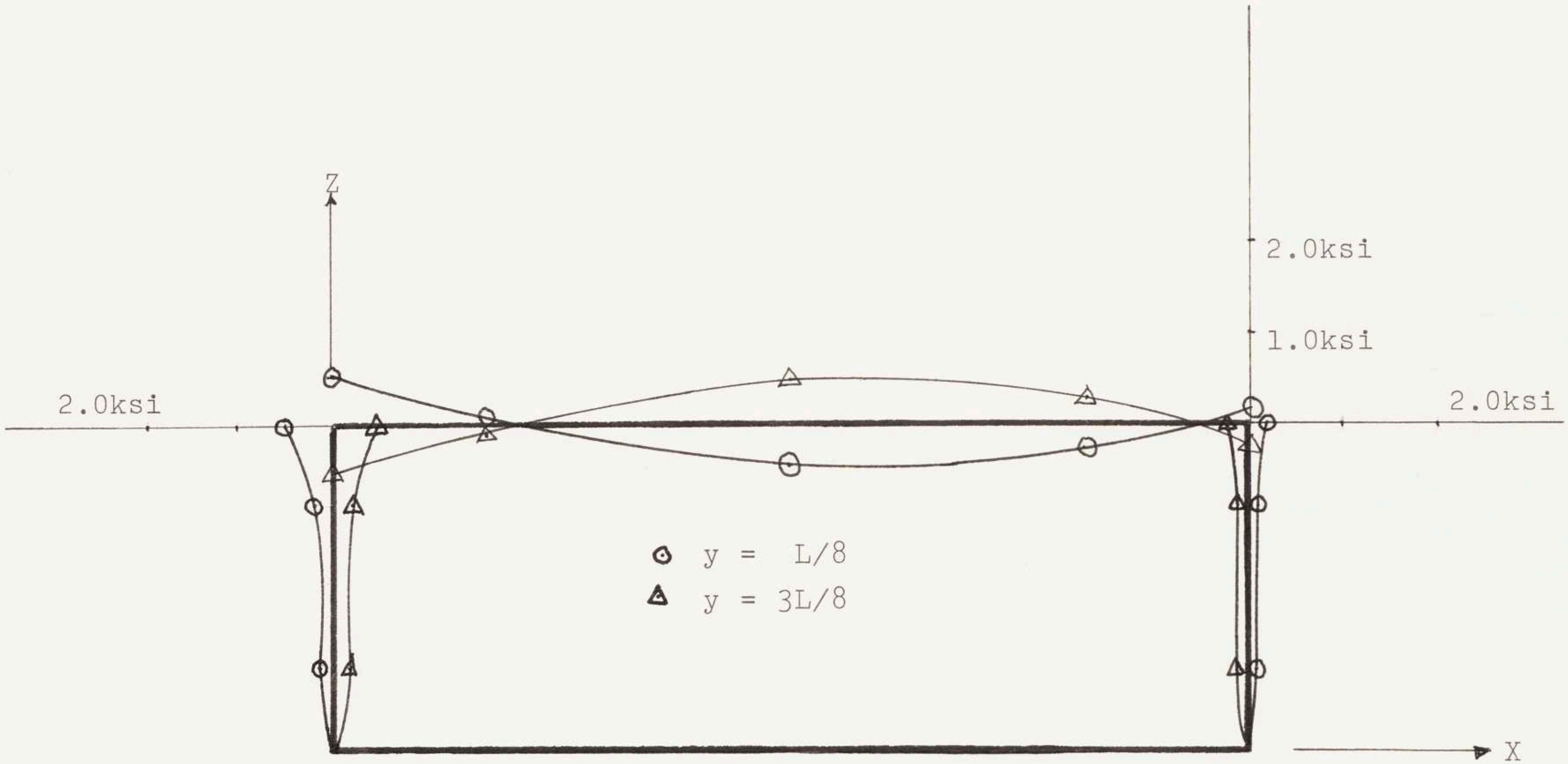

Stress Results For

L/B=.7
B/D=3.0
A_f/A_w=3.0

FIGURE XVIII
SYMMETRICAL BENDING MOMENT
GIRTH STRESS DISTRIBUTION OF QUARTER STRUCTURE

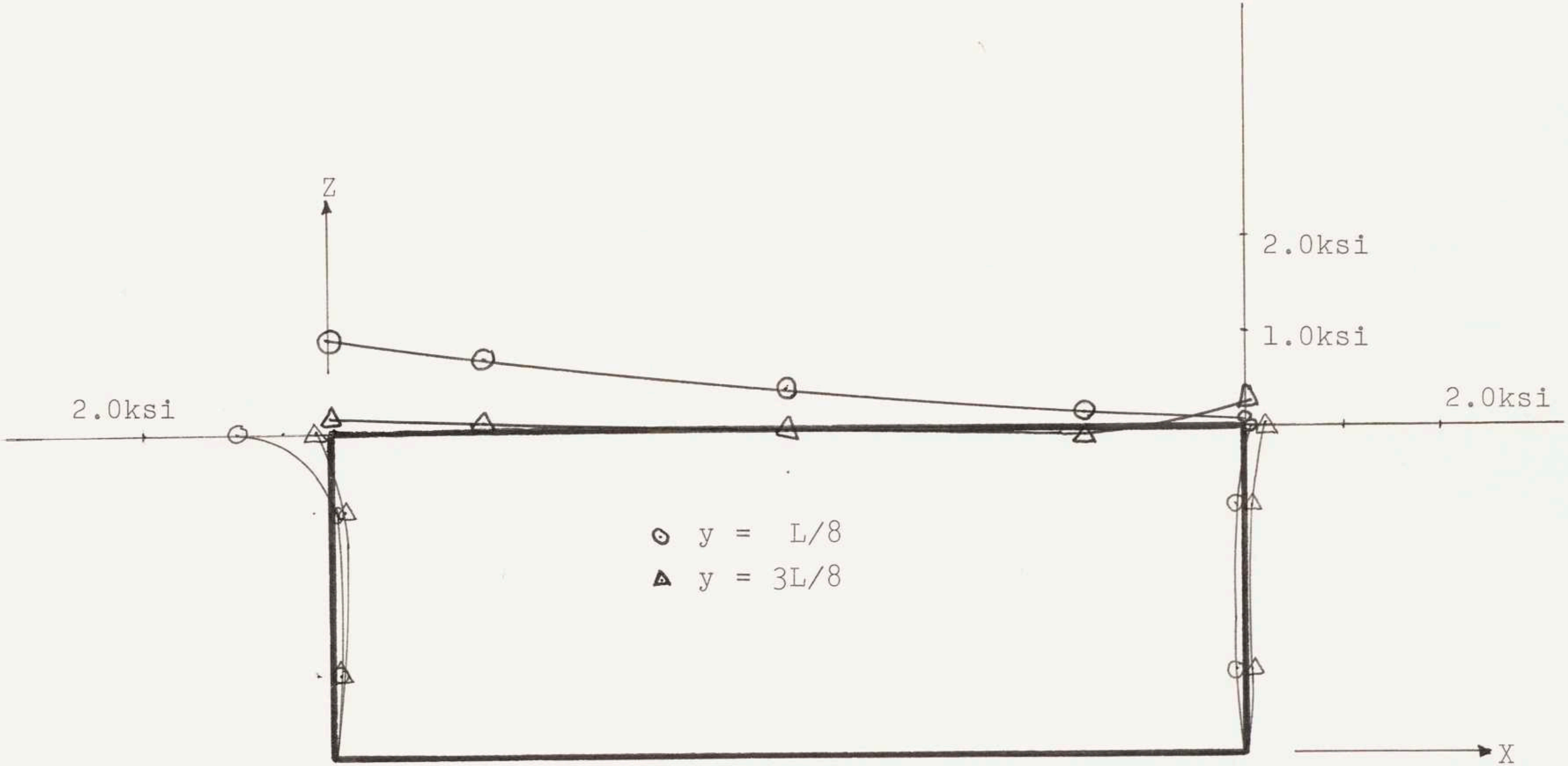

Stress Results for

L/B=.7
B/D=3.0
A_f/A_w=3.0

FIGURE XIX
ANTISYMMETRIC BENDING MOMENT + SHEAR
GIRTH STRESS DISTRIBUTION OF QUARTER STRUCTURE

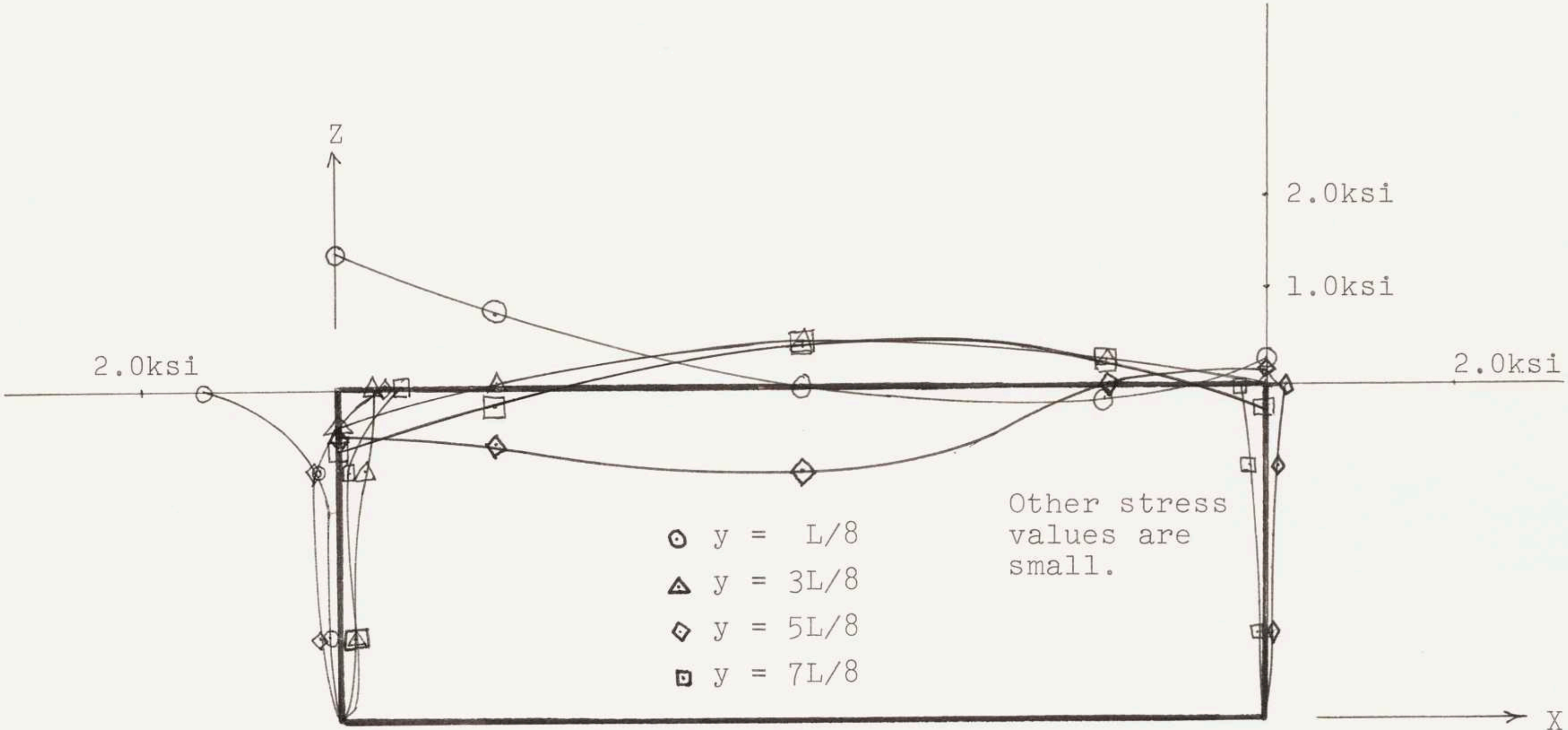

Stress Results for

L/B=.7
B/D=3.0
A_f/A_w=3.0

FIGURE XX
COMBINED GIRTH STRESS DISTRIBUTION OF QUARTER STRUCTURE

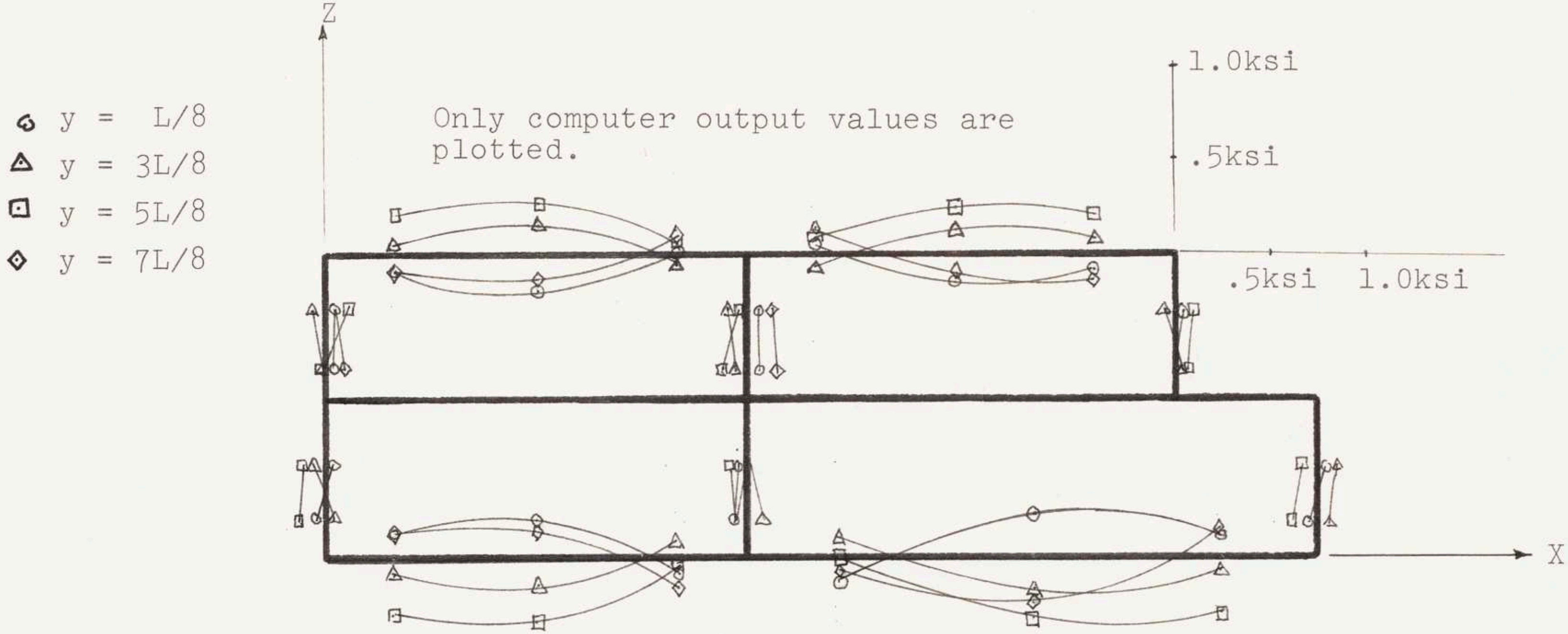

FIGURE XXI
COMBINED GIRTH STRESS DISTRIBUTION
FOR THE FORWARD ASR-21 CROSS STRUCTURE

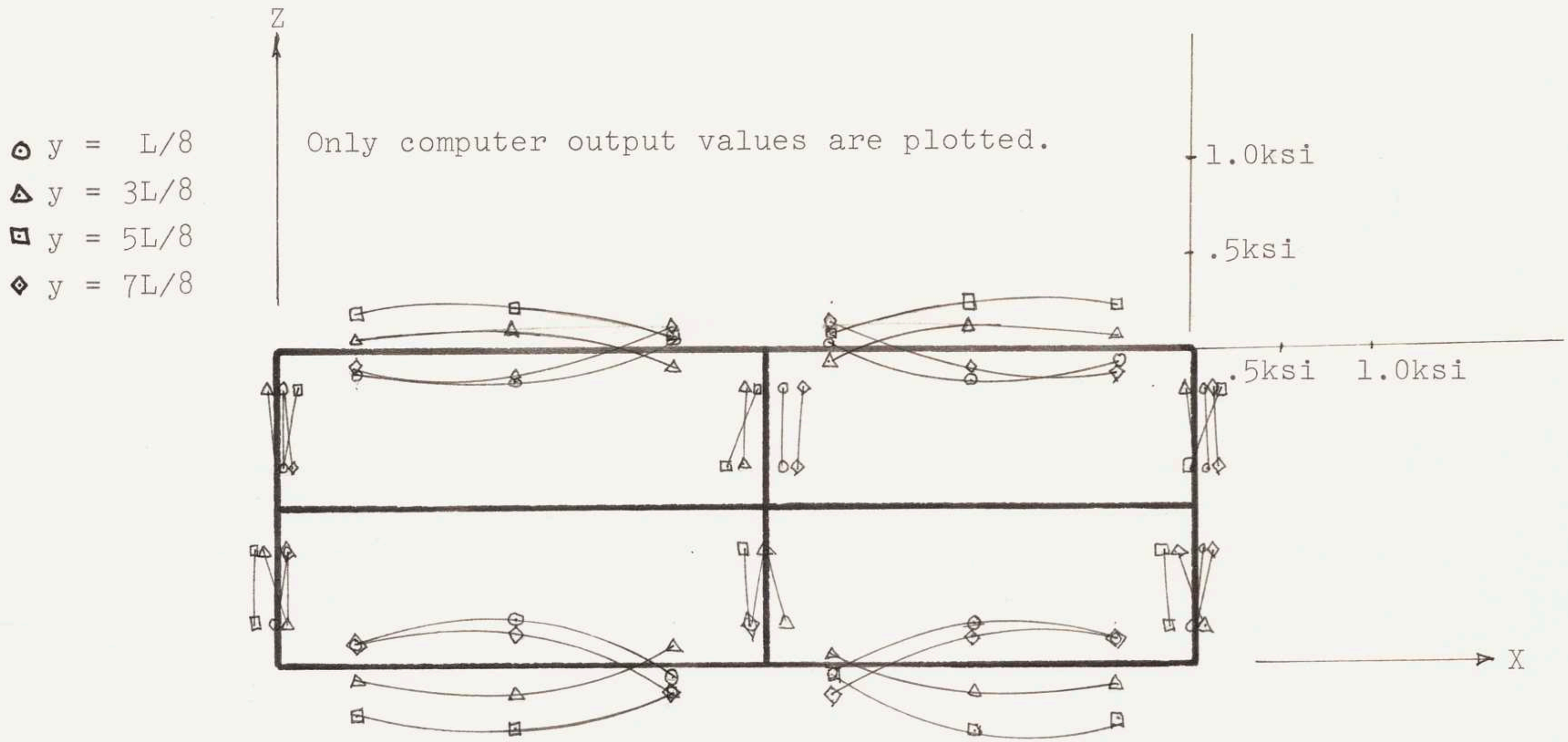

FIGURE XXII
COMBINED GIRTH STRESS DISTRIBUTION
FOR THE AFTER ASR-21 CROSS STRUCTURE

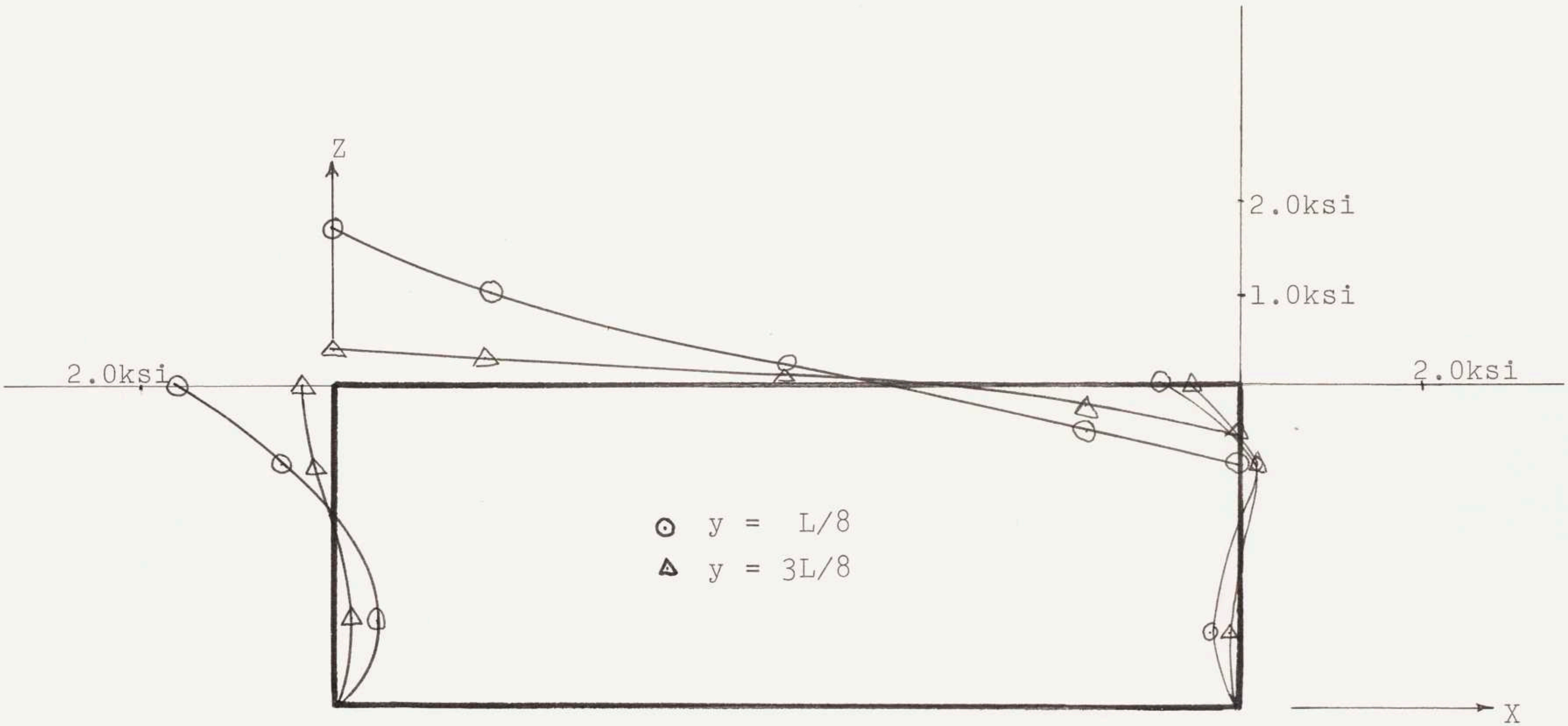

Stress Results For

L/B=.7
B/D=3.0
A_f/A_w=3.0

FIGURE XXIII
SYMMETRICAL BENDING MOMENT SHEAR STRESS DISTRIBUTION

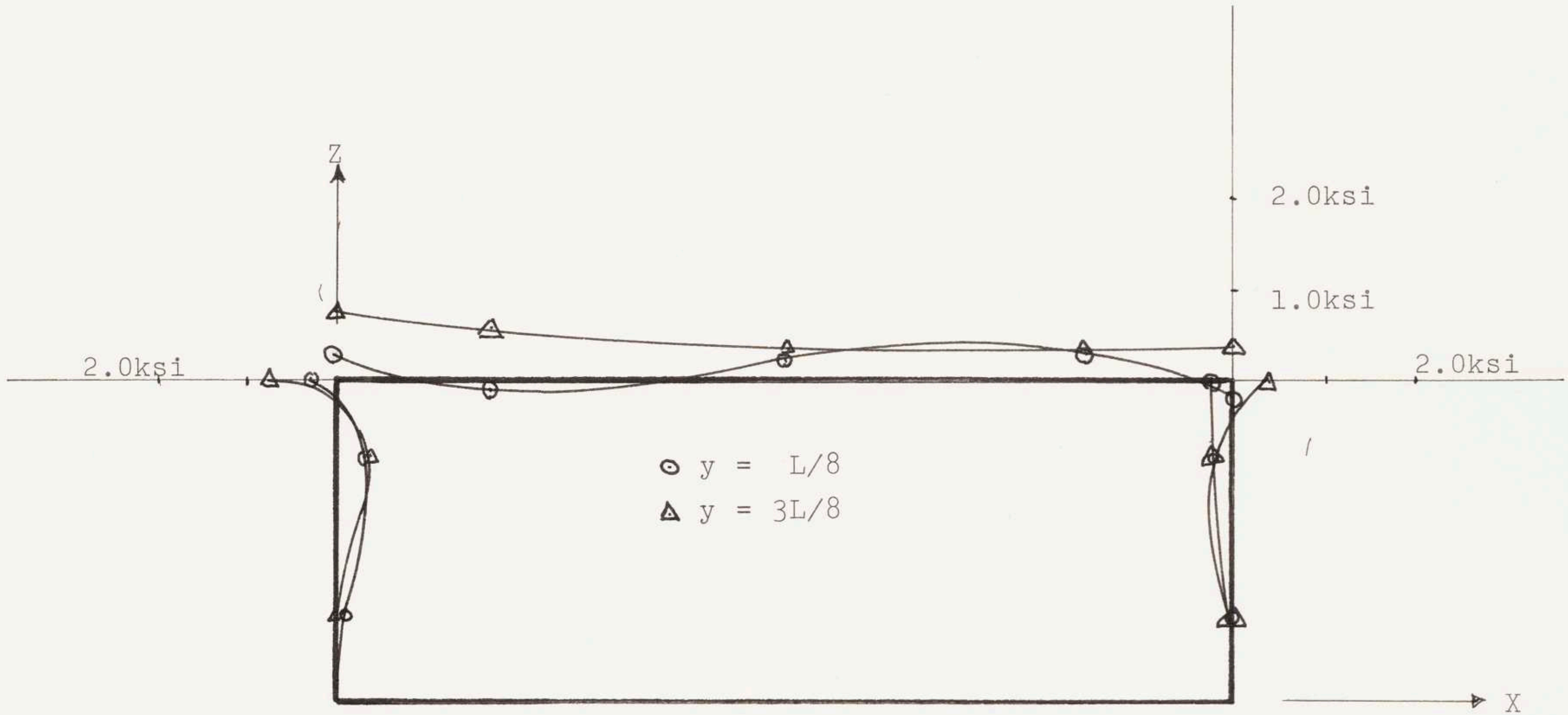

Stress Results For

L/B=.7
B/D=3.0
A_f/A_w=3.0

FIGURE XXIV
ANTISYMMETRIC BENDING MOMENT + SHEAR STRESS DISTRIBUTION

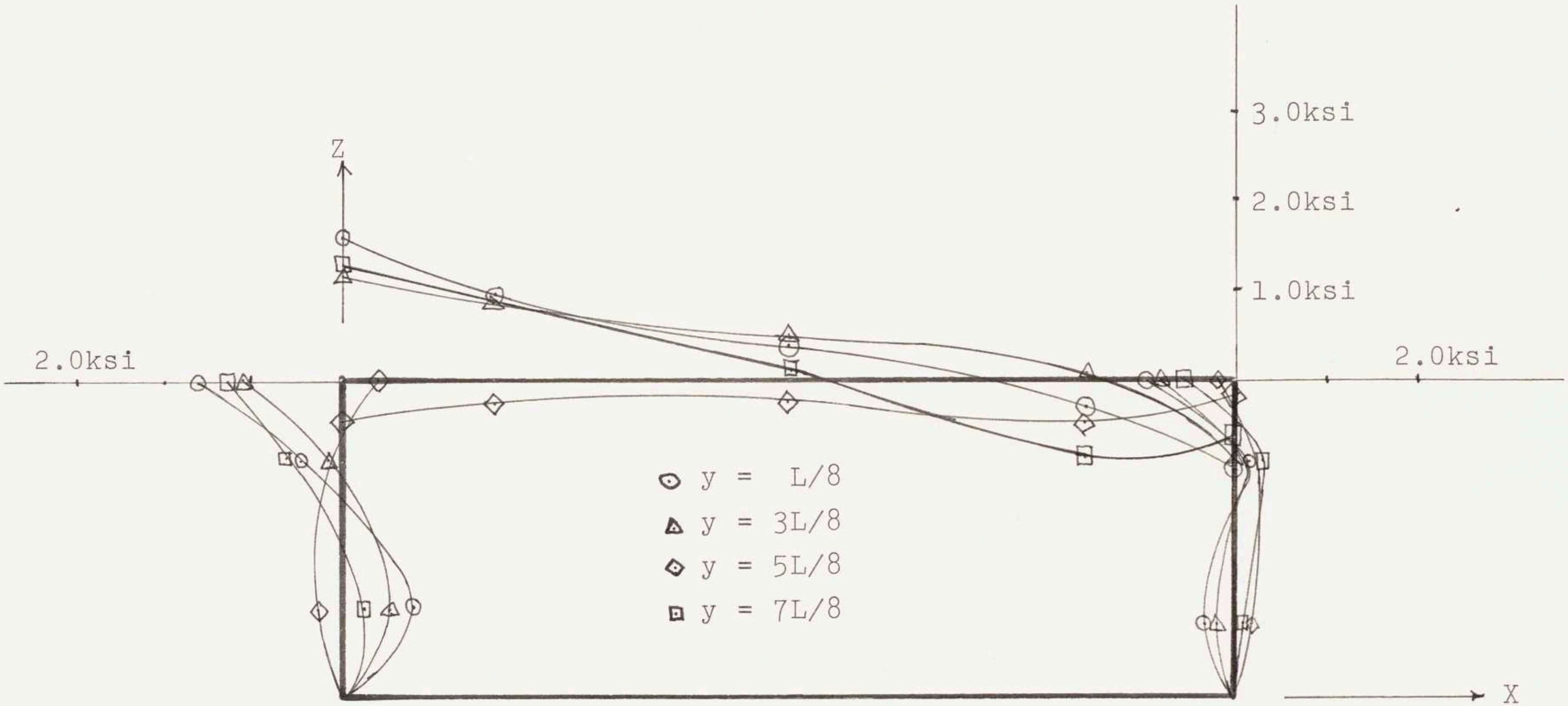

Stress Results For

L/B=.7
B/D=3.0
A_f/A_w=3.0

FIGURE XXV
COMBINED SHEAR STRESS DISTRIBUTION OF QUARTER STRUCTURE

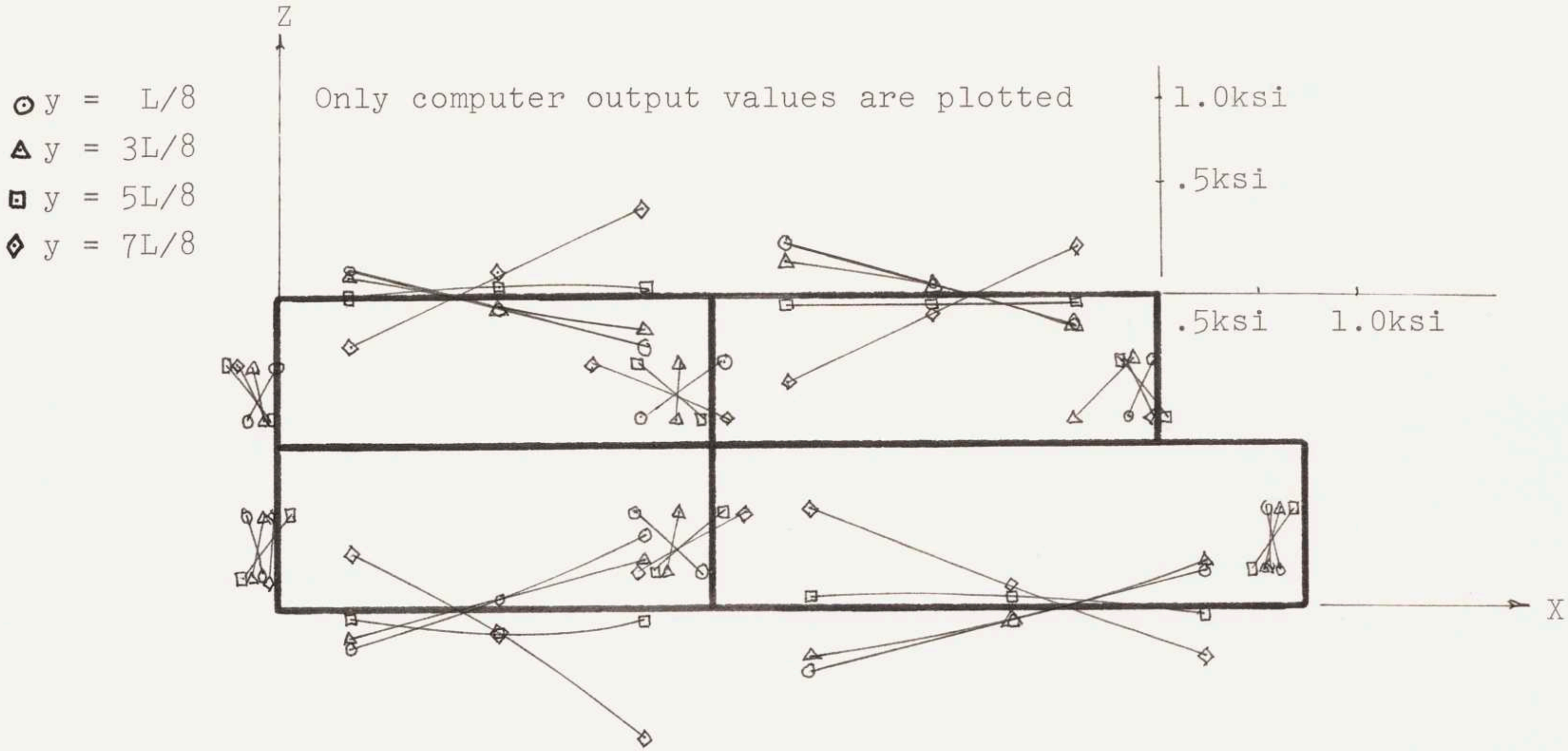

FIGURE XXVI
COMBINED SHEAR STRESS DISTRIBUTION
FOR THE FORWARD ASR-21 CROSS STRUCTURE

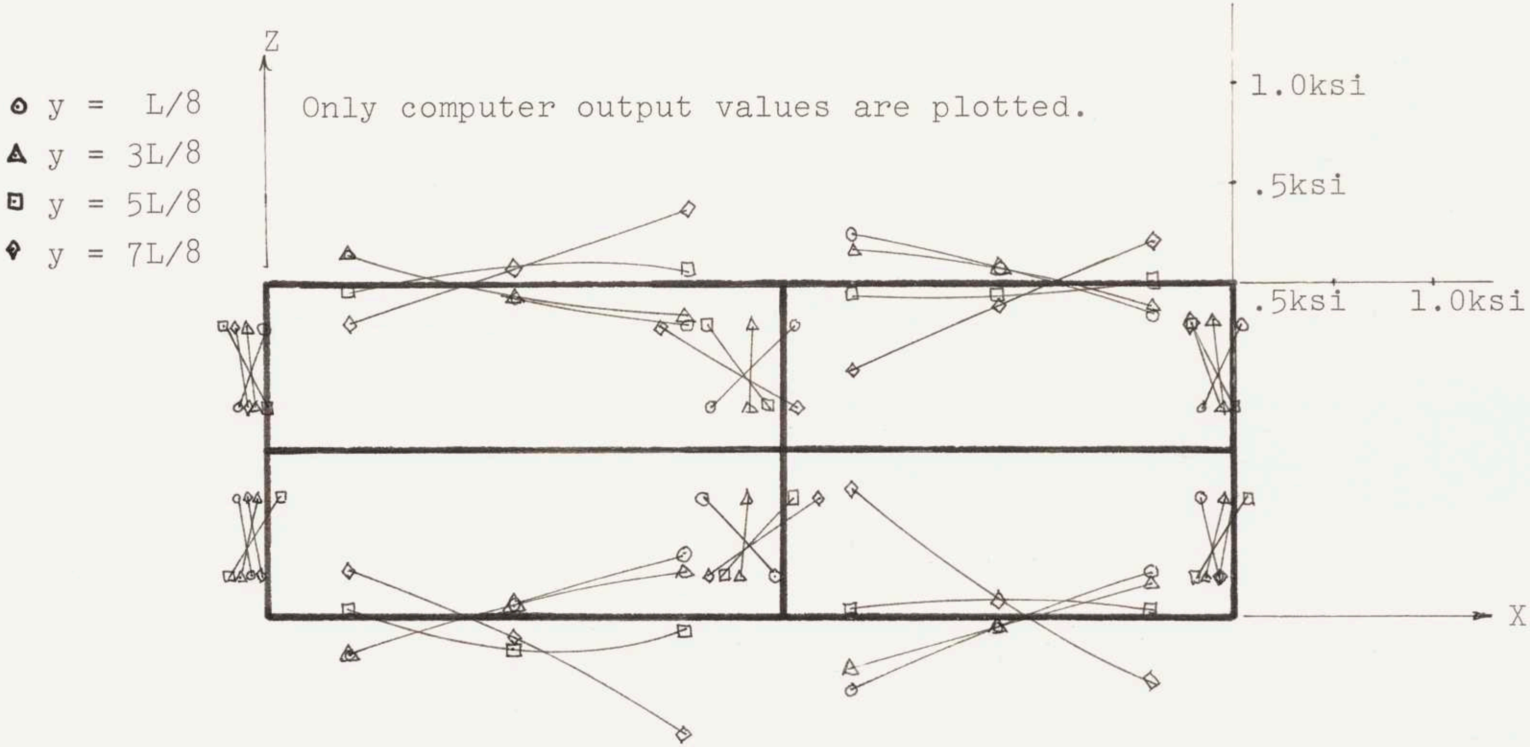

FIGURE XXVII
COMBINED SHEAR STRESS DISTRIBUTION
FOR AFTER ASR-21 CROSS STRUCTURE

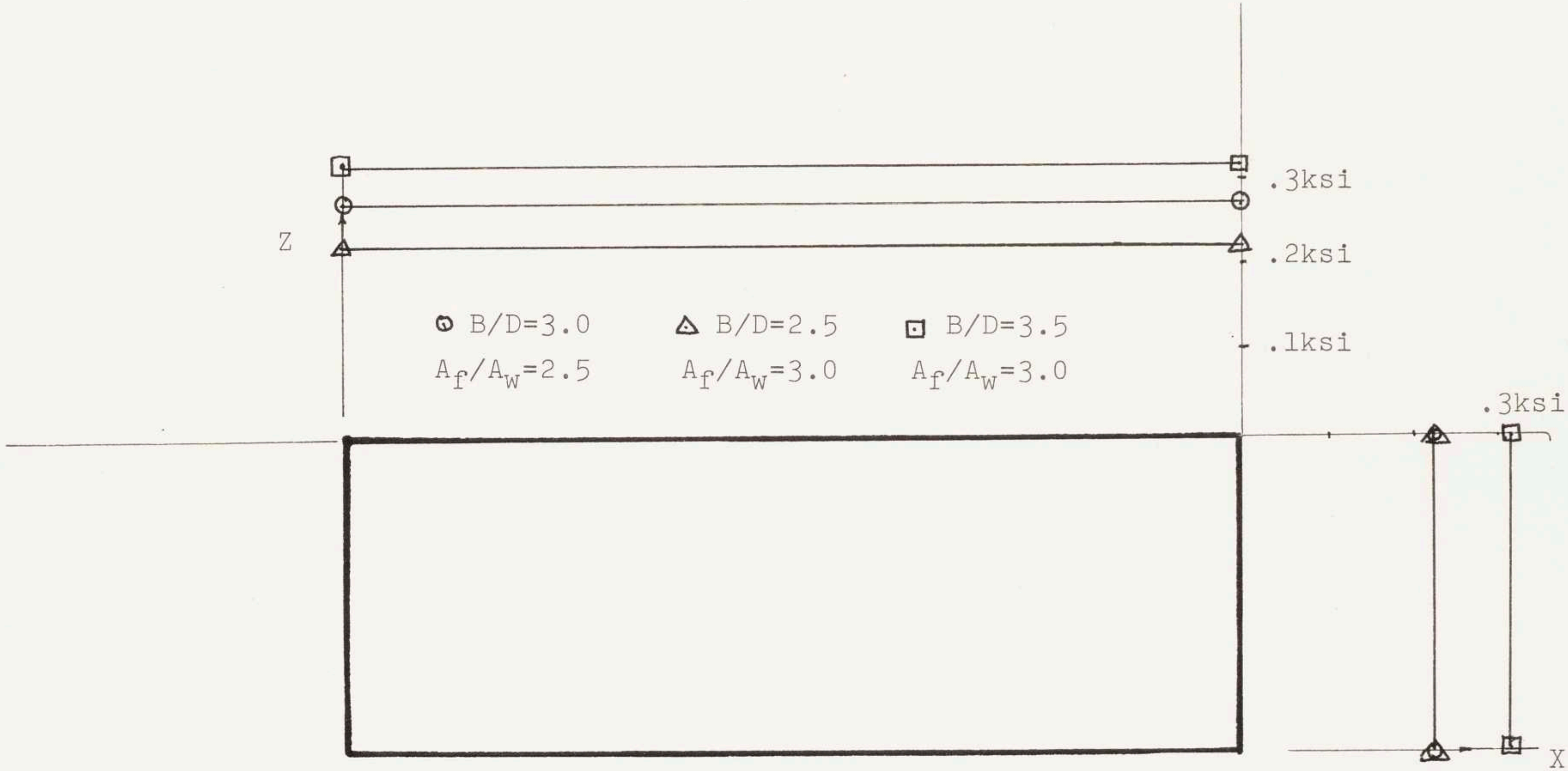

FIGURE XXVIII
TORSIONAL MOMENT SHEAR STRESS DISTRIBUTION OF QUARTER STRUCTURE

TABLE 8

TOP PLATING EFFECTIVENESS LOCATORS FOR THE ASR-21 CROSS STRUCTURES

Points plotted on Figures XXIX to XXXIV and designated by the following set of numbers indicate the effectiveness of the actual ASR-21 cross structures.

Number	Cross Structure	Y-Coordinate	Element Numbers
1	Forward	L/8	9,113,13
2	↓	3L/8	10,114,14
3	↓	5L/8	11,115,15
4	↓	7L/8	12,116,16
5	↓	L/8	49,45,41
6	↓	3L/8	50,46,42
7	↓	5L/8	51,47,43
8	↓	7L/8	52,48,44
9	After	L/8	9,13,17
10	↓	3L/8	10,14,18
11	↓	5L/8	11,15,19
12	↓	7L/8	12,16,20
13	↓	L/8	49,45,41
14	↓	3L/8	50,46,42
15	↓	5L/8	51,47,43
16	↓	7L/8	52,48,44

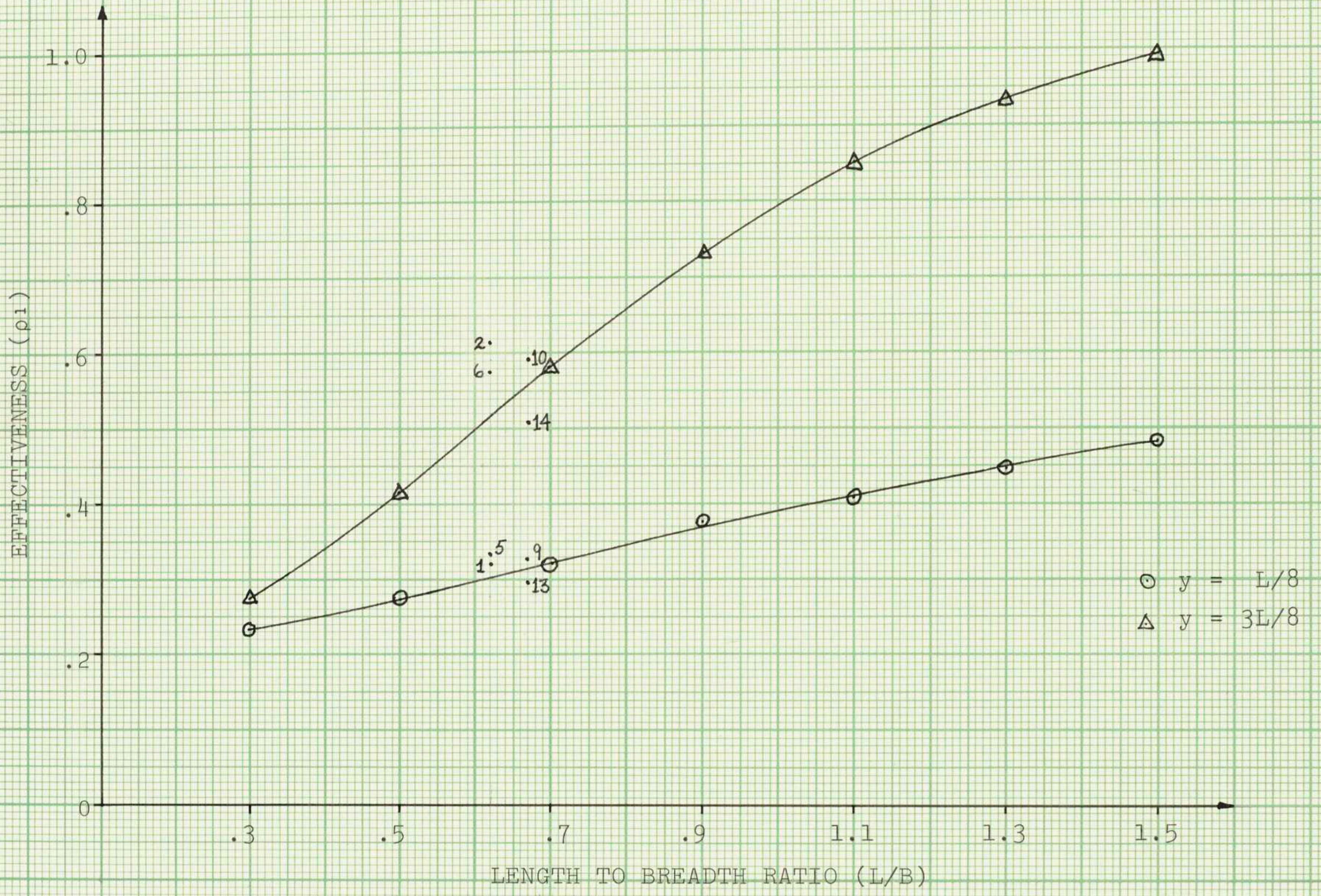

FIGURE XXIX
EFFECTIVENESS (ρ_I) VS L/B FOR SYMMETRIC BENDING MOMENT

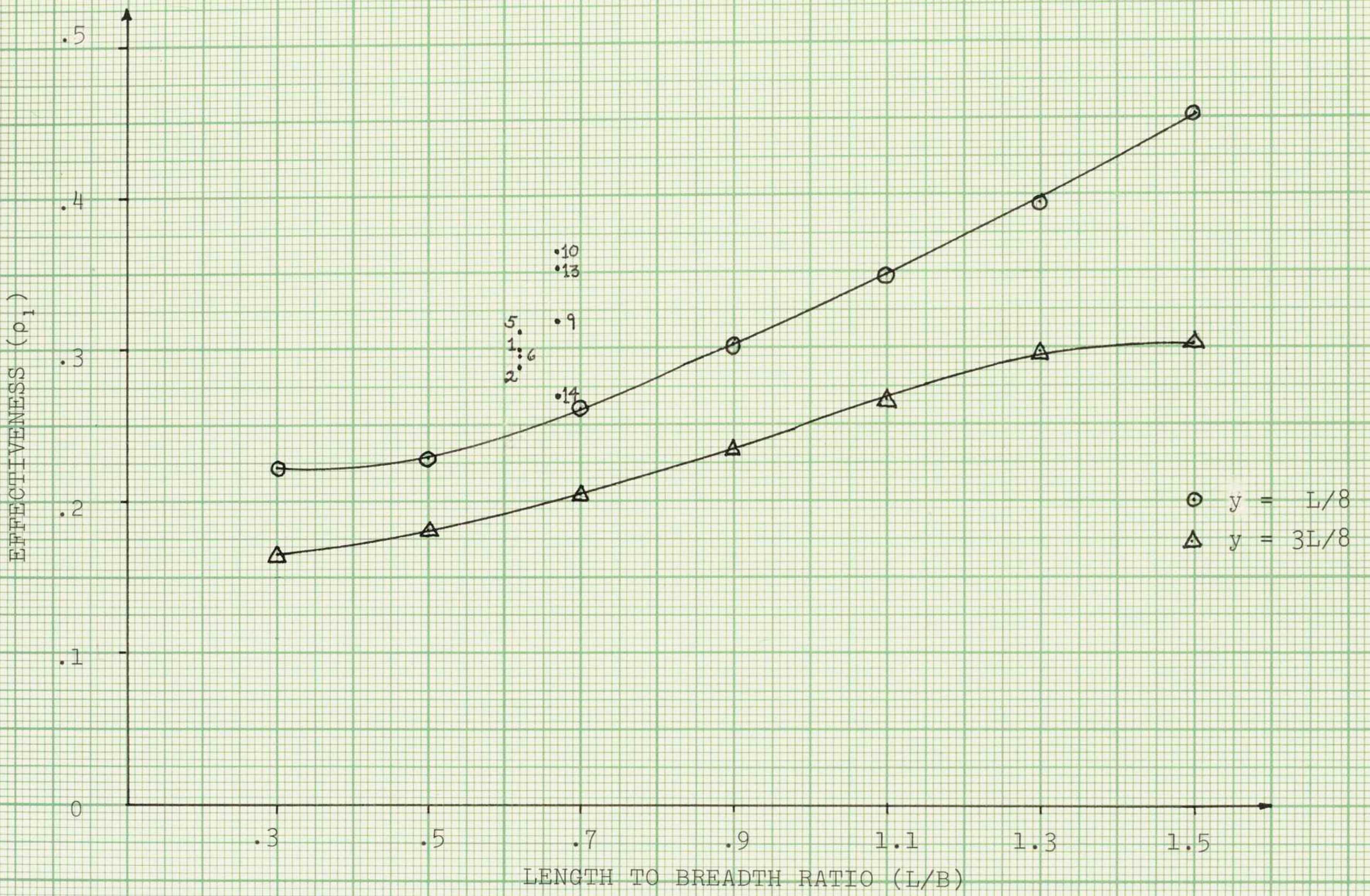

FIGURE XXX

EFFECTIVENESS (ρ_1) VS L/B FOR ANTISYMMETRIC BENDING MOMENT + SHEAR

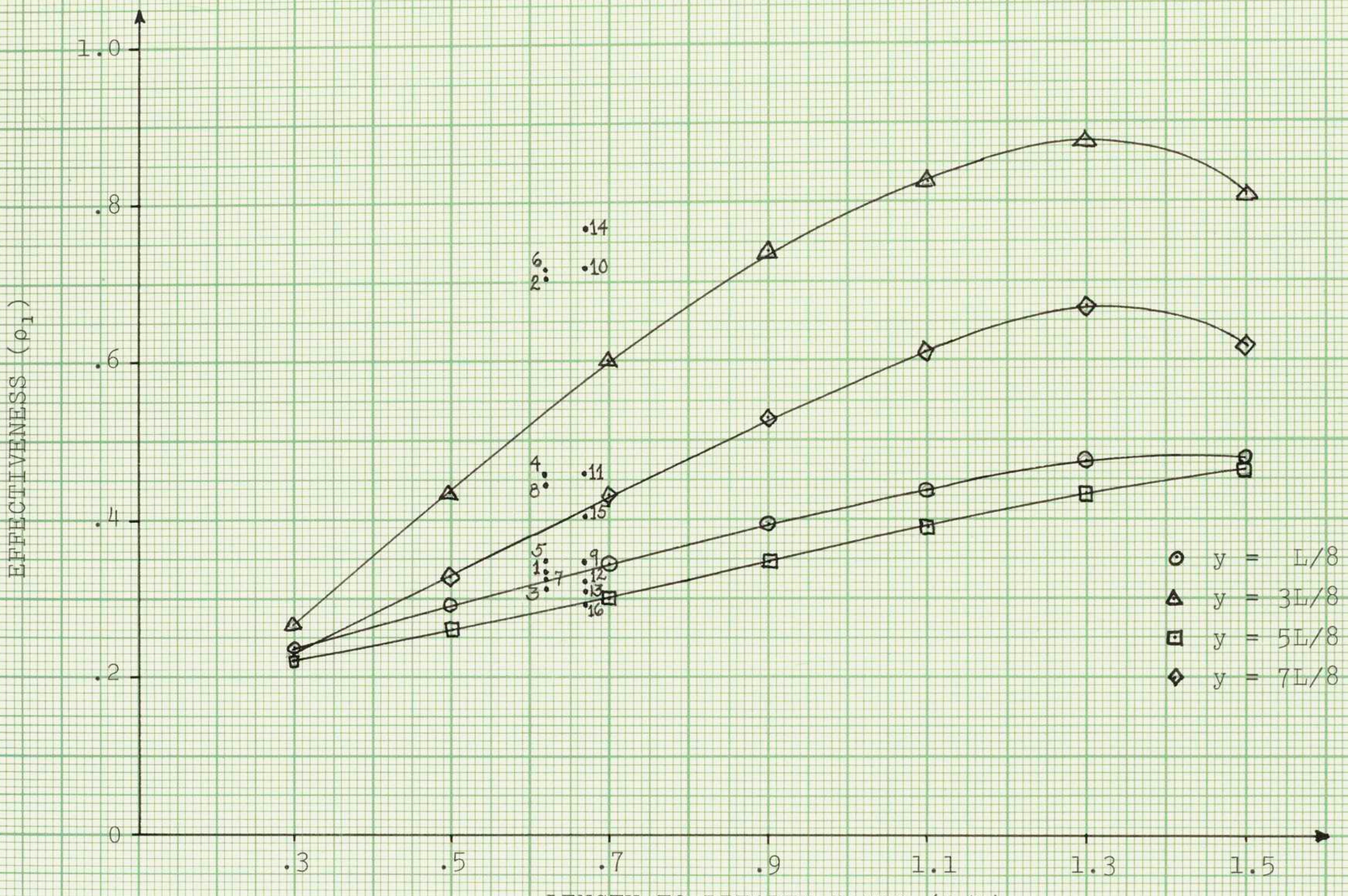

FIGURE XXXI
EFFECTIVENESS (ρ_1) VS L/B FOR COMBINED LOADING

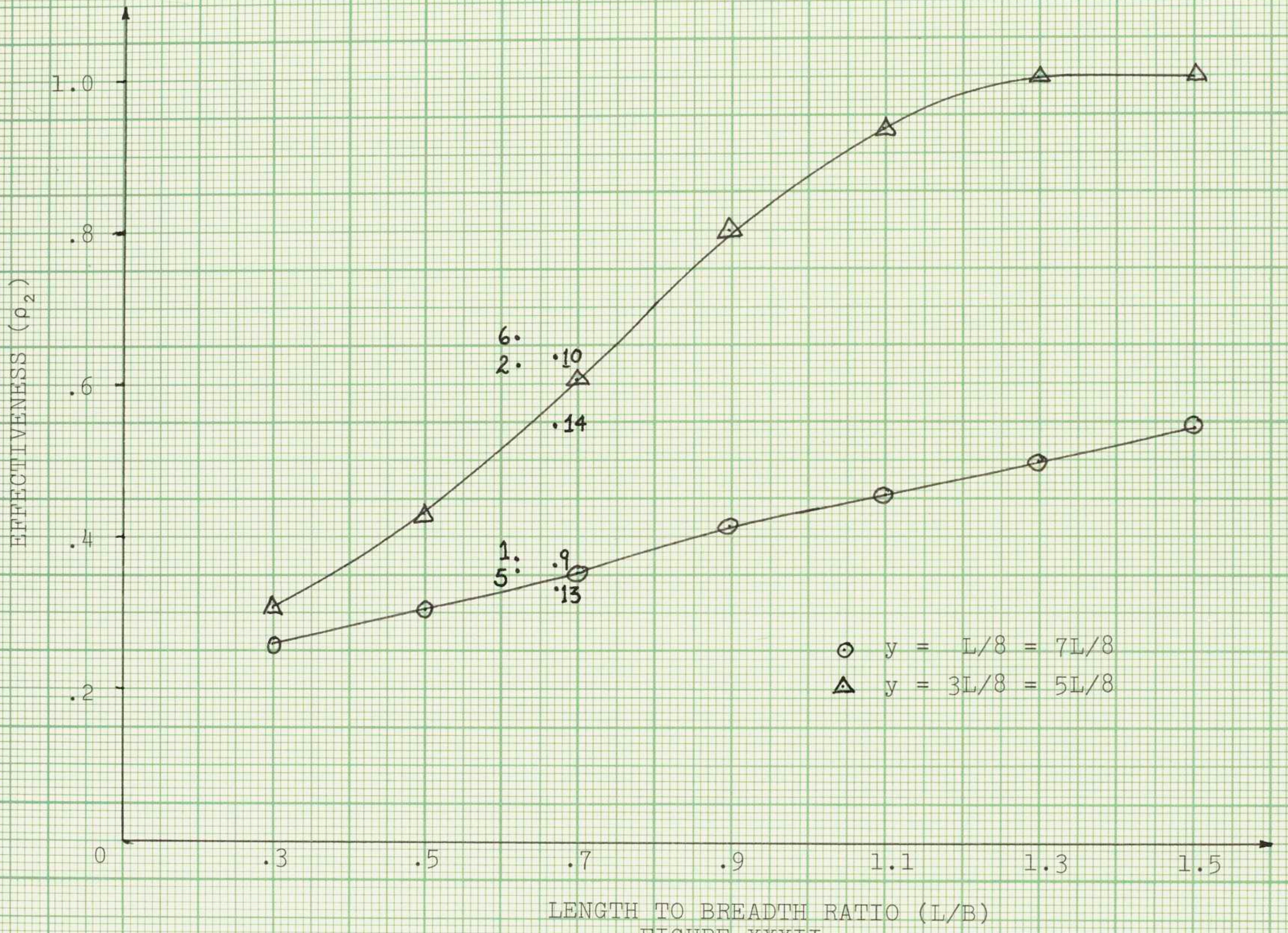

FIGURE XXXII

EFFECTIVENESS (ρ_2) VS L/B FOR SYMMETRIC BENDING MOMENT

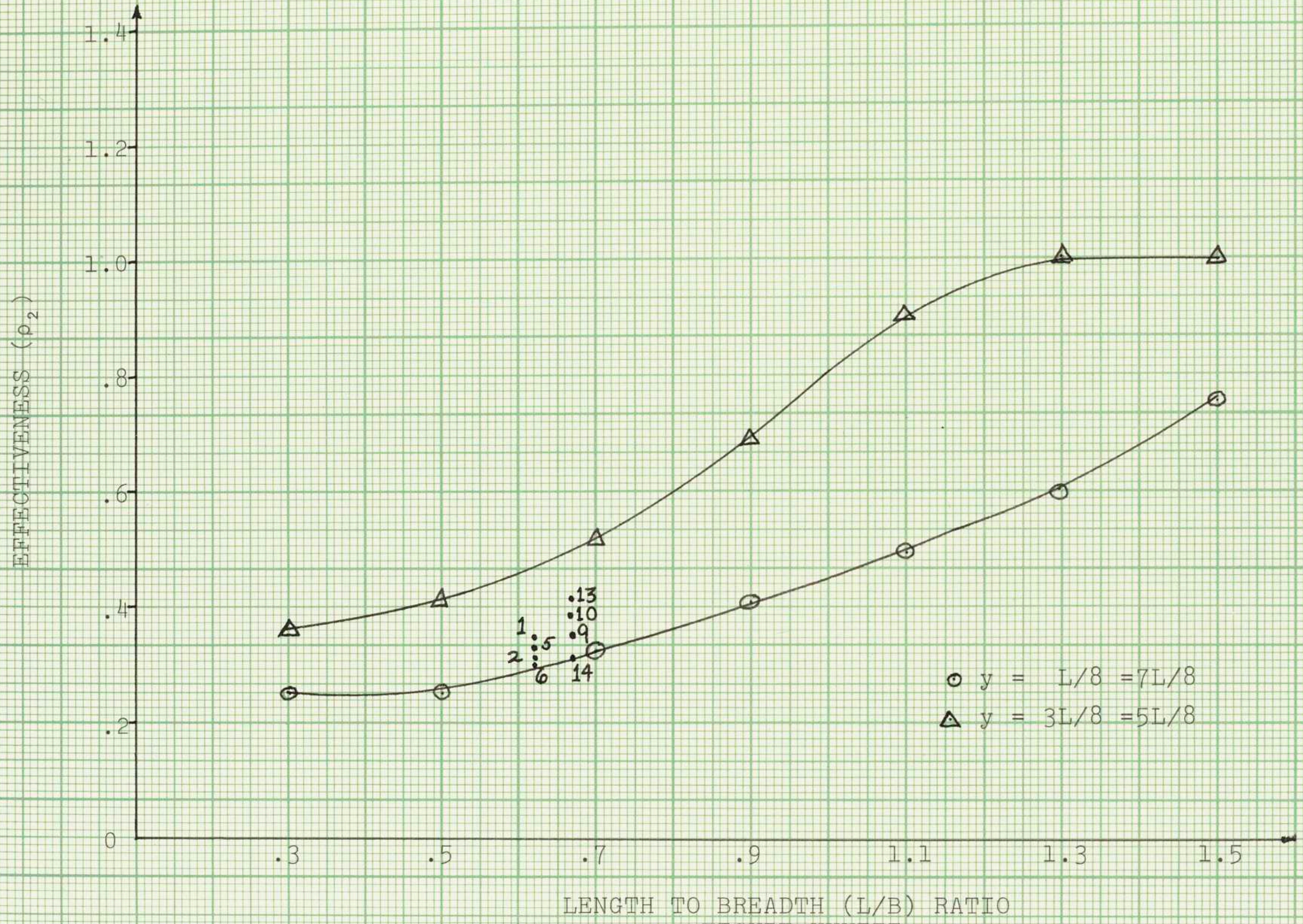

FIGURE XXXIII

EFFECTIVENESS (ρ_2) VS L/B FOR ANTISYMMETRIC BENDING MOMENT + SHEAR

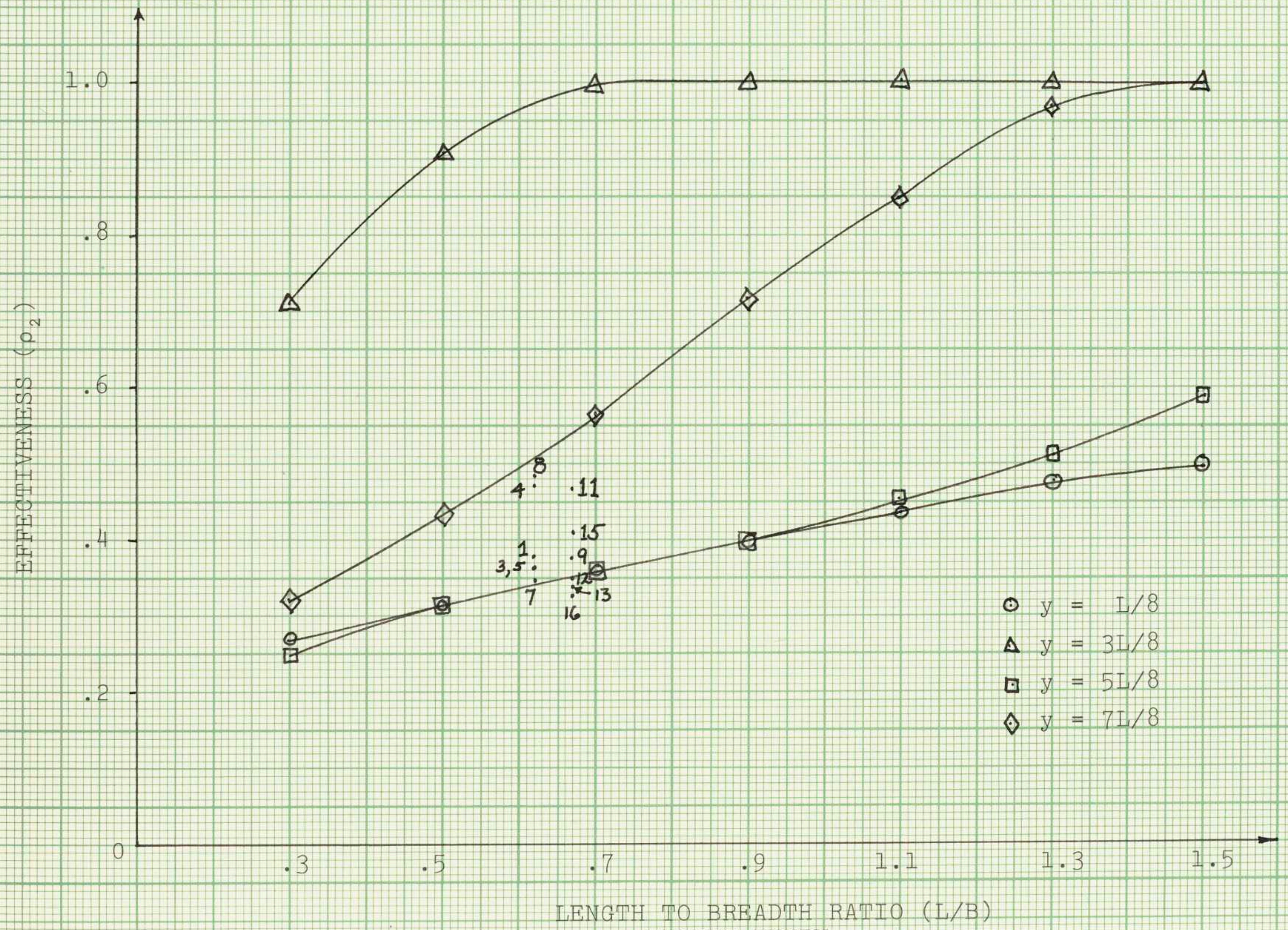

FIGURE XXXIV

EFFECTIVENESS (ρ_2) VS L/B FOR COMBINED CASE

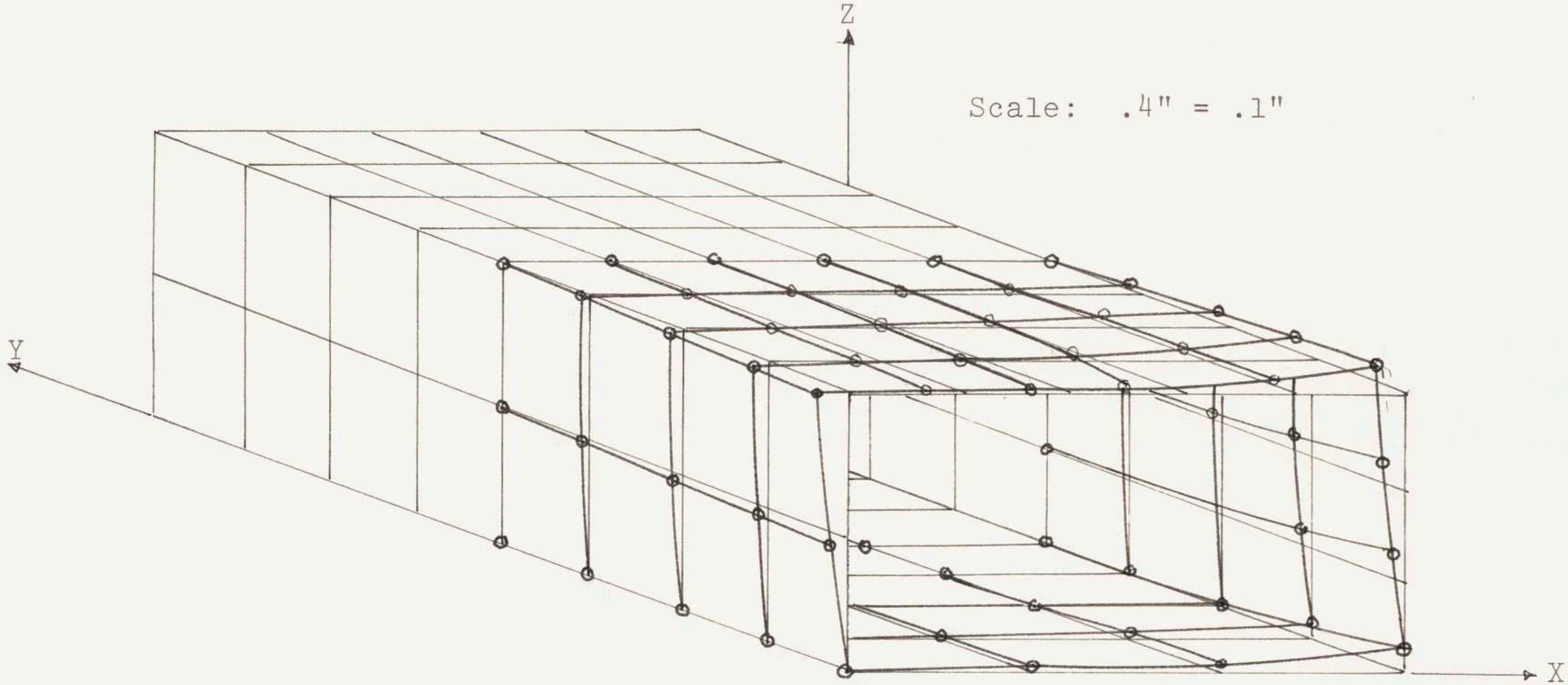

FIGURE XXXV
TORSIONAL MOMENT DISPLACEMENT (1/8 STRUCTURE)

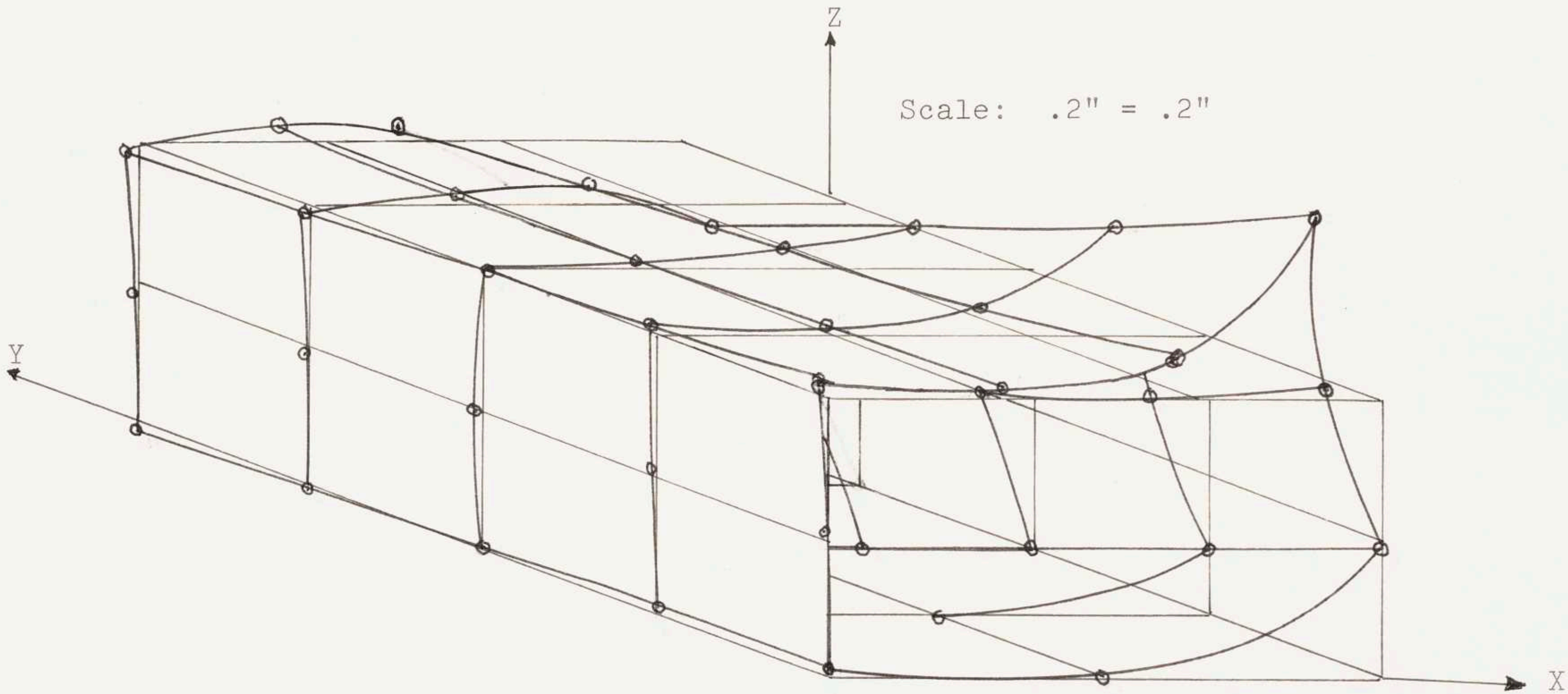

FIGURE XXXVI
ANTISYMMETRIC BENDING MOMENT + SHEAR DISPLACEMENT

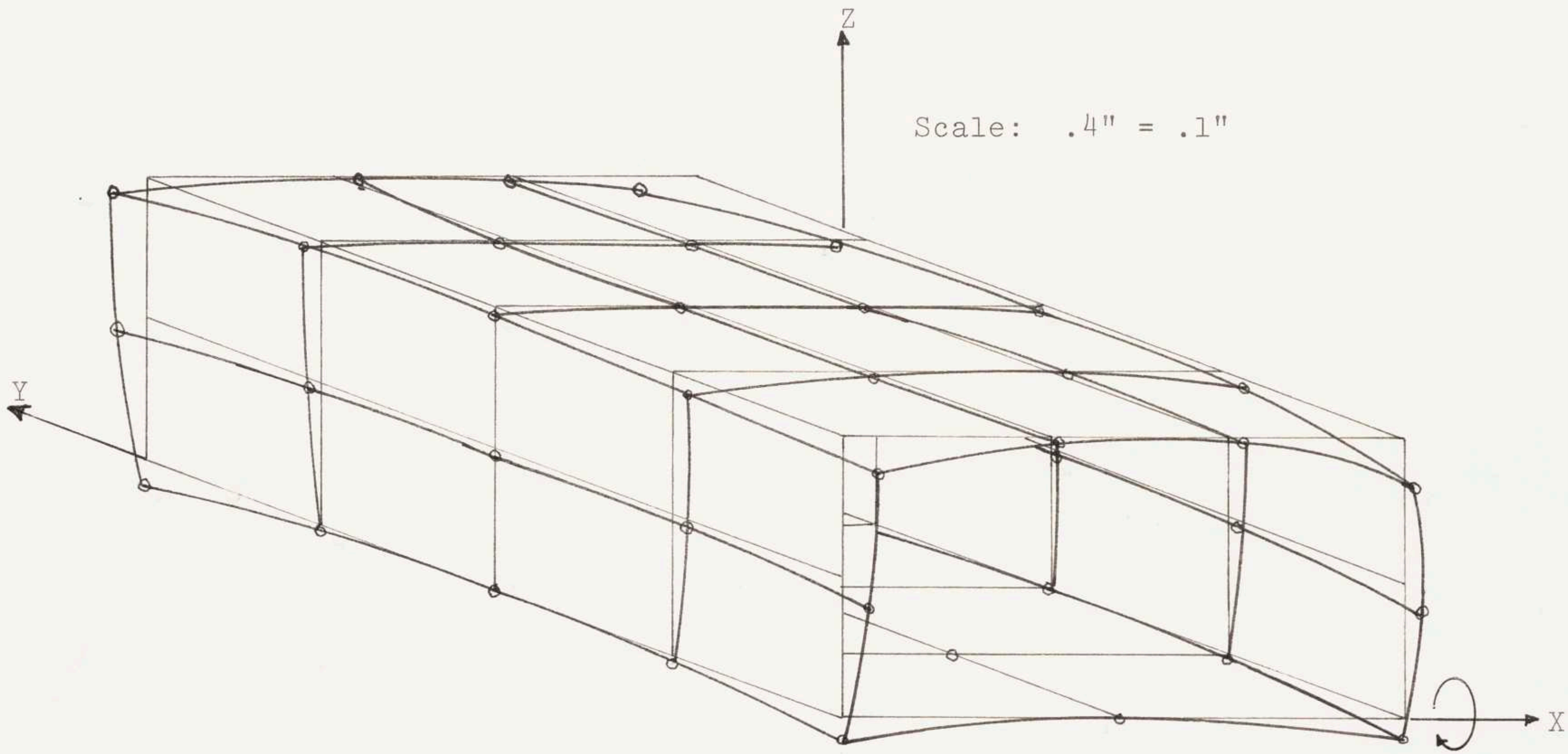

FIGURE XXXVII
SYMMETRIC BENDING MOMENT DISPLACEMENT

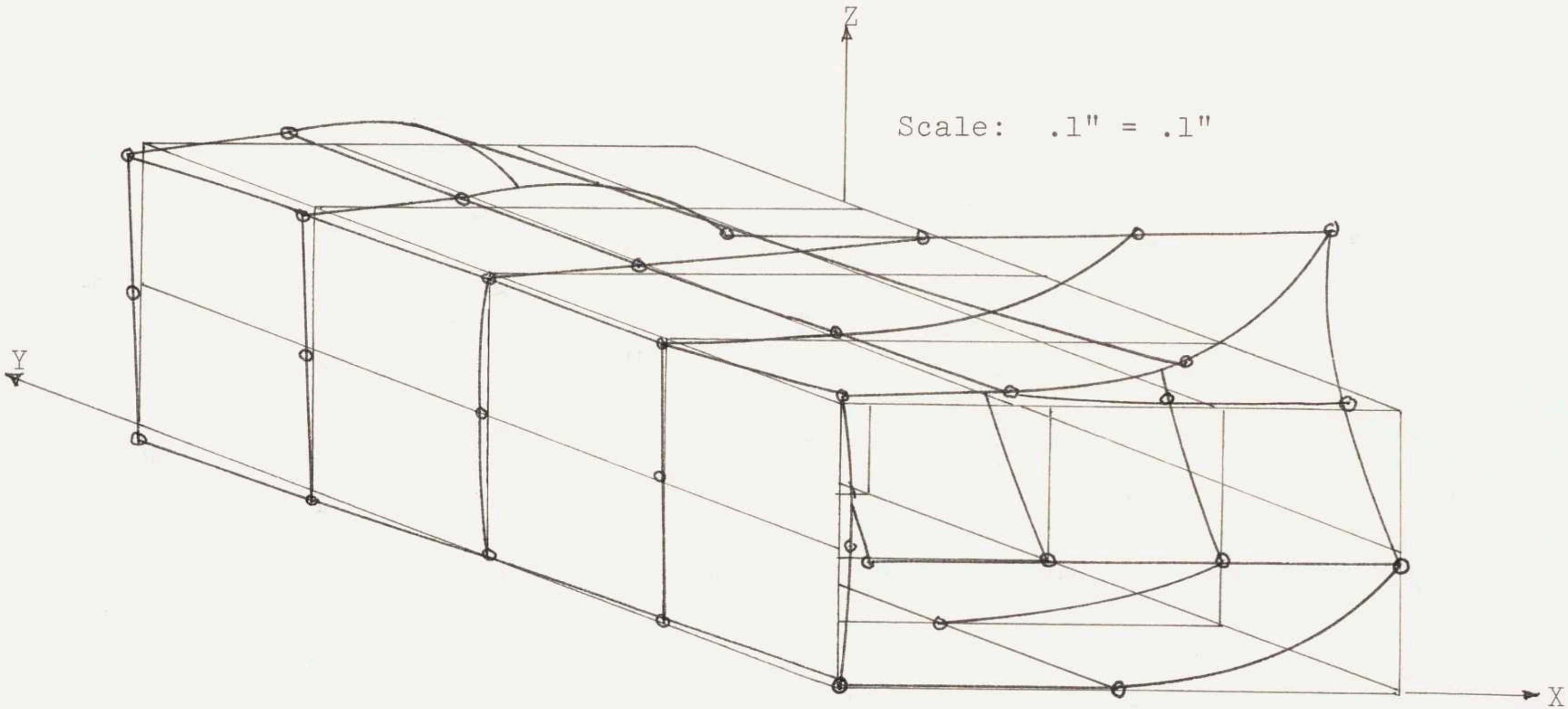

FIGURE XXXVIII
COMBINED LOADING DISPLACEMENT

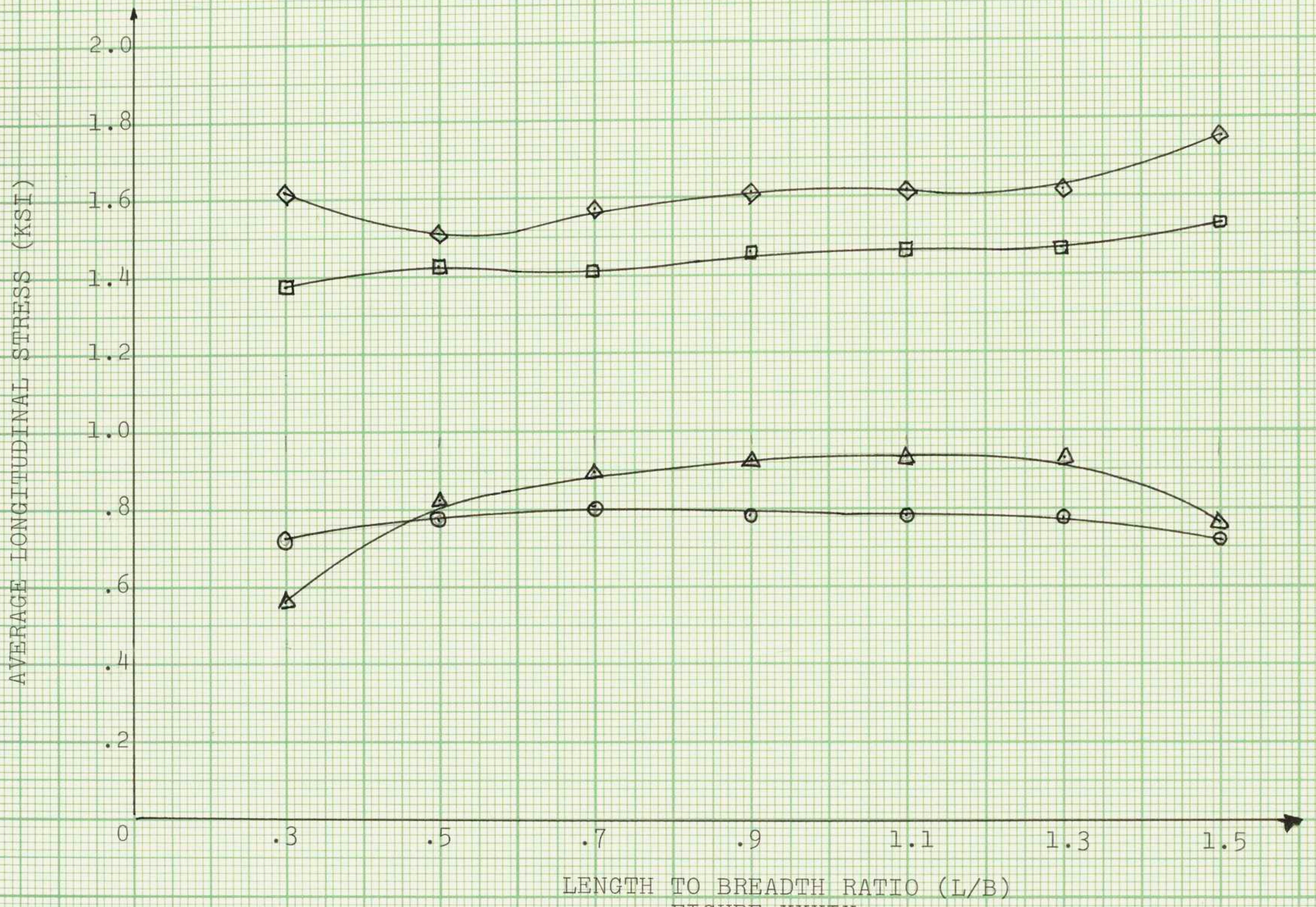

FIGURE XXXIX

AVERAGE STRESS VS L/B FOR THE QUARTER STRUCTURE

TABLE 9

EFFECTIVE BREADTHS OF THE MODEL AND

ACTUAL CROSS STRUCTURES

	Effective Breadth Assoc. With Center Bulkhead		Effective Breadth Assoc. With Side Bulkheads			
	Fwd. Cross Struc.	Aft. Cross Struc.	Fwd. Cross Struc.		Aft. Cross Struc.	
Model						
y=L/8	8.1'	8.45'	8.45'		8.75'	
y=3L/8	13.5'	14.2'	--		--	
y=5L/8	9.75	10.3	12.75		13.6	
y=7L/8	7.05	7.25	8.45		8.75	
ASR-21			Left Blkhd.	Right Blkhd.	Left Blkhd.	Right Blkhd.
y=L/8 Top Plate	8.17	8.53	8.72	9.05	9.61	8.93
Bot. Plate	8.48	8.15	9.57	10.7	10.1	9.31
y=3L/8 Top Plate	17.0	19.3	---		---	
Bot. Plate	20.82	19.97	---		---	
y=5L/8 Top Plate	7.67	11.2	8.29	8.64	11.4	11.2
Bot. Plate	8.07	10.9	9.06	9.74	12.5	11.8
y=7L/8 Top Plate	10.8	7.96	11.4	11.3	9.15	8.5
Bot. Plate	11.05	7.60	12.0	12.0	9.67	8.85

Effective breadth used in the actual ASR-21 design was 4 feet (Ref. 3).

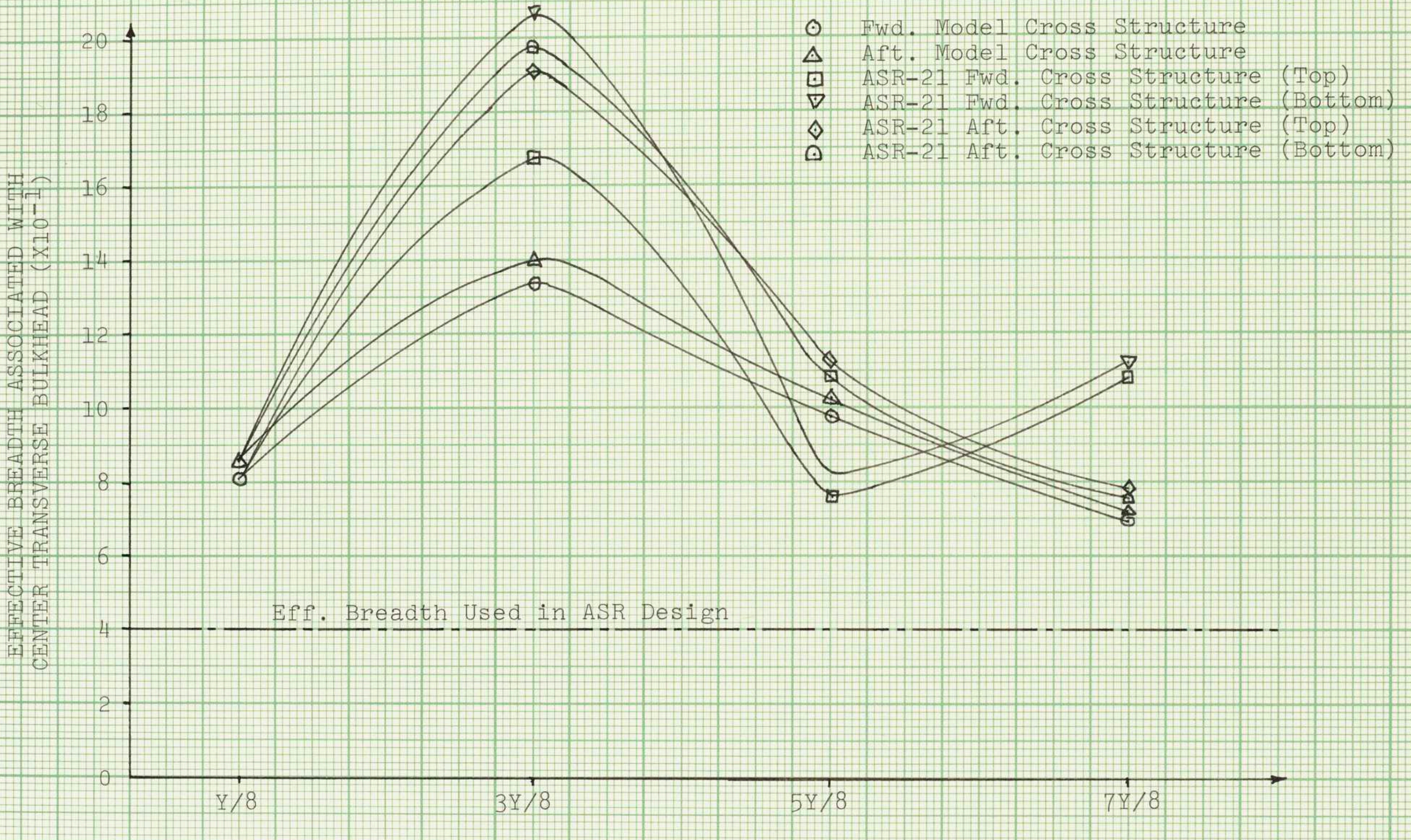

FIGURE XL
EFFECTIVE BREADTH ASSOCIATED WITH CENTER TRANSVERSE BULKHEAD VS LONGITUDINAL POSITION ALONG THE CROSS STRUCTURE

DISCUSSION OF RESULTS

From any finite element program there usually results a large amount of output. This was the case for this thesis, and in order to reduce the extensive volume of this information, sections of this output were either left out or reduced. In particular, the array of displacements that each computer run produced was not included in Appendix C. It was decided that since this thesis concentrated on the stress distribution in the structure, the presentation of the displacements in toto would be unnecessary and unwarranted. To fill this gap Figures XXXV to XXXVIII were included to show qualitatively what effect the separate loadings have on the displacement of the structure. As can be seen in the figures the structure responds as anticipated to a specific type of loading. Also, the stress results for the model contained in Tables C-3 to C-8 are only half of the stress output. Elemental stresses for the near end of the cross structure (y=L/8 and y=3L/8) are included. The stresses for the far end (y=5L/8 and y=7L/8) are omitted. The value of these stresses produced by the symmetric bending moment loading are equal to the stresses of the near end; the stresses for the far end of the beam with antisymmetric bending moment and shear loading are the negative of the stresses of the near end. The torsional moment loading stresses at the far end are also the negative of the near end.

It was mentioned in the effectiveness section part of the Procedure that a parabolic fit to the data was used to extrapolate to the plating edges for the purpose of determining the maximum stresses. The parabolic fit was then used to calculate the average stresses and the effectiveness of the section. The use of the parabolic fit resulted from investigation of the work done by Hildebrand and Reissner on shear lag (Ref. 28) in which they utilized a parabolic distribution of stresses in a box beam. The requirement to use the parabolic distribution was also occasioned by a need to conserve funds. For instance, the addition of two elements to the top plating of the cross structure (x-direction) of Figure VIII results in a computer cost increase of 28.8%. A check was made to determine what effect the use of five instead of three elements would have on the stress levels and consequently the average stress and effectiveness. Figure XLI shows the quarter structure with the added elements, and Figure XLII is a graph of the longitudinal stress level for both the three and five element cases. As can be observed the parabolic fit using three elements is only slightly different, and the difference between the average stresses was 1.8%. Thus, all the results in Tables C-12 to C-14 are based on the parabolic assumption. These results are then reflected in the effectiveness curves Figures XXVIII to XXXIV.

The effectiveness curves were plotted only for B/D=3.0 and A_f/A_w=3.0. The reasons for this result from the calculations summarized in Tables C-12 to C-14. The variation of the effectiveness with respect to the B/D and A_f/A_w ratios is very small, and because of this were not plotted. It must be noted that in the model and actual cross structures at y=3L/8 for all loading cases the longitudinal stress distribution changes significantly in shape as L/B increases. Figures XLIII and XLIV show this. Specifically, in all loading cases there is a point where the edge stress or the second maximum indicated by σ_{max2} in Figure XII drops below the average stress and causes ρ_2 to be greater than 1.0. As L/B increases further the curvature of the stress distribution reverses so that the maximum stresses in the plate occurs nearer the middle of the plate. Thus, for the longitudinal stresses at y=3L/8 a change in the definition of effectiveness as shown in Figure XII must be made. For distributions where the second maximum (σ_{max2}) drops below the average stress the plating is considered to be fully effective (i.e., ρ_2=1.0). For stress distributions where the curvature reverses and the maximum occurs nearer the center, ρ_1 is calculated using this maximum, and ρ_2 is considered equal to 1.0. These changes are reflected in the effectiveness curves plotted on Figures XXVIII to XXXIV. The computer results using the original definition are included in Tables C-12 to C-14 for comparison.

The values of the effectiveness of the actual structures are plotted on Figures XXVIII to XXXIV. Table 8 defines the locations of the effectiveness on the cross structures.

The effectiveness graphs can be very helpful to the designer. Given a cross structural shape and an allowable

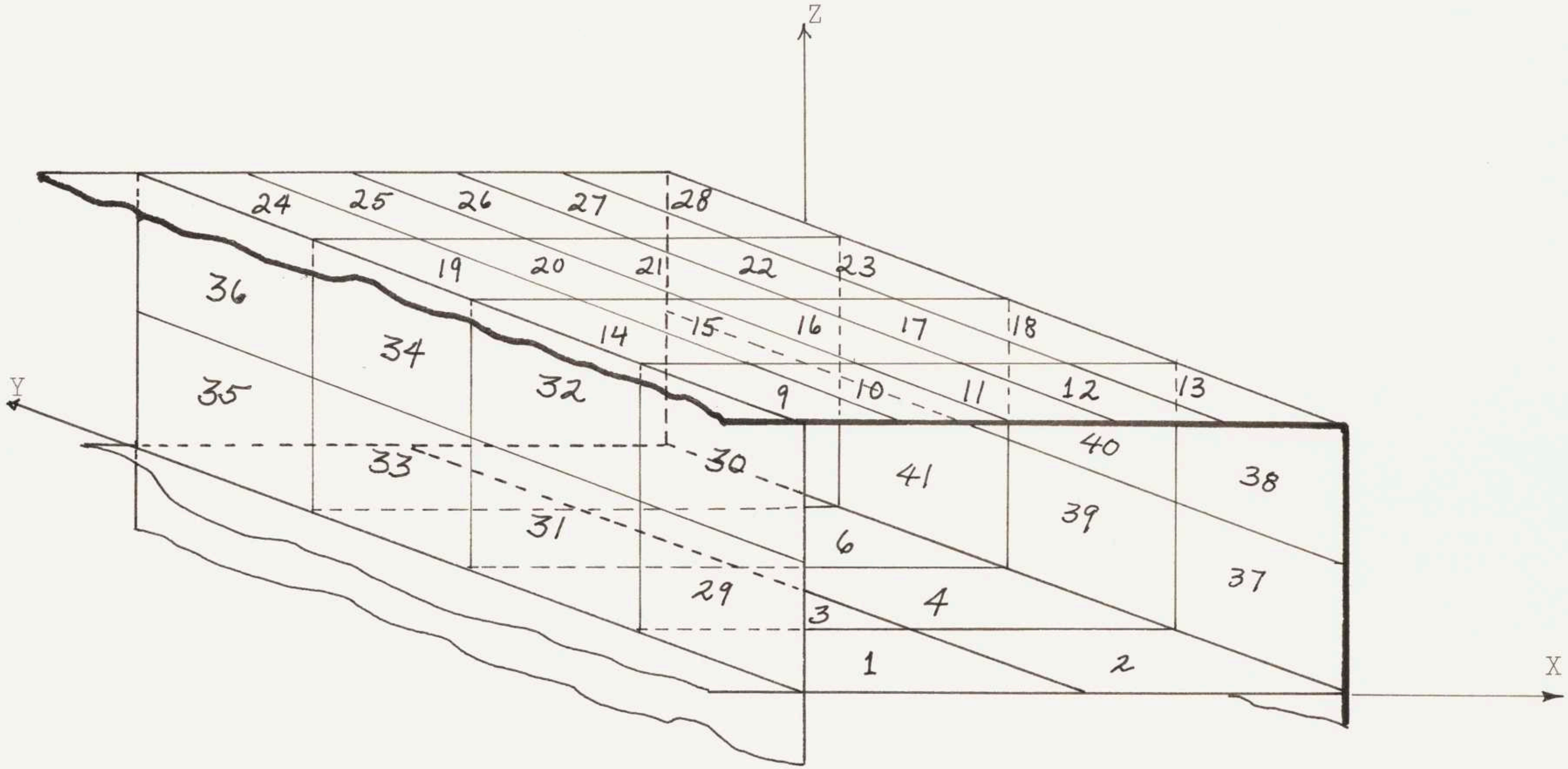

FIGURE XLI
THE FIVE ELEMENT MODEL NUMBERING SEQUENCE

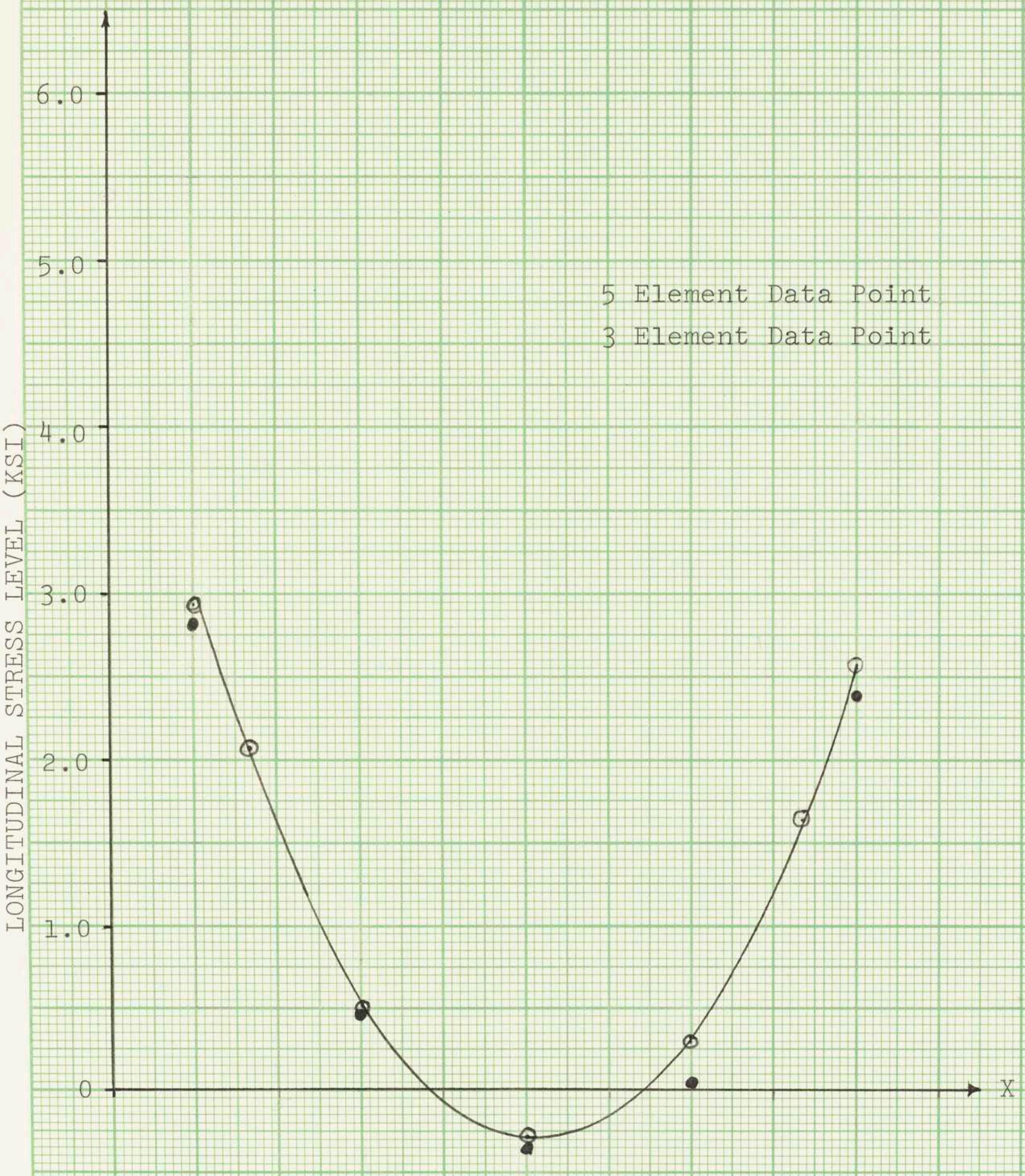

FIGURE XLII
PARABOLIC FIT VERIFICATION

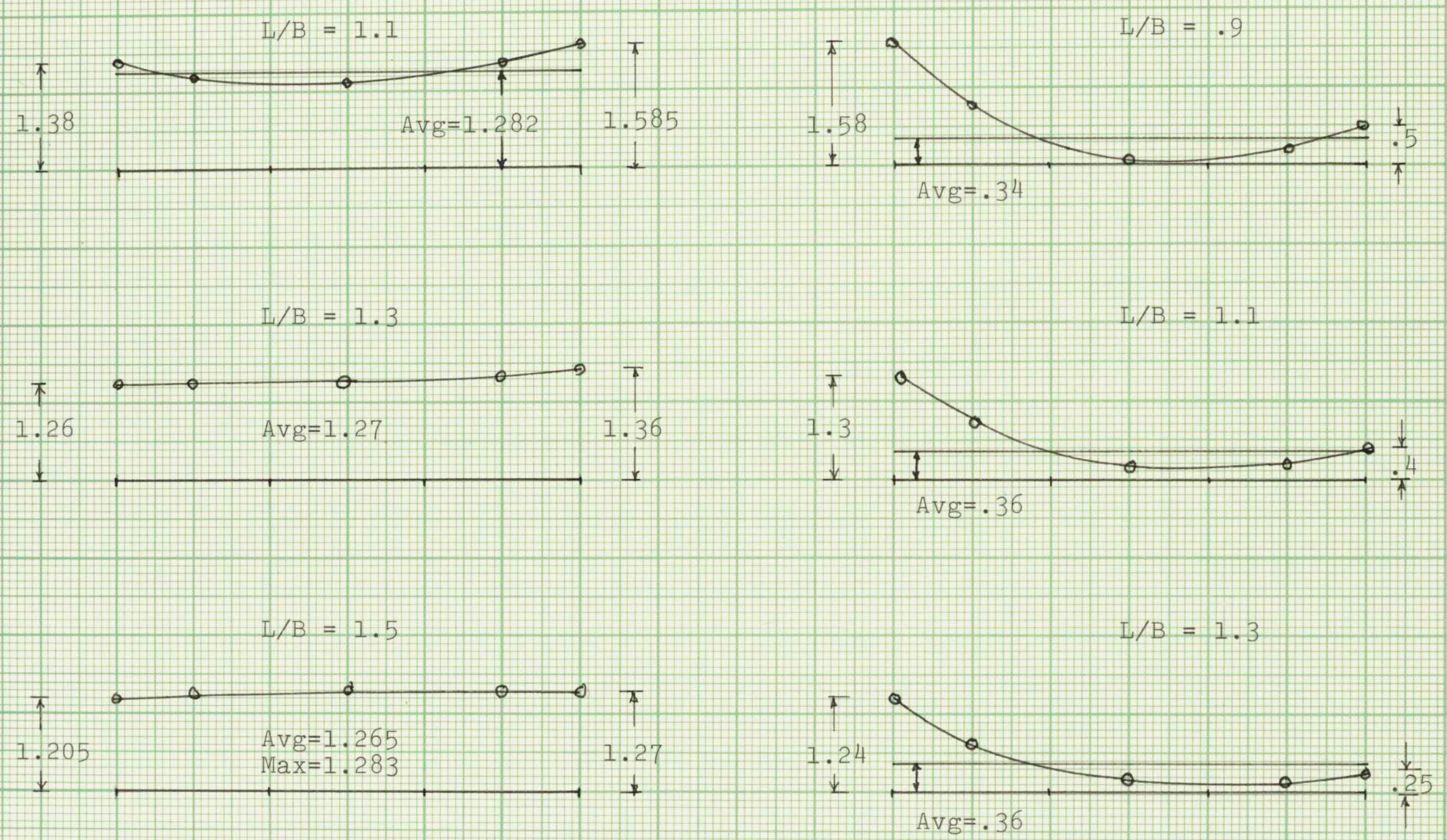

Numbers represent stress level in KSI.

FIGURE XLIII
SYMMETRIC AND ANTISYMMETRIC LONGITUDINAL STRESS DISTRIBUTIONS AT y=3L/8

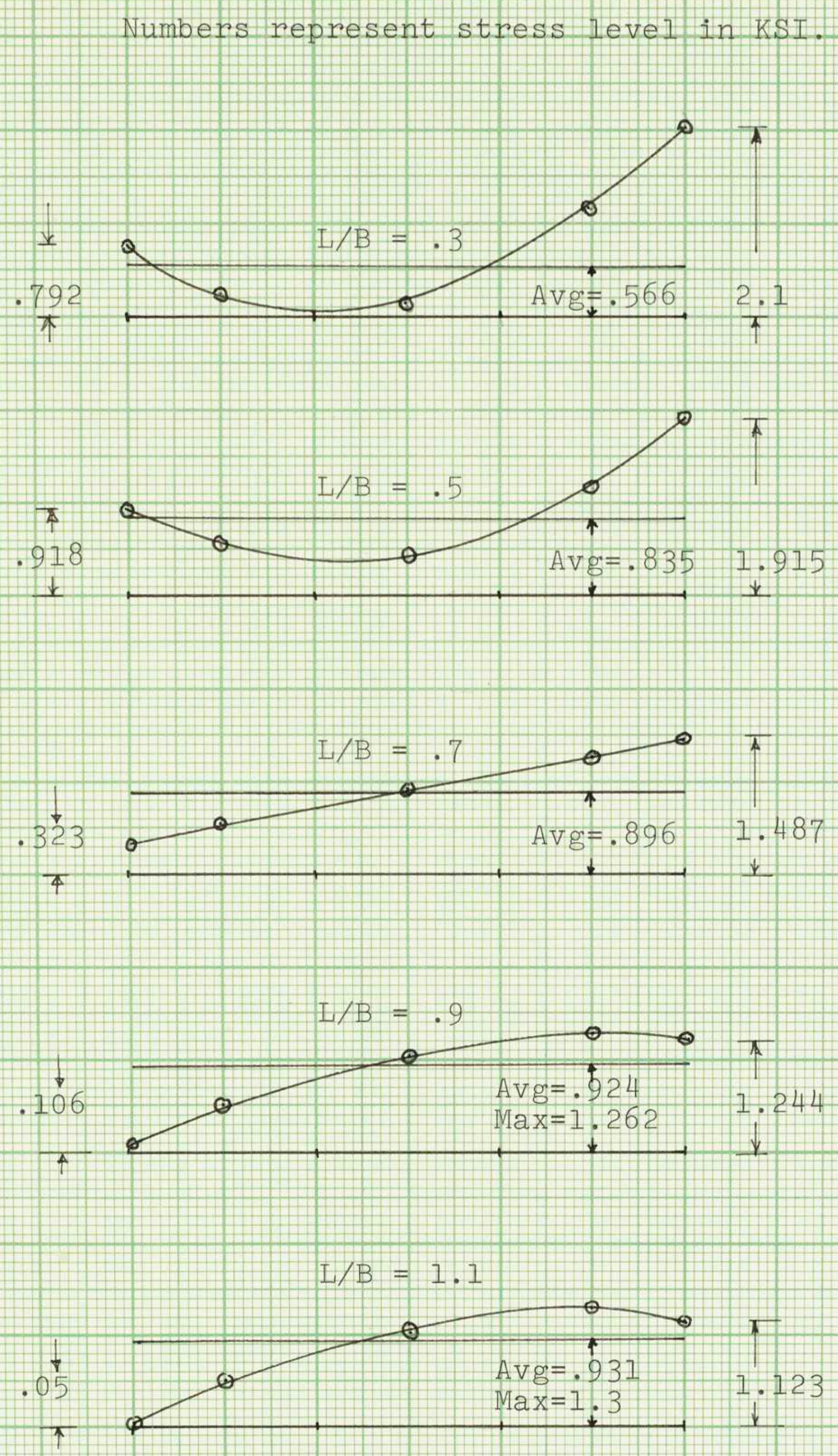

FIGURE XLIV
COMBINED LOAD LONGITUDINAL STRESS
DISTRIBUTIONS AT y=3L/8

average stress permitted for the structure, the designer can predict the maximum stresses in the structure. The apparent lack of dependence upon B/D and A_f/A_w in the ranges studied in this thesis show these curves to be of even greater importance. When varying the plating thicknesses of this structure, however, the designer must observe very carefully his average and maximum stresses. He could very easily have two structures that have the same effectiveness but because of the difference in plating thickness may have one structure that has stresses that exceed a reasonable level.

The torsional results are very interesting. It was found from several computer runs that the shear stresses did not vary along the length of the beam. Instead the shear stress remained constant, as one might predict them from the Bredt Formula (Equation 10) and the appropriate plate thicknesses. Additionally, it was also noted that in Table C-10 the longitudinal and girth stresses produced by the torsional moment were several orders of magnitude smaller than the same stresses produced by the bending moment loadings, and thus did not have any effect on the total longitudinal and girth stresses in the structure. These small values are actually a verification of the theory discussed by Oden (Ref. 20) and Venkatraman and Patel (Ref. 22). As a result of this, the remaining parametric cases were calculated by known analytical methods. (Appendix A and Table C-11).

The longitudinal stress resultants for all the loadings (Tables C-1 through C-4 and C-9, and Figures XIII through XVII) describe quite graphically the shear lag effect. The standard assumption in elasticity that plane sections remain plane is no longer true, and, hence, the simple theory of bending is not applicable. The main cause of the distortion of the cross sections is shear strain in the flange area of the box beams. Considerable effort was expended to relate the longitudinal stress results of this thesis to some applicable shear lag theory. Not only the loading but also the boundary conditions and geometry made the cross structure quite different from the single-celled box beams for which a suitable theory exists. Additional comments on this subject can be found in Appendix B.

All the figures showing the qualitative stress results of the structure are based on the data for L/B=.7, B/D=3.0, and A_f/A_w=3.0. This particular case was the closest model to the actual cross structures.

The average stresses that were calculated show only a small increase in value as A_f/A_w increases for given L/B and B/D ratios. The average stress change is very small for the range of L/B values (Figure XXXIX).

A check was performed on the linearity of the stress response of the structure to a set of scaled loadings, and it was found that the response was linear as expected by theory.

Based on the effectiveness curves and the L/B ratios of the actual cross structures Table 9 and Figure XL were generated to illustrate the effective breadths of plating in the cross structures. These were obtained from the standard definition that the effective breadth is equal to the actual breadth times the effectiveness. Note should be taken that a four-foot effective breadth was utilized by the designers of the ASR-21 Catamaran.

CONCLUSIONS

1. The effect of varying the breadth to depth (B/D) and the flange area to web area (A_f/A_w) ratios over the ranges of this thesis on the plating effectiveness of a structure with a given L/B ratio is negligible. This means that the type of loading, and the length and the breadth of the plating determine the structural plating effectiveness.

2. Average stress in the top plating of the cross structure model varies by only a small amount as L/B increases for given B/D and A_f/A_w ratios, which is simply a substantiation of the simple beam formula.

3. The highest stress level in both the model and the actual cross structures occurs at the plane y=7L/8 and for the combined loading case.

4. The actual ASR-21 Catamaran cross structures in general tend to be higher in effectiveness than the model curves for equal L/B ratios. The length of the ASR cross structures are constrained to 35 feet because of the requirement of the ASR to handle the DSRV, and to reduce the deleterious effect of wave action upon the hydrodynamics of the hulls and the strength of the cross structures. This leads one to conclude that the breadth of the ASR cross structures can be decreased at least to the point where it equals the model curves. The advantage of this would be a decrease in structural weight.

5. The maximum longitudinal web stresses occur in the top of the center web at the location y=7L/8 in the combined load-

ing case.

6. The maximum shear stress occurs at the top of the web and at the edge of the plating at y=L/8.

7. The longitudinal stresses are by far the most predominant stresses in the structure. In all sections of the structure the shear lag effect is graphically visible causing the longitudinal stresses to peak at the web stiffeners of the top and bottom plating. By using the effectiveness curves the designer can calculate the maximum stress in the cross structure flanges and the webs. This is, given a desired average stress for a given structure, the designer can calculate the maximum longitudinal stress in the structure.

8. The forward ASR cross structure has a cut out section at its forward end between the 0-2 and 0-1 levels. The remaining structure from the 0-1 level to the main deck serves very little purpose except to accommodate the interior arrangements of the vessel. Additionally, it carries very little load and adds significantly to the total weight of the structure. Structually the cross structure can do without its forward section, be just as effective and would be much lighter without it.

9. It is significant to note that the A_f/A_W ratio for the catamaran cross structures is nearly two times the same ratio for normal ship girders, which leads one to believe again that the structures are too heavy.

10. The torsional moment produces longitudinal and girth stresses that are orders of magnitude below those produced

by the bending moment and, hence, do not have any appreciable effect on the structure.

11. Existing torsional techniques for computing shear stresses in a closed, multicell, box beam are preferable to calculate these stresses than a finite element solution. Essentially, they are faster and much cheaper to use.

RECOMMENDATIONS

Although this thesis has concentrated on the ASR-21 Catamaran cross structures, the information is applicable to any four-celled box beam cross structure which satisfies the same boundary conditions. However, this thesis is but a small piece of the picture. With new catamaran designs being conceived for both military and industrial uses that will have both higher L/B ratios and different cross structural shapes the need exists for more detailed and expanded studies to be conducted. An effort should be made to examine these new designs in much the same manner, and possibly try to optimize the size, shape and weight of the cross structure.

A satisfactory analytical stress solution for a doubly symmetric four-celled box beam should be developed utilizing the stress function approach as used by Hildebrand (Ref. 29).

APPENDICES

APPENDIX A

ANALYTICAL TORSIONAL ANALYSIS

The analysis of a four-celled box beam subjected to a torsional moment has many facets which could lead to problems in handling the analytical solution of its loading. Some basic assumptions must then be made to extend existing methods of torsional analysis to the catamaran cross structure. It is assumed that a uniform shear stress exists across the thickness of the web and flanges of the cross structure. Additionally, shear stresses are assumed to be directed tangent to the boundary curve of the box beam. Normal stresses are assumed to be negligible. The product of the shear stress (σ_{xy}) and the plate thickness (t) is constant at all points along the perimeter of a cell. Finally, it is assumed that there is no in plane distortion so that the angle of twist (θ) of cell (i) is identically equal to the angle of twist of cell (i+1) and so forth. (ie. $\theta_i=\theta_{i+1}\ldots=\theta_n$).

For the general four-celled box beam pictured in Figure A-1 the equation of equilibrium (equation 1) relates the twisting moment to the shear flows.

$$M_t = 2\sum_{j=1}^{4} q_j A_j \qquad (1)$$

q_j = shear flow in cell j

A_j = area enclosed by the perimeter of a cell

M_t = the applied twisting moment

The rate of twist for a cell (j) is indicated by equation (2).

$$\theta_j = \frac{q_j}{2GA_j} \oint_{s_j} \frac{ds}{t} \qquad (2)$$

t = thickness of the boundary

ds = an incremental distance along the perimeter

For the case represented by Figure (A-1) where adjacent cells and in particular the neighboring boundary affect the total twist, the shear flows in these adjacent cells must be taken into consideration. Applying equation (2) around the boundary of a cell (j), results in equation (3).

$$2GA_j\,\theta = \left(q_j \oint_{s_j} \frac{ds}{t} - q_i \int_{s_{ji}} \frac{ds}{t} - q_k \int_{s_{jk}} \frac{ds}{t}\right) \qquad (3)$$

For simplification in this Appendix the following definitions are utilized.

$$\delta_{ji} = -\frac{1}{G} \int_{s_{ji}} \frac{ds}{t} \qquad (4a)$$

$$\delta_{jk} = -\frac{1}{G} \int_{s_{jk}} \frac{ds}{t}$$

$$\delta_{jj} = \frac{1}{G} \oint_{s_j} \frac{ds}{t} \qquad (4b, c)$$

Thus equation (3) can be rewritten as

$$\theta = \frac{1}{2A_j} \left(q_j\,\delta_{jj} + q_i\,\delta_{ji} + q_k \delta_{jk}\right) \qquad (5)$$

If equation (5) is now applied to each cell of the four-celled box beam, four equations with four unknowns (i_{q_j}, j=1, 2, 3, 4) will be generated.

$$\begin{aligned} \delta_{11}q_1+\delta_{12}q_2+\delta_{13}q_3 - 2A_1\theta &= 0 \\ \delta_{21}q_1+\delta_{22}q_2+\delta_{23}q_4 - 2A_2\theta &= 0 \\ \delta_{31}q_1+\delta_{34}q_4+\delta_{33}q_3 - 2A_3\theta &= 0 \\ \delta_{42}q_2+\delta_{43}q_3+\delta_{44}q_4 - 2A_4\theta &= 0 \end{aligned} \qquad (6a\text{-}d)$$

Equation (6) can be much more clearly expressed as a matrix equation (7). Note the coefficient matrix $\underset{\sim}{\nabla}$ is symmetric with $\delta_{ji} = \delta_{ij}$.

$$\begin{bmatrix} \delta_{11} & \delta_{12} & \delta_{13} & 0 \\ \delta_{21} & \delta_{22} & 0 & \delta_{24} \\ \delta_{31} & 0 & \delta_{33} & \delta_{34} \\ 0 & \delta_{42} & \delta_{43} & \delta_{44} \end{bmatrix} \begin{bmatrix} q_1 \\ q_2 \\ q_3 \\ q_4 \end{bmatrix} = 2^{\theta} \begin{bmatrix} A_1 \\ A_2 \\ A_3 \\ A_4 \end{bmatrix} \qquad (7)$$

$$\underset{\sim}{\nabla} \quad \underset{\sim}{Q} = 2\theta \quad \underset{\sim}{A} \qquad (8)$$

Utilizing the generalized dimensions of Figure (A-1) in equations 4a-c, and substituting them into the matrix $\underset{\sim}{\nabla}$ gives the generalized $\underset{\sim}{\nabla}^{1}$ (Equation 9) which can be augmented with $2\theta\underset{\sim}{A}$ to solve for the q_j.

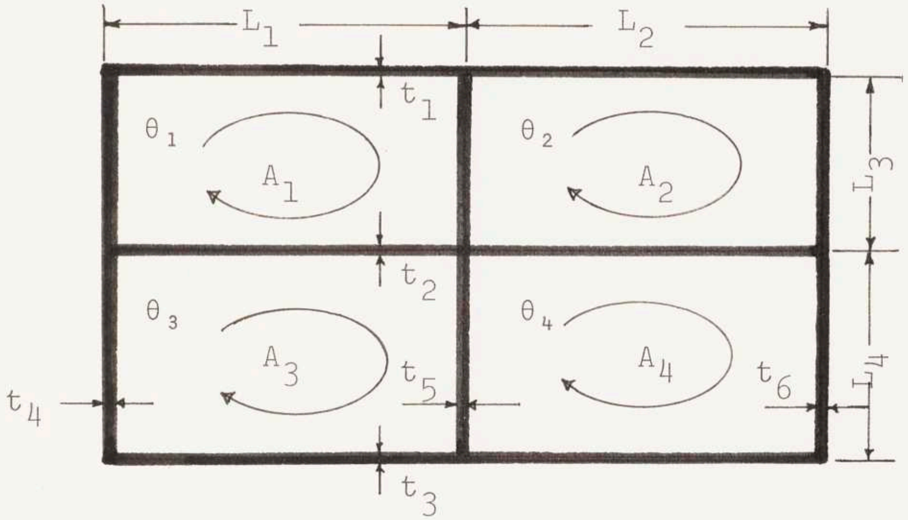

FIGURE A-I
CROSS SECTION OF FOUR-CELLED BOX BEAM

Equation (9)

$$
\underset{\sim}{\nabla}^{1} = \frac{1}{G}
\begin{bmatrix}
L_1\left(\frac{t_2 \;\; t_1}{t_1 \; t_2}\right) + L_3\left(\frac{t_5 + t_4}{t_4 \; t_5}\right) & -L_3\left(\frac{1}{t_5}\right) & -L_1\left(\frac{1}{t_2}\right) & 0 \\
-L_3\left(\frac{1}{t_5}\right) & L_2\left(\frac{t_2 + t_1}{t_1 \; t_2}\right) + L_3\left(\frac{t_6 + t_5}{t_5 \; t_6}\right) & 0 & -L_2\left(\frac{1}{t_2}\right) \\
-L_1\left(\frac{1}{t_2}\right) & 0 & L_1\left(\frac{t_3 + t_2}{t_3 \; t_2}\right) + L_4\left(\frac{t_5 + t_4}{t_4 \; t_5}\right) & -L_4\left(\frac{1}{t_5}\right) \\
0 & -L_2\left(\frac{1}{t_2}\right) & -L_4\left(\frac{1}{t_5}\right) & L_2\left(\frac{t_3 + t_2}{t_3 \; t_2}\right) + L_4\left(\frac{t_6 + t_5}{t_5 \; t_6}\right)
\end{bmatrix}
$$

Therefore, given a twisting moment and solving for the shear flows in equation (7) as functions of G and θ then the quantity Gθ can be determined by substituting into equation (1). The shear stresses can be calculated by dividing the shear flow by the appropriate thickness.

$$q_j = f_j(G\theta) \qquad (10)$$

$$M_t = 2\sum_{j=1}^{4} q_j A_j = 2\sum_{j=1}^{4} f_j(G\theta)\, A_j \qquad (11)$$

$$\sigma_{x_z} = \frac{q_j}{t_i} \qquad \begin{matrix} j = 1,4 \\ i = 1,6 \end{matrix} \qquad (12)$$

The calculations in Table C-XI were performed for the representative cases analyzed in this thesis. Because computer tests of the torsional loading (Table C-X) showed that the only stresses of importance in the structure could be obtained by the simple analytical method outlined above, the calculations in Table C-XI were done in lieu of additional computer runs for the Torsional Loading.

APPENDIX B

COMMENTS ON RELATING THE COMPUTER RESULTS TO EXISTING THEORY

In attempting to verify the computer results of this thesis by existing theory a significant effort was made to determine the applicable theory. Attempts at correlating both the stresses and the effectivenesses obtained from the computer results with theory proved futile. The major reasons for this are varied, but essentially all result from the fact that the catamaran cross structural shape has not been analyzed for the application of end bending moments. Sufficient theory exists to calculate the effects of torsional moments (Appendix A) and shear in the webs (Ref. 20). In addition to the geometrical shape differences, loading and boundary conditions vary significantly from existing box beam or box girder analyses.

Lankford (Ref. 3) and Dinsenbacher (Ref. 4) assumed "the cross structure bulkheads to be fixed ended beams undergoing a settlement of supports." Applying boundary conditions for a closed solution to "a settlement of supports" might be very difficult. The versatility of the finite element method allows one to solve problems with multiple degrees of indeterminancy and theoretically impossible boundary conditions. This makes the analysis of the cross structures relatively easy with the finite element method, and rather difficult to check in cases where a theoretical solution is only an approximation, or does not even exist.

When the first computer results were checked, it was obvious that some shear lag analysis must be used to verify the results. The extensive works on shear lag by Reissner (Refs. 23 and 24), Reissner and Hildebrand (Ref. 28), Hildebrand (Ref. 29), Kuhn (Refs. 25, 26 and 27), Smith (Ref. 34), and Yuille (Ref. 32) dealt principally with two types of structures, the box beam and stiffened plating.

Hildebrand and Reissner assumed a parabolic distribution of longitudinal stresses in the box beam in which the shear lag causes the stresses to vary around the stresses obtained by the standard beam formula (My/I). The analysis was done for single-cell box beams that were cantilevered, completely built-in, and simply supported. Some of the loading conditions that they examined were uniform lateral pressure and concentrated lateral loads. Hildebrand repeated many of the same boundary conditions and loadings for the identical geometry, but approached the shear lag solution by the use of an infinite series stress function whose variables were the geometric and material properties of the beams. Since neither of these two approaches could satisfy either the geometry of the four-celled box beam or the proper loading, it was not possible to use them.

Kuhn and others considered only the cantilevered box beam case with end moments and concentrated forces acting at the tip through the webs. Kuhn's interest was strictly the aircraft wing in all its geometric variations, and while interesting to read his results were not helpful to the analysis of the four-celled cross structure.

If one removes the top plate from the cross structure, and considers it as stiffened plating, it might very well be possible to compare the shear lag in this case to the shear lag for the cross structure. Smith and Yuille performed shear lag analysis on multiply stiffened plating. However, the only loads examined are uniform, concentrated, and sinusoidal loads in the plane of the plating which are highly applicable to the bottom plating of ships, but not to the cross structure. One of the difficult problems in solving the plating problem with edge loads in both flanges and webs is the difficulty encountered in convergence of the infinite series solution for this type of loading.

Schade (Refs. 12 and 13), Mansour (Ref. 11), Winter (Ref. 35) and Reissner (Ref. 24) either discuss or present curves of effectiveness (or as Reissner calls it "efficiency") and effective breadth. It was thought that a comparison might be made with some of their results. The problems of comparison are many. The effective breadth as defined by Schade is for lateral loads which cause the plate or panel to bend out of its original plane, and for which all of Schade's work was performed. This type of analysis is again very dependent upon loading. Neither Schade nor Mansour examined the loading of this thesis.

Various expressions exist for determining effective breadth of plating and beam flanges. The most common are listed below:

Reissner:

$$b_{eff} = b(1/3 \quad 2/3(\frac{\text{Stress at Plate Center}}{\text{Stress at Plate Edge}})$$

b_{eff}= Effective breadth

b= One half the plate breadth (from stiffener to midpoint)

Winter:

$$b_{eff} = \frac{\int_0^b (\text{stress})\, dy}{\text{Max Stress}} = \frac{\sigma avg}{\sigma max}$$

TABLE C-I

ACTUAL AFTER CATAMARAN CROSS STRUCTURE STRESSES (KSI)

SYMM. BEND. MOM.

Element	Girth Stress	Longitudinal Stress	Shear Stress
1	.00076	-.0109	-.0115
2	-.00338	-.0214	-.0047
3	-.00338	-.0214	.0047
4	.0076	-.0109	.0115
5	.00437	-.0097	.006
6	-.0700	-.0214	.00191
7	-.0700	-.0214	-.00191
8	.00437	-.0097	-.006
9	.0466	.5312	.3396
10	-.00399	.4632	.1061
11	-.00399	.4632	-.1061
12	.0466	.5312	-.3396
13	-.1418	.0173	.0623
14	.1845	.298	.0454
15	.1845	.298	-.0454
16	-.1418	.0173	-.0623
17	-.0862	.4658	-.1812
18	.1288	.4971	-.0672
19	.1288	.4971	.0672
20	-.0862	.4658	.1812
21	-.0928	-.832	-.516
22	.01778	-.7115	-.1578
23	.01778	-.7115	.1578

TABLE C-I (Cont'd.)

ACTUAL AFTER CATAMARAN CROSS STRUCTURE STRESSES (KSI)

SYMM. BEND. MOM.

Element	Girth Stress	Longitudinal Stress	Shear Stress
24	-.0928	-.832	.516
25	.1919	-.024	-.088
26	-.267	-.4399	-.0722
27	-.267	-.4399	.0722
28	.1919	-.024	.088
29	.1185	-.6483	.2516
30	-.1936	-.6702	.0839
31	-.1936	-.6702	-.0839
32	.1185	-.6483	-.2516
33	.00079	-.9948	.0100
34	-.00277	-.0189	.00434
35	-.00277	-.0189	-.00434
36	.00079	-.9948	-.0100
37	.00418	-.00757	-.00533
38	-.00616	-.0169	-.0019
39	-.00616	-.0169	.0019
40	.00418	-.00757	.00533
41	.0422	.5048	-.2996
42	-.0178	.4181	-.1047
43	-.0178	.4181	.1047
44	.0422	.5048	.2996
45	-.1492	-.03095	-.0501
46	.1736	.2069	-.0415

TABLE C-I (Cont'd.)

ACTUAL AFTER CATAMARAN CROSS STRUCTURE STRESSES (KSI)

SYMM. BEND. MOM.

Element	Girth Stress	Longitudinal Stress	Shear Stress
47	.1736	.2069	.0415
48	-.1492	-.03095	.0501
49	-.0879	.4294	.1605
50	.1124	.4548	.07408
51	.1124	.4548	-.07408
52	-.0879	.4294	-.1605
53	-.0871	-.792	.4538
54	-.0376	-.6467	.153
55	-.0376	-.6467	-.153
56	-.0871	-.792	-.4538
57	.1964	.0456	.631
58	-.246	-.303	.06308
59	-.246	-.303	-.06308
60	.1964	.0456	-.631
61	.166	-.5692	-.2143
62	-.1656	-.5769	-.0909
63	-.1656	-.5769	.0909
64	.166	-.5692	.2143
65	.1273	.5852	-.2197
66	-.09348	.1702	-.0498
67	-.09348	.1702	.0498
68	.1273	.5852	.2197
69	.0995	1.078	.3407

TABLE C-I (Cont'd.)

ACTUAL AFTER CATAMARAN CROSS STRUCTURE STRESSES (KSI)

SYMM. BEND. MOM.

Element	Girth Stress	Longitudinal Stress	Shear Stress
70	-.0651	.5261	.1121
71	-.0651	.5261	-.1121
72	.0995	1.078	-.3407
73	.0478	.3076	-.0421
74	-.0068	.1727	-.0216
75	-.0068	.1727	.0216
76	.0478	.3076	.0421
77	.03223	.7711	.1133
78	.0088	.5441	.0570
79	.0088	.5441	-.0570
80	.03223	.7711	-.1133
81	.0298	.2563	-.0120
82	.01221	.177	-.0159
83	.01221	.177	.0159
84	.0298	.2563	.0120
85	.0177	.7047	.0673
86	.0243	.5549	.04314
87	.0243	.5549	-.04314
88	.0177	.7047	-.0673
89	-.0851	-.6247	-.2897
90	-.03013	-.3382	-.10142
91	-.03013	-.3382	.10142
92	-.0851	-.6247	.2897

TABLE C-I (Cont'd.)

ACTUAL AFTER CATAMARAN CROSS STRUCTURE STRESSES (KSI)

SYMM. BEND. MOM.

Element	Girth Stress	Longitudinal Stress	Shear Stress
93	-.055	-1.398	.1787
94	.01636	-.812	.03912
95	.01636	-.812	-.03912
96	-.055	-1.398	-.1787
97	.0237	-.3436	-.0777
98	-.07102	-.29579	-.0504
99	-.07102	-.29579	.0504
100	.0237	-.3436	.0777
101	-.00432	-.9798	.0065
102	-.043	-.7345	.01498
103	-.043	-.7345	-.01498
104	-.00432	-.9798	-.0065
105	.0262	-.2876	-.0381
106	-.0741	-.2794	-.0379
107	-.0741	-.2794	.0379
108	.0262	-.2876	.0381
109	.0044	-.8725	-.0171
110	-.0523	-.7088	.0108
111	-.0523	-.7088	-.0108
112	.0044	-.8725	.0171

TABLE C-I

ACTUAL AFTER CATAMARAN CROSS STRUCTURE STRESSES (KSI)

ANTISYMM. B.M. + SHEAR

Element	Girth Stress	Longitudinal Stress	Shear Stress
1	.00148	.00509	.00506
2	.0039	.0141	-.00298
3	-.0039	-.0141	-.00298
4	-.00148	-.00509	.00506
5	-.00015	.0038	-.0018
6	.00489	.0119	.00392
7	-.00489	-.0119	.00392
8	.00015	-.0038	-.0018
9	-.0319	-.2054	-.1049
10	-.03845	-.2812	.0738
11	.03845	.2812	.0738
12	.0319	.2054	-.1049
13	-.0149	.00796	-.0199
14	-.0701	.0331	-.0111
15	.0701	-.0331	-.0111
16	.0149	-.00796	-.0199
17	.00742	-.1738	.0387
18	-.0783	-.2633	-.0698
19	.0783	.2633	-.0698
20	-.00742	.1738	.0387
21	.0616	.3147	.157
22	.0554	.4045	-.1014
23	-.0554	-.4045	-.1014

TABLE C-I (Cont'd.)

ACTUAL AFTER CATAMARAN CROSS STRUCTURE STRESSES (KSI)

ANTISYMM. B.M. + SHEAR

Element	Girth Stress	Longitudinal Stress	Shear Stress
24	-.0616	-.3147	.157[illegible]
25	.03017	-.0128	.0278
26	.1007	-.0416	.0281
27	-.1007	.0416	.0281
28	-.03017	.0128	.0278
29	-.0052	.2342	-.0472
30	.1039	.3388	.1033
31	-.1039	-.3388	.1033
32	.0052	-.2342	-.0472
33	.00147	.0046	-.00417
34	.00375	.0139	.00239
35	-.00375	-.0139	.00239
36	-.00147	-.0046	-.00417
37	.00010	.00273	.00142
38	.00397	.00875	-.00319
39	-.00397	-.00875	-.00319
40	-.00010	-.00273	.00142
41	-.0319	-.1962	.0884
42	-.03769	-.2717	-.0617
43	.03769	.2717	-.0617
44	.0319	.1962	.0884
45	-.0173	.0253	.0137
46	-.0583	.0530	.0129

TABLE C-I (Cont'd.)

ACTUAL AFTER CATAMARAN CROSS STRUCTURE STRESSES (KSI)

ANTISYMM. B.M. + SHEAR

Element	Girth Stress	Longitudinal Stress	Shear Stress
47	.0583	-.0530	.0129
48	.0173	-.0253	.0137
49	.00528	-.1601	-.0283
50	-.0704	-.2422	.0550
51	.0704	.2422	.0550
52	-.00528	.1601	-.0283
53	.06141	.301	-.1333
54	.0549	.3906	.0852
55	-.0549	-.3906	.0852
56	-.06141	-.301	-.1333
57	.0335	-.03649	-.0167
58	.0832	.0678	-.03215
59	-.0832	-.0678	-.03215
60	-.0335	.03649	-.0167
61	-.0018	.2053	.0317
62	.0889	.298	-.0797
63	-.0889	-.298	-.0797
64	.0018	-.2053	.0317
65	-.0553	-.2187	-.1345
66	.0281	-.0346	-.1272
67	-.0281	.0346	-.1272
68	.0553	.2187	-.1345
69	-.02605	-.4149	-.2774
70	-.2067	-.3608	-.2664

TABLE C-I (Cont'd.)

ACTUAL AFTER CATAMARAN CROSS STRUCTURE STRESSES (KSI)

ANTISYMM. B.M. + SHEAR

Element	Girth Stress	Longitudinal Stress	Shear Stress
71	.0267	.3608	-.2664
72	.02605	.4149	-.2774
73	-.02736	-.1227	-.0837
74	.00131	-.0294	-.0285
75	-.00131	.0294	-.0285
76	.02736	.1227	-.0837
77	-.0104	-.3057	-.0988
78	-.04549	-.3333	-.1436
79	.04549	.3333	-.1436
80	.0104	.3057	-.0988
81	-.0185	-.10333	-.07836
82	-.00455	-.02949	-.0176
83	.00455	.02949	-.0176
84	.0185	.10333	-.07836
85	-.00068	-.2799	-.07236
86	-.0489	-.3184	-.125
87	.0489	.3184	-.125
88	.00068	.2799	-.07236
89	-.00014	.2407	-.1017
90	.0216	.1015	-.0605
91	-.0216	-.1015	-.0605
92	.00014	-.2407	-.1017

TABLE C-I (Cont'd.)

ACTUAL AFTER CATAMARAN CROSS STRUCTURE STRESSES (KSI)

ANTISYMM. B.M. + SHEAR

Element	Girth Stress	Longitudinal Stress	Shear Stress
93	.0030	.5415	-.1925
94	.0671	.5112	-.2518
95	-.0671	-.5112	-.2518
96	-.0030	-.5415	-.1925
97	-.0037	.141	-.0698
98	-.0306	.08224	.0111
99	.0306	-.08224	.0111
100	.0037	-.141	-.0698
101	-.00271	.3866	-.0487
102	.07137	.4298	-.1402
103	-.07137	-.4298	-.1402
104	.00271	-.3866	-.0487
105	-.005	.1184	-.0689
106	.0297	.073	.01279
107	-.0297	-.073	.01279
108	.005	-.1184	-.0689
109	-.0093	.3443	-.0338
110	.0692	.3939	-.1236
111	-.0692	-.3939	-.1236
112	.0093	-.3443	-.0338

TABLE C-I

ACTUAL AFTER CATAMARAN CROSS STRUCTURE STRESSES (KSI)

COMBINED

Element	Girth Stress	Longitudinal Stress	Shear Stress
1	.00224	-.00589	-.00647
2	.00053	-.00724	-.0077
3	-.00729	-.0355	.00175
4	-.00072	-.0161	.0166
5	.0042	-.00588	.00419
6	-.0021	-.0095	.00584
7	-.0119	-.0333	.00201
8	.00453	-.0135	-.00790
9	.01467	.3258	.2347
10	-.0424	.1819	.1799
11	.03445	.7445	-.0323
12	.07866	.7367	-.4446
13	-.1568	.0253	.04238
14	.1144	.3312	.03427
15	.2547	.265	-.0565
16	-.1269	.00936	-.0823
17	-.0787	.292	-.1424
18	.05004	.2338	-.1371
19	.2077	.7605	-.00265
20	-.09363	.6398	.220
21	-.03119	-.51778	-.3592
22	.0732	-.3069	-.2592
23	-.0377	-1.116	.05637

TABLE C-I (Cont'd.)

ACTUAL AFTER CATAMARAN CROSS STRUCTURE STRESSES (KSI)

COMBINED

Element	Girth Stress	Longitudinal Stress	Shear Stress
24	-.1546	-1.147	.6742
25	.2221	-.03696	-.06011
26	-.1664	-.4816	-.04407
27	-.3678	-.3983	.1004
28	.1618	-.01121	.1159
29	.1133	-.4141	.2044
30	-.08977	-.3314	.1872
31	-.2976	-1.009	.01936
32	.1239	-.8826	-.2989
33	.00227	-.00534	.00586
34	.000974	-.00506	.00674
35	-.00653	-.03289	-.00195
36	-.000676	-.0146	-.0142
37	.00429	-.00484	-.00391
38	-.00219	-.00823	-.00513
39	-.01014	-.02574	-.00127
40	.00408	-.0103	.00675
41	.01035	.3086	-.2112
42	-.05557	.1464	-.1666
43	.0198	.68988	.0430
44	.07423	.7012	.3881
45	-.1666	-.0056	-.0364
46	.1152	.260	-.0286

TABLE C-I (Cont'd.)

ACTUAL AFTER CATAMARAN CROSS STRUCTURE STRESSES (KSI)

COMBINED

Element	Girth Stress	Longitudinal Stress	Shear Stress
47	.2320	.1539	.0545
48	-.1318	-.0563	.0638
49	-.0827	.2693	.1322
50	.04199	.2126	.1291
51	.1828	.6971	-.01905
52	-.0933	.5895	-.1889
53	-.02576	-.4911	.3205
54	.09257	-.2561	.2383
55	-.01735	-1.037	-.06774
56	-.1486	-1.093	-.5872
57	.2301	.00918	.0463
58	-.1628	-.3709	.03183
59	-.3293	-.2351	-.0943
60	.1629	.0822	-.07992
61	.1142	-.364	-.1826
62	-.0766	-.2789	-.1707
63	-.2546	-.8750	.0111
64	.1178	-.7745	.2461
65	.07198	.3665	-.3542
66	-.06531	.1356	-.1771
67	-.1216	.2049	-.0774
68	.1827	.8040	.0852
69	.0735	.6630	.0633

TABLE C-I (Cont'd.)

ACTUAL AFTER CATAMARAN CROSS STRUCTURE STRESSES (KSI)

COMBINED

Element	Girth Stress	Longitudinal Stress	Shear Stress
70	-.0924	.1653	-.1544
71	-.0389	.8871	-.3786
72	.1256	1.493	-.618
73	.02049	.18496	-.1259
74	-.005497	.1433	-.05012
75	-.00812	.2022	-.00689
76	.0752	.4304	-.0416
77	.02174	.4654	.0145
78	-.03667	.2108	-.0865
79	.0543	.8775	-.2007
80	.0427	1.0769	-.2121
81	.01131	.1529	-.09042
82	.00766	.1476	-.0336
83	.01677	.2066	-.00161
84	.0483	.3597	-.0663
85	.01702	.4248	-.00502
86	-.0246	.2365	-.08188
87	.07330	.8734	-.1682
88	.01839	.9847	-.1397
89	-.00866	-.3840	-.3915
90	-.00849	-.2367	-.1620
91	-.0518	-.4398	.04087
92	-.00838	-.8654	.1881

TABLE C-I (Cont'd.)

ACTUAL AFTER CATAMARAN CROSS STRUCTURE STRESSES (KSI)

COMBINED

Element	Girth Stress	Longitudinal Stress	Shear Stress
93	-.05198	-.8564	-.02377
94	.0835	-.301	-.2128
95	-.05082	-1.323	-.291
96	-.05804	-1.940	-.3612
97	.01996	-.203	-.1476
98	-.0404	-.2135	-.0393
99	-.1016	-.378	.0615
100	.0274	-.485	.0078
101	-.00704	-.593	-.0422
102	.0284	-.305	-.1252
103	-.1144	-1.164	-.1552
104	-.001608	-1.366	-.0553
105	.0212	-.1692	-.107
106	-.04439	-.2064	-.0251
107	-.1038	-.3524	.05074
108	.03121	-.4062	-.03078
109	-.0049	-.5283	-.05101
110	.0169	-.315	-.1129
111	-.1215	-1.103	-.1345
112	.0137	-1.217	-.01672

TABLE C-II

ACTUAL FORWARD CATAMARAN CROSS STRUCTURE STRESSES (KSI)

SYMM. BEND. MOM.

Element	Girth Stress	Longitudinal Stress	Shear Stress
1	-.00358	-.0102	-.0084
2	.0053	-.0179	-.0049
3	.0053	-.0179	.0049
4	-.00358	-.0102	.0084
5	.00646	.00445	-.0072
6	-.0047	.01715	-.0056
7	-.0047	.01715	.0056
8	.00646	.00445	.0072
9	.0433	.543	.3308
10	-.0026	.459	.101
11	-.0026	.459	-.101
12	.0433	.543	-.3308
13	-.0824	.447	-.1746
14	.1231	.465	-.065
15	.1231	.465	.065
16	-.0824	.447	.1746
17	.0139	.709	.0474
18	.0228	.5198	.0275
19	.0228	.5198	-.0275
20	.0139	.709	-.0474
21	-.0792	-.7457	-.4138
22	.0504	-.5963	-.1548
23	.0504	-.5963	.1548

TABLE II (Cont'd.)

ACTUAL FORWARD CATAMARAN CROSS STRUCTURE STRESSES (KSI)

SYMM. BEND. MOM.

Element	Girth Stress	Longitudinal Stress	Shear Stress
24	-.0792	-.7457	.4138
25	.2164	.0979	-.0638
26	-.2452	-.2122	-.05976
27	-.2452	-.2122	.05976
28	.2164	.0979	.0638
29	.1268	-.6108	.2084
30	-.1557	-.6248	.1032
31	-.1557	-.6248	-.1032
32	.1268	-.6108	-.2084
33	-.0027	-.0118	.01009
34	-.0007	-.0218	.00343
35	-.0007	-.0218	-.00343
36	-.0027	-.0118	-.01009
37	.00163	-.0025	-.0028
38	-.00508	-.0058	.00042
39	-.00508	-.0058	-.00042
40	.00163	-.0025	.0028
41	.0384	.5435	-.3399
42	.00146	.459	-.108
43	.00146	.459	.108
44	.0384	.5435	.3399
45	-.152	.0134	-.0634
46	.192	.3051	-.0446

TABLE II (Cont'd.)

ACTUAL FORWARD CATAMARAN CROSS STRUCTURE STRESSES (KSI)

SYMM. BEND. MOM.

Element	Girth Stress	Longitudinal Stress	Shear Stress
47	.192	.3051	.0446
48	-.152	.0134	.0634
49	-.0906	.5	.1917
50	.1305	.525	.0733
51	.1305	.525	-.0733
52	-.0906	.5	-.1917
53	-.0987	-.815	.513
54	.0223	-.715	.154
55	.0223	-.715	-.154
56	-.0987	-.815	-.513
57	.1812	-.0283	.0851
58	-.2576	-.4298	.0717
59	-.2576	-.4298	-.0717
60	.1812	-.0283	-.0851
61	.1134	-.606	-.2393
62	-.1899	-.6346	-.0779
63	-.1899	-.6346	.0779
64	.1134	-.606	.2393
65	.1263	.5848	-.221
66	-.0919	.168	-.0514
67	-.0919	.168	.0514
68	.1263	.5848	.221
69	.1001	1.09	.3379

TABLE II (Cont'd.)

ACTUAL FORWARD CATAMARAN CROSS STRUCTURE STRESSES (KSI)

SYMM. BEND. MOM.

Element	Girth Stress	Longitudinal Stress	Shear Stress
70	-.0657	.5217	.1138
71	-.0657	.5217	-.1138
72	.1001	1.09	-.3379
73	.00602	.0106	.0126
74	-.00076	.0122	.0100
75	-.00076	.0122	-.0100
76	.00602	.0106	-.0126
77	.00816	.2629	-.0474
78	.02869	.2146	-.0275
79	.02869	.2146	.0275
80	.00816	.2629	.0474
81	.0398	.3403	-.06108
82	.00456	.20913	-.0253
83	.00456	.20913	.0253
84	.0398	.3403	.06108
85	.0308	.833	.1074
86	.0134	.585	.0544
87	.0134	.585	-.0544
88	.0308	.833	-.1074
89	-.00958	-.624	-.288
90	-.0284	-.339	-.0993
91	-.0284	-.339	.0993
92	-.00958	-.624	.288

TABLE II (Cont'd.)

ACTUAL FORWARD CATAMARAN CROSS STRUCTURE STRESSES (KSI)

SYMM. BEND. MOM.

Element	Girth Stress	Longitudinal Stress	Shear Stress
93	-.0542	-1.37	.1719
94	.0162	-.816	.0369
95	.0162	-.816	-.0369
96	-.0542	-1.37	-.1719
97	.00337	-.3286	-.0181
98	-.0633	-.3077	-.0285
99	-.0633	-.3077	.0285
100	.00337	-.3286	.0181
101	-.00227	-.9928	.0181
102	-.0576	-.8403	.0285
103	-.0576	-.8403	-.0285
104	-.00227	-.9928	-.0181
105	.01426	-.3139	-.0634
106	-.0574	-.2566	-.0469
107	-.0574	-.2566	.0469
108	.01426	-.3139	.0634
109	-.00687	-.912	-.0170
110	-.03629	-.6855	.0178
111	-.03629	-.6855	-.0178
112	-.00687	-.912	.0170
113	-.138	.0131	.0554
114	.1793	.2898	.0432
115	.1793	.2898	-.0432
116	-.138	.0131	-.0554

TABLE C-II (Cont'd.)

ACTUAL FORWARD CATAMARAN CROSS STRUCTURE STRESSES (KSI)

ANTISYMM. B.M. + SHEAR

Element	Girth Stress	Longitudinal Stress	Shear Stress
1	.0235	.00813	-.00715
2	.0128	.0239	-.02059
3	-.0128	-.0239	-.02059
4	-.0235	-.00813	-.00715
5	.04747	.01299	-.02918
6	-.00261	.00579	.00143
7	.00261	-.00579	.00143
8	-.04747	-.01299	-.02918
9	-.03198	-.2092	-.106
10	-.0385	-.2866	.0748
11	.0385	.2866	.0748
12	.03198	.2092	-.106
13	.00653	-.1667	.0369
14	-.075	-.2486	-.068
15	.075	.2486	-.068
16	-.00653	.1667	.0369
17	.00186	-.2804	-.0657
18	-.04912	-.3139	-.1194
19	.04912	.3139	-.1194
20	-.00186	.2804	-.0657
21	-.0446	.2824	.1105
22	.0526	.3789	-.078
23	-.0526	-.3789	-.078

TABLE C-II (Cont'd.)

ACTUAL FORWARD CATAMARAN CROSS STRUCTURE STRESSES (KSI)

ANTISYMM. B.M. + SHEAR

Element	Girth Stress	Longitudinal Stress	Shear Stress
24	.0446	-.2824	.1105
25	.0262	-.0584	.02239
26	.0769	-.1096	.0101
27	-.0769	.1096	.0101
28	-.0262	.0584	.02239
29	-.0113	.2586	-.04063
30	.1174	.4251	.0731
31	-.1174	-.4251	.0731
32	.0113	-.2586	-.04063
33	.00988	.00596	-.00624
34	.00836	.0175	-.00374
35	-.00836	-.0175	-.00374
36	-.00988	-.00596	-.00624
37	.00307	.0011	-.0009
38	.00454	.00554	-.00907
39	-.00454	-.00554	-.00907
40	-.00307	-.0011	-.0009
41	-.0318	-.2082	.1069
42	-.03918	-.2858	-.0758
43	.03918	.2858	-.0758
44	.0318	.2082	.1069
45	-.01458	.00878	.0218
46	-.073	.0347	.0093

TABLE C-II (Cont'd.)

ACTUAL FORWARD CATAMARAN CROSS STRUCTURE STRESSES (KSI)

ANTISYMM. B.M. + SHEAR

Element	Girth Stress	Longitudinal Stress	Shear Stress
47	.073	-.0347	.0093
48	.01458	-.00878	.0218
49	.00822	-.1876	-.0416
50	-.0833	-.2802	.0728
51	.0833	.2802	.0728
52	-.00822	.1876	-.0416
53	.0452	.3095	-.150
54	.0523	.4030	.1068
55	-.0523	-.4030	.1068
56	-.0452	-.3095	-.150
57	.02096	-.0119	-.0219
58	.0955	-.0148	-.02138
59	-.0955	.0148	-.02138
60	-.02096	.0119	-.0219
61	.0081	.2215	.0491
62	.0999	.3279	-.0924
63	-.0999	-.3279	-.0924
64	-.0081	-.2215	.0491
65	-.0529	-.2192	-.1323
66	.0271	-.0331	-.1244
67	-.0271	.0331	-.1244
68	.0529	.2192	-.1323
69	-.0248	-.4183	-.2739

TABLE C-II (Cont'd.)

ACTUAL FORWARD CATAMARAN CROSS STRUCTURE STRESSES (KSI)

ANTISYMM. B.M. + SHEAR

Element	Girth Stress	Longitudinal Stress	Shear Stress
70	-.0282	-.3667	-.2647
71	.0282	.3667	-.2647
72	.0248	.4183	-.2739
73	-.0526	.0386	.0652
74	-.136	-.03578	.0479
75	.136	.03578	.0479
76	.0526	-.0386	.0652
77	-.00858	-.1047	-.0665
78	-.0104	-.0363	-.0129
79	.0104	.0363	-.0129
80	.00858	.1047	-.0665
81	-.016	-.132	-.0843
82	-.0042	-.0395	-.028
83	.0042	.0395	-.028
84	.016	.132	-.0843
85	-.00171	-.328	-.1025
86	-.0508	-.354	-.15
87	.0508	.354	-.15
88	.00171	.328	-.1025
89	-.0022	.2404	-.1046
90	.02098	.1034	-.0628
91	-.02098	-.1034	-.0628
92	.0022	-.2404	-.1046

TABLE C-II (Cont'd.)

ACTUAL FORWARD CATAMARAN CROSS STRUCTURE STRESSES (KSI)

ANTISYMM. B.M. + SHEAR

Element	Girth Stress	Longitudinal Stress	Shear Stress
93	.00378	.5391	-.195
94	.0668	.5103	-.254
95	-.0668	-.5103	-.254
96	-.00378	-.5391	-.195
97	.0147	.0609	-.159
98	-.0023	-.0809	-.0805
99	.0023	.0809	-.0805
100	-.0147	-.0609	-.159
101	-.0111	.419	-.1409
102	.0889	.5509	-.2204
103	-.0889	-.5509	-.2204
104	.0111	-.419	-.1409
105	.0038	.1318	-.0819
106	.0258	.0716	-.0026
107	-.0258	-.0716	-.0026
108	-.0038	-.1318	-.0819
109	-.00607	.3635	-.0589
110	.0703	.4158	-.146
111	-.0703	-.4158	-.146
112	.00607	-.3635	-.0589
113	-.01512	.0077	-.018
114	-.0689	.0319	-.01313
115	.0689	-.0319	-.01313
116	.01512	-.0077	-.018

TABLE C-II (Cont'd.)

ACTUAL FORWARD CATAMARAN CROSS STRUCTURE STRESSES (KSI)

COMBINED

Element	Girth Stress	Longitudinal Stress	Shear Stress
1	.01992	-.00207	-.01555
2	.0181	.006	-.02549
3	-.0075	-.0418	-.01569
4	-.02708	-.01833	.00125
5	.05393	.01744	-.03638
6	-.00731	.02294	-.00417
7	-.00209	.01136	.00703
8	-.04101	-.00854	-.02198
9	.01132	.3341	.2248
10	-.0411	.1729	.1758
11	.0359	.7521	-.0262
12	.07528	.7449	-.4368
13	-.07587	.2805	-.1377
14	.0481	.2164	-.133
15	.1981	.6139	-.003
16	-.08893	.7136	.2115
17	.01576	.4286	-.0183
18	-.02632	.2059	-.0919
19	.07192	.8337	-.1469
20	.01204	.9894	-.1131
21	-.1238	-.464	-.3033
22	.1030	-.2171	-.2328
23	-.0022	-1.028	.0768

TABLE C-II (Cont'd.)

ACTUAL FORWARD CATAMARAN CROSS STRUCTURE STRESSES (KSI)

COMBINED

Element	Girth Stress	Longitudinal Stress	Shear Stress
24	-.0346	-.9749	.5243
25	.2426	.0395	-.04141
26	-.1683	.3218	-.04966
27	-.3221	.1563	.06986
28	.1902	-.1026	.08619
29	.1155	-.3523	.16777
30	-.0383	-.1998	.1763
31	-.2731	-.8695	-.0301
32	.1381	-1.6498	-.2490
33	.00718	-.00588	.00385
34	.00766	-.0043	-.00031
35	-.00906	-.0393	-.00717
36	-.01258	-.01772	-.01633
37	.00476	-.0014	-.0037
38	-.00054	-.00026	-.00865
39	-.00962	-.01134	-.00949
40	-.00144	-.0036	.0021
41	.0066	.3353	-.233
42	-.03772	.1735	-.1838
43	.04064	.7517	.0322
44	.0702	.7451	.4468
45	-.1666	.0222	-.0416
46	.119	.3398	-.0353

TABLE C-II (Cont'd.)

ACTUAL FORWARD CATAMARAN CROSS STRUCTURE STRESSES (KSI)

COMBINED

Element	Girth Stress	Longitudinal Stress	Shear Stress
47	.265	.0046	.0539
48	-.1374	.2704	.0852
49	-.08238	.3124	.1501
50	.0472	.2448	.1461
51	.2138	.6876	-.0005
52	-.09882	.8052	-.2333
53	-.0535	-.5055	+.363
54	.0746	-.312	.2608
55	-.0300	-1.1245	-.0472
56	-.1439	-1.118	-.663
57	.2022	-.0402	.0632
58	-.1421	-.4698	.05032
59	-.3531	-.0164	-.09308
60	.1602	-.3862	-.1070
61	.1215	-.3850	-.1902
62	-.0900	-.3068	-.1703
63	-.2898	-.828	-.0145
64	.1053	-.9626	.2884
65	.0734	.3656	-.3533
66	-.0648	.1349	-.1758
67	-.1190	.2011	-.073
68	.1792	.8040	.0887
69	.0753	.6717	.064

TABLE C-II (Cont'd.)

ACTUAL FORWARD CATAMARAN CROSS STRUCTURE STRESSES (KSI)

COMBINED

Element	Girth Stress	Longitudinal Stress	Shear Stress
70	-.0939	.1550	-.1509
71	-.0375	.8884	-.3785
72	.1249	1.5083	-.6118
73	-.04658	.0492	.0778
74	-.13676	-.02358	.0579
75	+.13524	.04798	.0379
76	.05862	-.0280	.0526
77	-.00042	.1582	-.1139
78	.01829	.1783	-.404
79	.03909	.2509	+.0146
80	.01674	.3676	-.0191
81	.0238	.2083	-.14538
82	.00036	.16963	-.0533
83	.00876	.24863	-.0027
84	.0558	.4723	-.02322
85	.02909	.505	.0049
86	-.0374	.231	-.0956
87	.0642	.939	-.2644
88	.03251	1.161	-.2099
89	-.01178	-.3836	-.3926
90	-.00742	-.2356	-.1621
91	-.04938	-.4424	.0365
92	-.00738	-.8644	.1834

TABLE C-II (Cont'd.)

ACTUAL FORWARD CATAMARAN CROSS STRUCTURE STRESSES (KSI)

COMBINED

Element	Girth Stress	Longitudinal Stress	Shear Stress
93	-.05042	-.8309	-.0231
94	.0830	-.3057	-.2171
95	-.0506	-1.3263	-.2909
96	-.05798	-1.9091	-.3669
97	.01807	-.2677	-.1771
98	-.0656	-.3886	-.109
99	-.0610	-.2268	-.0520
100	-.01133	-.3895	-.1409
101	-.01337	-.5738	-.1228
102	.0313	-.2892	-.1919
103	-.1465	-1.3912	-.2489
104	+.0088	-1.4118	-.159
105	.01806	-.1821	-.1453
106	-.0316	-.185	-.0495
107	-.0832	-.3282	.0443
108	.01046	-.4457	-.0185
109	-.01294	-.5485	-.0759
110	.03401	-.2697	-.1282
111	-.1066	-1.1013	-.1638
112	-.0008	-1.2755	-.0419
113	-.15312	.0209	.0374
114	.1104	.3217	.0301
115	.2482	.0055	-.0563
116	-.1229	.2579	-.0734

TABLE C-III

NORMAL STRESSES FOR SYMM. BEND. MOM. (σyy) in KSI

L/B	.3	.3	.3	.5	.5	.5	.7
B/D	2.5	3.0	3.5	3.0	3.0	3.0	3.0
A_f/A_w	3.0	3.0	3.0	2.5	3.0	3.5	2.5
SYMM. BEND. MOM.							
Left	3.772	4.554	5.371	3.81	3.99	4.14	3.31
9	1.45	1.761	2.081	1.60	1.67	1.73	1.515
10	-.477	-.57	-.670	-.252	-.266	-.281	.0104
11	1.20	1.441	1.683	1.310	1.405	1.495	1.28
Right	3.342	4.074	4.777	3.35	3.69	3.80	2.95
Left	3.27	3.999	4.776	2.70	2.82	2.91	1.94
12	1.376	1.69	2.009	1.422	1.475	1.52	1.295
13	-.205	-.248	-.294	.366	.384	.399	.792
14	1.165	1.401	1.641	1.314	1.405	1.509	1.33
Right	2.956	3.569	4.198	2.54	2.71	2.89	1.99

TABLE C-III (Cont'd.)

NORMAL STRESSES FOR SYMM. BEND. MOM (σyy) in KSI

L/B	.3	.3	.3	.5	.5	.5	.7
B/D	2.5	3.0	3.5	3.0	3.0	3.0	3.0
A_f/A_w	3.0	3.0	3.0	2.5	3.0	3.5	2.5
SYMM. BEND. MOM.							
21	1.698	1.943	2.178	1.33	1.585	1.860	1.132
22	3.291	3.872	4.458	2.940	3.27	3.61	2.57
23	1.351	1.439	1.526	.796	.861	.924	.533
24	2.844	3.27	3.704	2.075	2.19	2.29	1.48
29	.799	.943	1.094	.744	.865	1.01	.687
30	2.229	2.663	3.106	2.182	2.41	2.66	1.97
31	.764	.893	1.025	.657	.715	.776	.521
32	2.118	2.522	2.936	1.860	2.000	2.15	1.49

TABLE C-III (Cont'd.)

NORMAL STRESSES FOR SYMM. BEND. MOM. (σyy) in KSI

L/B	.7	.7	.9	.9	.9	1.1	1.1
B/D	3.0	3.0	3.0	3.0	3.0	3.0	3.0
A_f/A_w	3.0	3.5	2.5	3.0	3.5	2.5	3.0
			SYMM. BEND. MOM.				
Left	3.48	3.61	2.93	3.08	3.20	2.63	2.76
9	1.585	1.64	1.45	1.52	1.57	1.40	1.46
10	.00638	-.00218	.209	.214	.218	.359	.372
11	1.372	1.46	1.245	1.33	1.415	1.205	1.29
Right	3.16	3.43	2.61	2.80	2.97	2.33	2.51
Left	1.995	2.04	1.545	1.57	1.59	1.34	1.365
12	1.335	1.365	1.245	1.28	1.30	1.225	1.255
13	.829	.861	1.031	1.075	1.115	1.15	1.198
14	1.415	1.490	1.315	1.39	1.452	1.29	1.351
Right	2.12	2.24	1.65	1.74	1.825	1.44	1.505

TABLE C-III (Cont'd.)

NORMAL STRESSES FOR SYMM. BEND. MOM. (σyy) in KSI

L/B	.7	.7	.9	.9	.9	1.1	1.1
B/D	3.0	3.0	3.0	3.0	3.0	3.0	3.0
A_f/A_w	3.0	3.5	2.5	3.0	3.5	2.5	3.0
SYMM. BEND MOM.							
21	1.133	1.54	.99	1.15	1.315	.88	.974
22	2.84	3.10	2.29	2.51	2.73	2.07	2.18
23	.55	.564	.394	.398	.394	.328	.314
24	1.52	1.55	1.16	1.175	1.18	1.000	.976
29	.789	.905	.634	.719	.815	.585	.636
30	2.16	2.37	1.78	1.95	2.13	1.62	1.710
31	.557	.59	.427	.45	.47	.368	.371
32	1.58	1.675	1.24	1.31	1.37	1.085	1.10

TABLE C-III (Cont'd.)

NORMAL STRESSES FOR SYMM. BEND. MOM. (σyy) in KSI

L/B	1.1	1.3	1.3	1.3	1.3	1.3	1.5
B/D	3.0	2.5	3.0	3.0	3.0	3.5	3.0
A_f/A_w	3.5	3.0	2.5	3.0	3.5	3.0	3.0
SYMM. BEND. MOM.							
Left	2.88	2.123	2.39	2.51	2.62	2.90	2.308
9	1.52	1.194	1.355	1.415	1.47	1.64	1.378
10	.382	.414	.473	.493	.509	.564	.584
11	1.37	1.072	1.168	1.25	1.325	1.418	1.212
Right	2.66	1.938	2.11	2.26	2.41	2.567	2.059
Left	1.38	1.063	1.24	1.26	1.28	1.463	1.205
12	1.28	1.053	1.212	1.25	1.28	1.443	1.238
13	1.24	1.064	1.215	1.26	1.30	1.446	1.278
14	1.41	1.116	1.260	1.315	1.365	1.509	1.283
Right	1.585	1.159	1.305	1.36	1.455	1.563	1.27

TABLE C-III (Cont'd.)

NORMAL STRESSES FOR SYMM. BEND. MOM. (σyy) in KSI

L/B	1.1	1.3	1.3	1.3	1.3	1.3	1.5
B/D	3.0	2.5	3.0	3.0	3.0	3.5	3.0
A_f/A_w	3.5	3.0	2.5	3.0	3.5	3.0	3.0
SYMM. BEND. MOM.							
21	1.14	.829	.789	.891	1.000	.964	.804
22	2.44	1.795	1.875	2.04	2.19	2.290	1.867
23	.316	.177	.294	.289	.282	.335	.272
24	1.01	.785	.92	.921	.926	1.075	.882
29	.737	.534	.540	.600	.671	.668	.554
30	1.925	1.405	1.480	1.61	1.75	1.816	1.485
31	.396	.295	.330	.342	.350	.388	.415
32	1.18	.878	.987	1.030	1.060	1.176	.959

TABLE C-IV

NORMAL STRESSES FOR ANTISYM. B.M. + SHEAR (σyy) in KSI

L/B	.3	.3	.3	.5	.5	.5	.7
B/D	2.5	3.0	3.5	3.0	3.0	3.0	3.0
A_f/A_w	3.0	3.0	3.0	2.5	3.0	3.5	2.5
			ANTISYM. B.M. + SHEAR*				
Left	-1.242	-1.465	-1.672	-1.269	-1.411	-1.444	-1.172
9	-.465	-.546	-.622	-.520	-.559	-.591	-.523
10	+.179	+.213	+.245	+.129	+.138	+.147	+.054
11	-.389	-.466	-.541	-.353	-.38	-.806	-.342
Right	-1.128	-1.345	-1.554	-1.019	-1.33	-1.167	-.883
Left	-2.704	-3.209	-3.691	-1.799	-1.902	-1.99	-1.591
12	-1.19	-1.409	-1.622	-.828	-.8754	-.914	-.782
13	+.315	+.378	+.432	+.152	+.1602	+.167	+.0611
14	-.211	-.252	-.293	-.149	-.141	-.173	-.129
Right	-1.236	-1.4734	-1.697	-.785	-.830	-.941	-.611

*Note: For Asym. B.M. + Shear the signs of the stress are opposite when considering the opposite end of the

TABLE C-IV (Cont'd.)

NORMAL STRESSES FOR ANTISYM. B.M. + SHEAR (σyy) in KSI

L/B	.3	.3	.3	.5	.5	.5	.7
B/D	2.5	3.0	3.5	3.0	3.0	3.0	3.0
A_f/A_W	3.0	3.0	3.0	2.5	3.0	3.5	2.5
ANTISYM. B.M. + SHEAR*							
21	-.378	-.5019	-.6329	-.487	-.575	-.669	-.466
22	-1.859	-2.25	-2.655	-1.308	-1.434	-1.567	-1.120
23	+.073	+.0255	-.048	-.133	-.149	-.166	-.178
24	-1.737	-2.121	-2.521	-1.194	-1.266	-1.341	-1.078
29	-.211	-.251	-.291	-.210	-.248	-.294	-.203
30	-.699	-.833	-.968	-.646	-.717	-.793	-.590
31	-.0776	-.092	-.108	-.075	-.084	-.094	-.0674
32	-.259	-.309	-.360	-.234	-.255	-.278	-.20

*Note: For Asym. B.M. + Shear the signs of the stress are opposite when considering the opposite end of the

TABLE C-IV (Cont'd.)

NORMAL STRESSES FOR ANTISYM. B.M. + SHEAR (σ_{yy}) in KSI

L/B	.7	.7	.9	.9	.9	1.1	1.1
B/D	3.0	3.0	3.0	3.0	3.0	3.0	3.0
A_f/A_w	3.0	3.5	2.5	3.0	3.5	2.5	3.0
ANTISYM. B.M. + SHEAR*							
Left	-1.249	-1.316	-1.048	-1.11	-1.164	-.932	-.984
9	-.557	-.585	-.5104	-.5402	-.564	-.493	-.519
10	+.0575	+.0608	-.0218	-.0233	-.024	-.0868	-.092
11	-.305	-.381	-.3156	-.3400	-.364	-.307	-.331
Right	-.946	-1.017	-.755	-.813	-.864	-.652	-.699
Left	-1.679	-1.753	-1.396	-1.596	-1.534	-1.23	-1.294
12	-.825	-.861	-.7368	-.7766	-.8091	-.694	-.731
13	+.0634	+.065	-.0236	-.0263	-.0286	-.093	-.0992
14	-.129	-.149	-.119	-.128	-.136	-.116	-.124
Right	-.651	-.687	-.471	-.499	-.525	-.363	-.382

*Note: For Asym. B.M. + Shear the signs of the stress are opposite when considering the opposite end of the

TABLE C-IV (Cont'd.)

NORMAL STRESSES FOR ANTISYM. B.M. + SHEAR (σyy) in KSI

L/B	.7	.7	.9	.9	.9	1.1	1.1
B/D	3.0	3.0	3.0	3.0	3.0	3.0	3.0
A_f/A_w	3.0	3.5	2.5	3.0	3.5	2.5	3.0
				ANTISYM. B.M. + SHEAR*			
21	-.537	-.611	-.417	-.475	-.534	-.365	-.413
22	-1.22	-1.315	-.96	-1.042	-1.125	-.833	-.900
23	-.189	-.198	-.192	-.200	-.205	-.1925	-.198
24	-1.035	-1.182	-.962	-1.01	-1.05	-.861	-.900
29	-.235	-.272	-.189	-.215	-.246	-.173	-.194
30	-.655	-.718	-.529	-.582	-.639	-.472	-.506
31	-.073	-.079	-.055	-.0585	-.0613	-.0435	-.0449
32	-.216	-.233	-.161	-.173	-.1825	-.1285	-.134

*Note: For Asym. B.M. + Shear the signs of the stress are opposite when considering the opposite end of the

TABLE C-IV (Cont'd.)

NORMAL STRESSES FOR ANTISYM. B.M. + SHEAR (σyy) in KSI

L/B	1.1	1.3	1.3	1.3	1.3	1.3	1.5
B/D	3.0	2.5	3.0	3.0	3.0	3.5	3.0
A_f/A_w	3.5	3.0	2.5	3.0	3.5	3.0	3.0
				ANTISYM. B.M. + SHEAR*			
Left	-1.027	-.825	-.835	-.878	-.915	-1.128	-.886
9	-.541	-.496	-.477	-.501	-.521	-.673	-.569
10	-.096	-.168	-.139	-.146	-.153	-.223	-.246
11	-.354	-.289	-.302	-.324	-.359	-.385	-.336
Right	-.744	-.516	-.478	-.612	-.654	-.696	-.537
Left	-1.37	-1.575	-1.106	-1.162	-1.208	-2.007	-1.68
12	-.761	-.928	-.664	-.698	-.726	-1.191	-1.04
13	-.104	-.165	-.146	-.155	-.162	-.208	-.255
14	-.131	-.114	-.118	-.124	-.131	-.177	-.141
Right	-.403	-.355	-.286	-.301	-.328	-.483	-.335

*Note: For Asym. B.M. + Shear the signs of the stress are opposite when considering the opposite end of the [illegible]

TABLE C-IV (Cont'd.)

NORMAL STRESSES FOR ANTISYM. B.M. + SHEAR (σ_{yy}) in KSI

L/B	1.1	1.3	1.3	1.3	1.3	1.3	1.5
B/D	3.0	2.5	3.0	3.0	3.0	3.5	3.0
A_f/A_w	3.5	3.0	2.5	3.0	3.5	3.0	3.0
ANTISYM. B.M. + SHEAR*							
21	-.447	-.379	-.320	-.359	-.398	-.441	-.363
22	-.965	-.794	-.731	-.79	-.843	-1.009	-.804
23	-.201	-.228	-.189	-.193	-.195	-.370	-.402
24	-.931	-1.076	-.782	-.816	-.845	-1.201	-1.198
29	-.22	-.158	-.155	-.176	-.197	-.198	-.161
30	-.564	-.411	-.422	-.461	-.502	-.532	-.426
31	-.0457	-.033	-.0341	-.0345	-.0342	-.045	-.029
32	-.140	-.098	-.1035	-.107	-.110	-.148	-.093

*Note: For Asym. B.M. + Shear the signs of the stress are opposite when considering the opposite end of the

TABLE C-V

NORMAL STRESSES FOR SYMM. BEND. MOM. (σ_{xx}) in KSI

L/B	.3	.3	.3	.5	.5	.5	.7
B/D	2.5	3.0	3.5	3.0	3.0	3.0	3.0
A_f/A_w	3.0	3.0	3.0	2.5	3.0	3.5	2.5
SYMM. BEND. MOM.							
9	.1761	.212	.250	.180	.186	.190	.0847
10	-.3441	-.417	-.492	-.485	-.514	-.542	-.432
11	-.1747	-.210	-.247	-.275	-.293	-.310	-.241
12	-.1761	-.212	-.250	-.183	-.188	-.193	-.0855
13	.3441	.417	.492	.484	.522	.546	.435
14	.1747	.210	.247	.280	.298	.315	.243
21	.252	.302	.311	.162	.217	.278	.1168
22	.279	.307	.316	.177	.233	.294	.1375
23	-.252	-.302	-.311	-.162	-.221	-.282	-.1180
24	-.279	-.307	-.316	-.177	-.237	-.299	-.1395
29	.0339	.038	.0393	.0312	-.0495	.074	.033
30	.0385	.0427	.0443	.0418	.0611	.086	.0464
31	-.0339	-.038	-.0393	-.0318	-.0506	-.075	-.0334
32	-.0385	-.0427	-.0443	-.0424	-.0621	-.0874	-.0469

TABLE C-V (Cont'd.)

NORMAL STRESSES FOR SYMM. BEND. MOM. (σxx) in KSI

L/B	.7	.7	.9	.9	.9	1.1	1.1
B/D	3.0	3.0	3.0	3.0	3.0	3.0	3.0
$A_f A_w$	3.0	3.5	2.5	3.0	3.5	2.5	3.0
				SYMM. BEND. MOM.			
9	.0834	.0798	.0168	.0111	.00356	-.0143	-.0209
10	-.456	-.479	-.351	-.371	-.390	-.277	-.284
11	-.254	-.266	-.186	-.196	-.204	-.142	-.143
12	-.084	-.0806	-.0169	-.0111	-.00351	.0144	.0211
13	.462	.485	+.354	.371	.393	.279	.286
14	.257	.269	+.188	.197	.206	.142	.144
21	.151	.189	.085	.109	.134	.065	.0815
22	.1735	.213	.108	.1332	.1595	.086	.104
23	-.153	-.1915	-.0867	-.110	-.1352	-.0654	-.0823
24	-.176	-.216	-.109	-.1344	-.162	-.0866	-.1055
29	.0454	.0615	.029	.038	.0492	.0243	.0312
30	.0605	.0777	.0428	.0535	.0665	.0374	.0457
31	-.0463	-.0623	-.0293	-.0384	-.0495	-.0246	-.0314
32	-.0612	-.0787	-.0432	-.054	-.0672	-.0375	-.0461

TABLE C-V (Cont'd.)

NORMAL STRESSES FOR SYMM. BEND. MOM. (σ_{xx}) in KSI

L/B	1.1	1.3	1.3	1.3	1.3	1.3	1.5
B/D	3.0	2.5	3.0	3.0	3.0	3.5	3.0
A_f/A_w	3.5	3.0	2.5	3.0	3.5	3.0	3.0
				SYMM. BEND. MOM.			
9	-.0304	-.0298	-.023	-.0303	-.039	-.0291	-.0284
10	-.309	-.198	-.217	-.23	-.243	-.263	-.1819
11	-.1535	-.095	-.107	-.112	-.116	-.129	-.0863
12	.0306	.0298	.0232	.0306	.039	.0291	.0284
13	.311	.198	.218	.232	.244	.263	.1819
14	.155	.095	.108	.112	.117	.129	.0863
21	.099	.0704	.0508	.063	.076	.0582	.0502
22	.124	.0882	.0697	.0837	.0982	.0821	.0687
23	-.100	-.0704	-.0510	-.0634	-.0768	-.0582	-.0502
24	-.125	-.0882	-.0702	-.0844	-.0992	-.0821	-.0687
29	.0394	.0278	.0203	.0256	.032	.0243	.0211
30	.0559	.0396	.0319	.0386	.0469	.0389	.0328
31	-.0398	-.0278	-.0207	-.0257	-.0322	-.0242	-.0211
32	-.0564	-.0396	-.0320	-.0389	-.0472	-.0389	-.0328

TABLE C-VI

NORMAL STRESSES FOR ANTISYM. B.M. + SHEAR (σ_{yy}) in KSI

L/B	.3	.3	.3	.5	.5	.5	.7
B/D	2.5	3.0	3.5	3.0	3.0	3.0	3.0
A_f/A_w	3.0	3.0	3.0	2.5	3.0	3.5	2.5
			ANTISYM. B.M. + SHEAR*				
9	5.14	6.167	7.196	+1.447	+1.45	+1.45	+.766
10	3.03	3.637	4.294	+ .854	+.854	+.855	+.457
11	.999	1.198	1.398	+.275	+.273	+.274	+.145
12	1.347	1.619	1.893	+.289	+.284	+.280	+.103
13	1.009	1.210	1.414	+.193	+.188	+.182	+.0207
14	.318	.381	.445	+.0604	+.058	+.055	+.00232
21	-.27	-.227	-.1916	-.075	-.0938	-.1144	-.0414
22	-.22	-.169	-.123	-.0428	-.0597	-.079	-.0117
23	-.105	-.132	-.163	-.0377	-.0255	-.0101	-.0202
24	-.365	-.429	-.496	-.179	-.1742	-.165	-.1299
29	-.134	-.116	-.1019	-.0398	-.0482	-.0582	-.0235
30	-.149	-.142	-.1199	-.0501	-.0591	-.0697	-.0339
31	-.0185	-.0128	-.0098	+.0011	+.0062	+.0131	+.0056
32	-.020	-.0141	-.0109	+.0014	+.0063	+.01303	+.0074

*Note: Signs shift at the opposite end of the quarter structure model

TABLE C-VI (Cont'd.)

NORMAL STRESSES FOR ANTISYM. B.M. + SHEAR (σ_{yy}) in KSI

L/B	.7	.7	.9	.9	.9	1.1	1.1
B/D	3.0	3.0	3.0	3.0	3.0	3.0	3.0
$A_f A_w$	3.0	3.5	2.5	3.0	3.5	2.5	3.0
ANTISYM. B.M. + SHEAR*							
9	+.768	+.769	+.476	+.476	+.479	+.326	+.328
10	+.459	+.460	+.29	+.291	+.293	+.204	+.204
11	+.145	+.145	+.091	+.091	+.091	+.0627	+.626
12	+.0992	+.096	+.03	+.0267	+.0235	-.00396	-.00736
13	+.013	+.0063	-.048	-.0555	-.063	-.0741	-.0811
14	-.00597	-.0095	-.0285	-.0321	-.0355	-.0372	-.0391
21	-.0528	-.0653	-.0266	-.0344	-.043	-.0183	-.0240
22	-.0215	-.0326	-.00035	-.0067	-.014	+.0048	+.00034
23	-.0089	+.0044	-.0124	-.00326	+.00778	-.0094	-.00205
24	-.135	-.127	-.1149	-.1112	-.1048	-.0983	-.0956
29	-.0285	-.0346	-.0186	-.0204	-.0247	-.0133	-.0160
30	-.0384	-.0451	-.0254	-.0296	-.0346	-.0213	-.0247
31	+.0103	+.0164	+.00839	+.0124	+.0178	+.0096	+.0133
32	+.0121	+.0184	+.0118	+.0163	+.022	+.0143	+.0185

*Note: Signs shift at the opposite end of the quarter structure model

TABLE C-VI (Cont'd.)

NORMAL STRESSES FOR ANTISYM. B.M. + SHEAR (σyy) in KSI

L/B	1.1	1.3	1.3	1.3	1.3	1.3	1.5
B/D	3.0	2.5	3.0	3.0	3.0	3.5	3.0
A_f/A_w	3.5	3.0	2.5	3.0	3.5	3.0	3.0
ANTISYM. B.M. + SHEAR*							
9	+.329	.341	+.242	+.243	+.242	.450	.318
10	+.205	.205	+.153	+.154	+.155	.276	.192
11	+.626	.064	+.0461	+.046	+.046	.088	.059
12	-.0103	-.0411	-.0204	-.0235	-.0265	-.0457	-.054
13	-.0875	-.083	-.0802	-.0865	-.0925	-.1106	-.095
14	-.0432	-.039	-.038	-.0405	-.0428	-.0535	-.043
21	-.0303	-.0165	-.0128	-.0166	-.021	-.008	-.0049
22	-.0049	+.0209	+.0073	+.0040	+.000058	+.0390	+.0323
23	+.0067	-.0181	-.0093	-.0034	+.0035	-.0255	-.0289
24	-.0907	-.1422	-.0879	-.0862	-.0826	-.1857	-.1584
29	-.0193	-.0139	-.0108	-.0129	-.0155	-.0135	-.0108
30	-.0287	-.0211	-.0188	-.0217	-.0250	-.0215	-.0194
31	+.0177	+.0125	+.0097	+.0128	+.0166	+.0176	+.0117
32	+.0236	+.0176	+.0152	+.01904	+.0236	+.0195	+.0180

*Note: Signs shift at the opposite end of the quarter structure model

TABLE C-VII

SHEAR STRESS (σxy) in KSI

L/B	.3	.3	.3	.5	.5	.5	.7
B/D	2.5	3.0	3.5	3.0	3.0	3.0	3.0
A_f/A_W	3.0	3.0	3.0	2.5	3.0	3.5	2.5
ELEMENT			SYMMET. BEND. MOM.				
9	.600	.732	.8698	.882	.921	.955	.926
10	.00756	.0045	.00104	.113	.125	.137	.147
11	-.201	-.242	-.283	-.408	-.434	-.462	-.500
12	.243	.297	.352	.336	.351	.365	.293
13	.438	.051	.0587	.112	.119	.125	.1065
14	-.118	-.142	-.1678	-.231	-.245	-.258	-.251
21	-.405	-.516	-.608	-.418	-.562	-.726	-.426
22	.405	.516	.608	.418	.562	.726	.726
23	-.203	-.242	-.262	-.151	-.195	-.244	-.110
24	.203	.242	.262	.151	.195	.244	.110
29	-.0496	-.0636	-.0746	-.0718	-.121	-.184	-.106
30	.0496	.0635	.0746	.0718	.121	.184	.106
31	-.0276	-.0338	-.0374	-.0406	-.0564	-.0766	-.047
32	.0276	.0337	.0374	.0406	.0564	.0766	.047

TABLE C-VII (Cont'd.)

SHEAR STRESS (σxy) in KSI

L/B	.7	.7	.9	.9	.9	1.1	1.1
B/D	3.0	3.0	3.0	3.0	3.0	3.0	3.0
A_f/A_W	3.0	3.5	2.5	3.0	3.5	2.5	3.0
ELEMENT			SYMMET. BEND. MOM.				
9	.965	.995	.850	.881	.905	.761	.788
10	.157	.167	.133	.139	.145	.112	.116
11	-.528	-.555	-.50	-.53	-.555	-.473	-.502
12	.303	.312	.204	.208	.210	.126	.125
13	.110	.114	.0698	-.0704	-.0694	+.038	.036
14	-.264	-.276	-.216	-.217	-.237	-.172	-.180
21	-.56	-.707	-.39	-.506	-.634	-.353	-.455
22	.56	.707	.39	.506	.634	.353	.455
23	-.134	-.158	-.066	-.0742	-.0817	-.0318	-.0308
24	.134	.158	.066	.0742	.0817	.0318	.0308
29	-.153	-.214	-.114	-.157	-.212	-.114	-.153
30	.153	.214	.114	.157	.212	.114	.153
31	-.057	-.0693	-.038	-.0434	-.049	-.0258	-.0278
32	.057	.0693	.038	.0434	.049	.0258	.0278

TABLE C-VII (Cont'd.)

SHEAR STRESS (σxy) in KSI

L/B	1.1	1.3	1.3	1.3	1.3	1.3	1.5
B/D	3.0	2.5	3.0	3.0	3.0	3.5	3.0
A_f/A_w	3.5	3.0	2.5	3.0	3.5	3.0	3.0
ELEMENT				SYMMET. BEND. MOM.			
9	.81	.594	.681	.705	.725	.818	.635
10	.118	.081	.0957	.0971	.0975	.114	.085
11	-.527	-.398	-.439	-.465	-.49	-.530	-.426
12	.124	.054	.0684	.064	.0604	.076	.0222
13	+.0328	.009	.0172	.0138	.00935	.019	.0013
14	-.187	-.116	-.129	-.135	-.140	-.155	-.097
21	-.565	-.395	-.320	-.408	-.508	-.426	-.374
22	.565	.395	.320	.408	.508	.426	.374
23	-.0285	-.0225	-.0705	-.00061	-.00742	.019	.0204
24	.0285	.0225	.0705	.00061	.00742	-.019	-.0204
29	-.202	-.139	-.111	-.146	-.189	-.154	-.139
30	.202	.139	.111	.146	.189	.154	.139
31	-.0292	-.0219	-.0146	-.0141	-.0129	-.0061	-.003
32	.0292	.0219	.0146	.0141	.0129	.00604	.0027

TABLE C-VIII

SHEAR STRESS (σ_{xy}) in KSI

L/B	.3	.3	.3	.5	.5	.5	.7
B/D	2.5	3.0	3.5	3.0	3.0	3.0	3.0
A_f/A_w	3.0	3.0	3.0	2.5	3.0	3.5	2.5
ELEMENT				ANTISYMM B.M. + SHEAR			
9	.596	.718	.841	.138	.126	.119	-.0024
10	.6657	.797	.928	.310	.312	.318	.226
11	.6099	.732	.854	.284	.286	.292	.244
12	1.231	1.475	1.718	.655	.669	.686	.573
13	1.162	1.396	1.630	.582	.481	.485	.346
14	1.218	1.460	1.704	.508	.500	.510	.328
21	-.2793	-.330	-.387	-.286	-.376	-.484	-.218
22	-.598	-.547	-.489	-.145	-.145	-.144	-.0945
23	.1031	.155	.2108	-.494	-.566	-.650	-.346
24	-.981	-1.031	-1.088	+.063	.045	.0231	.0337
29	-.0823	-.0817	-.0818	-.185	-.226	-.279	-.142
30	-.3565	-.357	-.356	-.0351	-.035	-.0344	-.0178
31	-.0056	-.0060	-.0061	-.213	-.246	-.287	-.146
32	-.433	-.432	-.432	-.0073	-.0151	-.0262	-.0133

TABLE C-VIII (Cont'd.)

SHEAR STRESS (σ_{xy}) in KSI

L/B	.7	.7	.9	.9	.9	1.1	1.1
B/D	3.0	3.0	3.0	3.0	3.0	3.0	3.0
A_f/A_w	3.0	3.5	2.5	3.0	3.5	2.5	3.0
ELEMENT			ANTISYMM B.M. + SHEAR				
9	-.0113	-.0226	-.0681	-.0821	-.094	-.104	-.117
10	.228	.229	.169	.169	.169	.13	.13
11	.249	.253	.225	.231	.236	.214	.22
12	.586	.596	.511	.524	.535	.465	.479
13	.344	.345	.271	.271	.271	.229	.229
14	.324	.319	.214	.208	.203	.145	.1395
21	-.29	-.372	-.183	-.243	-.310	-.164	-.215
22	-.0875	-.0775	-.0558	-.0462	-.0341	-.0312	-.0209
23	-.392	-.439	-.249	-.279	-.311	-.189	-.211
24	.0137	+.0102	+.0095	-.00995	-.0326	-.0067	-.025
29	-.174	-.214	-.117	-.144	-.176	-.103	-.125
30	-.0149	-.0107	-.0051	-.00116	-.00436	-.00261	+.0071
31	-.167	-.191	-.104	-.118	-.134	-.078	-.0885
32	-.0219	-.0333	-.0185	-.0269	-.0378	-.022	-.0301

TABLE C-VIII (Cont'd.)

SHEAR STRESS (σ_{xy}) in KSI

L/B	1.1	1.3	1.3	1.3	1.3	1.3	1.5
B/D	3.0	2.5	3.0	3.0	3.0	3.5	3.0
A_f/A_w	3.5	3.0	2.5	3.0	3.5	3.0	3.0
ELEMENT				ANTISYMM B.M. + SHEAR			
9	-.128	-.129	-.120	-.1325	-.143	-.168	-.159
10	.130	.151	.104	.104	.103	.199	.148
11	.225	.251	.202	.208	.213	.337	.277
12	.495	.550	.430	.442	.453	.716	.604
13	.231	.271	.202	.204	.204	.360	.297
14	.134	.180	.105	.0994	.094	.234	.168
21	-.272	-.043	-.146	-.191	-.24	-.0355	-.032
22	-.0846	-.159	-.131	-.00242	.0103	-.166	-.156
23	-.235	.0028	-.147	-.164	-.181	-.007	-.0162
24	-.0464	-.205	-.0134	-.0299	-.0486	-.195	-.172
29	-.154	.0082	-.0905	-.110	-.1345	.0118	.00999
30	+.00129	-.109	.00844	.01325	.0194	-.113	-.104
31	-.100	-.028	-.060	-.0675	-.0765	-.337	-.034
32	-.0402	-.0728	-.0223	-.0294	-.0387	-.0671	-.060

TABLE C-IX

COMBINED RESULTS FOR LONGITUDINAL STRESS (σ_{yy}) KSI

L/B	.3	.3	.3	.5	.5	.5	.7
B/D	2.5	3.0	3.5	3.0	3.0	3.0	3.0
A_f/A_w	3.0	3.0	3.0	2.5	3.0	3.5	2.5
*Left	2.524	3.089	3.696	2.538	2.628	2.562	2.131
9	.987	1.214	1.459	1.08	1.111	1.139	.992
10	-.295	-.358	-.425	-.123	-.128	-.134	-.0644
11	.813	.975	1.144	.957	1.025	.689	.938
*Right	2.263	2.731	3.22	2.353	2.498	1.886	2.050
Left	.568	.792	1.057	.903	.918	.742	.346
12	.186	.277	.387	.594	.5996	.506	.513
13	.111	.126	.139	.518	.5442	.566	.8531
14	.954	1.148	1.348	1.165	1.264	1.336	1.201
Right	1.720	2.099	2.50	1.760	1.915	1.99	1.378

*Values extrapolated to plating edge.

TABLE C-IX(Cont'd.)

COMBINED RESULTS FOR LONGITUDINAL STRESS (σ_{yy}) KSI

L/B	.7	.7	.9	.9	.9	1.1	1.1
B/D	3.0	3.0	3.0	3.0	3.0	3.0	3.0
A_f/A_w	3.0	3.5	2.5	3.0	3.5	2.5	3.0
*Left	2.478	2.309	1.876	1.962	2.038	1.697	1.774
9	1.028	1.055	.9396	.9798	1.006	.907	.941
10	.0639	.05862	.1872	.1967	.194	.2722	.280
11	1.067	1.079	.9294	.99	1.051	.898	.959
*Right	2.306	2.345	1.861	1.978	2.105	1.684	1.801
Left	.323	.290	.142	.106	.0559	.115	.0689
12	.510	.504	.5082	.5034	.4909	.531	.524
13	.8924	.926	1.0074	1.0487	1.0864	1.057	1.099
14	1.286	1.341	1.196	1.262	1.316	1.174	1.227
Right	1.487	1.546	1.174	1.244	1.293	1.079	1.123

*Values extrapolated to plating edge.

TABLE C-IX (Cont'd.)

COMBINED RESULTS FOR LONGITUDINAL STRESS (σ_{yy}) KSI

L/B	1.1	1.3	1.3	1.3	1.3	1.3	1.5
B/D	3.0	2.5	3.0	3.0	3.0	3.5	3.0
A_f/A_w	3.5	3.0	2.5	3.0	3.5	3.0	3.0
*Left	1.859	1.281	1.554	1.627	1.697	1.774	1.423
9	.979	.6986	.878	.914	.949	.967	.809
10	.286	.246	.334	.347	.356	.341	.338
11	1.016	.742	.866	.926	.966	1.032	.876
*Right	1.915	1.346	1.536	1.645	1.722	1.871	1.523
Left	.0328	-.514	.1195	.100	.068	-.45162	-.472
12	.519	.125	.548	.552	.554	.251	.2008
13	1.136	.899	1.069	1.105	1.147	1.213	1.022
14	1.279	1.002	1.142	1.191	1.234	1.584	1.142
Right	1.173	.802	1.011	1.059	1.088	1.5487	.939

*Values extrapolated to plating edge.

TABLE C-IX (Cont'd.)

COMBINED RESULTS FOR LONGITUDINAL STRESS (σyy) KSI

L/B	.3	.3	.3	.5	.5	.5	.7
B/D	2.5	3.0	3.5	3.0	3.0	3.0	3.0
A_f/A_w	3.0	3.0	3.0	2.5	3.0	3.5	2.5
*Left	5.975	7.206	8.439	4.50	4.708	4.904	3.528
15	2.565	3.097	3.63	2.25	2.3504	2.434	2.077
16	-.520	-.623	-.726	.214	.2234	.232	.7309
17	1.376	1.653	1.934	1.463	1.546	1.682	1.459
*Right	4.192	5.040	5.895	3.32	3.50	3.776	2.601
Left	5.01	6.019	7.047	5.075	5.468	5.750	4.484
18	1.918	2.307	2.703	2.12	2.29	2.321	2.038
19	-.6535	-.783	-.9156	-.381	-.404	-.428	-.0436
20	1.591	1.907	2.225	1.663	1.785	2.301	1.622
Right	4.519	5.419	6.33	4.389	4.711	5.720	3.860

*Values extrapolated to plating edge.

TABLE C-IX (Cont'd.)

COMBINED RESULTS FOR LONGITUDINAL STRESS (σ_{yy}) KSI

L/B	.7	.7	.9	.9	.9	1.1	1.1
B/D	3.0	3.0	3.0	3.0	3.0	3.0	3.0
A_f/A_w	3.0	3.5	2.5	3.0	3.5	2.5	3.0
*Left	3.653	3.793	2.935	3.049	3.121	2.572	2.655
15	2.15	2.226	1.9818	2.0566	2.1091	1.919	1.986
16	.7656	.796	1.0546	1.1013	1.1436	1.243	1.297
17	1.544	1.639	1.434	1.518	1.588	1.406	1.475
*Right	2.744	2.913	2.114	2.241	2.339	1.802	1.889
Left	4.707	4.941	3.972	4.192	4.366	3.559	3.738
18	2.141	2.225	1.9604	2.0602	2.134	1.893	1.979
19	-.05112	-.06298	.2308	.2373	.242	.4458	.464
20	1.677	1.841	1.5606	1.67	1.779	1.512	1.621
Right	4.011	4.365	3.373	3.607	3.833	2.988	3.201

*Values extrapolated to plating edge.

TABLE C-IX (Cont'd.)

COMBINED RESULTS FOR LONGITUDINAL STRESS (σ_{yy}) KSI

L/B	1.1	1.3	1.3	1.3	1.3	1.3	1.5
B/D	3.0	2.5	3.0	3.0	3.0	3.5	3.0
A_f/A_w	3.5	3.0	2.5	3.0	3.5	3.0	3.0
*Left	2.725	2.638	2.333	2.423	2.506	3.399	2.885
15	2.041	1.98	1.876	1.948	2.006	2.58	2.275
16	1.344	1.229	1.361	1.415	1.453	1.642	1.532
17	1.541	1.23	1.378	1.439	1.496	1.638	1.425
*Right	1.975	1.512	1.586	1.660	1.741	1.986	1.61
Left	3.912	2.95	3.221	3.384	3.537	4.009	3.288
18	2.06	1.69	1.832	1.916	1.991	2.298	1.997
19	.478	.583	.612	.639	.662	.776	.830
20	1.724	1.36	1.470	1.574	1.684	1.788	1.549
Right	3.408	2.455	2.678	2.871	3.077	3.244	2.616

*Values extrapolated to plating edge.

TABLE C-IX (Cont'd.)

COMBINED RESULTS FOR LONGITUDINAL STRESS (σyy) KSI

L/B	.3	.3	.3	.5	.5	.5	.7
B/D	2.5	3.0	3.5	3.0	3.0	3.0	3.0
A_f/A_w	3.0	3.0	3.0	2.5	3.0	3.5	2.5
21	1.31	1.441	1.545	.843	1.01	1.191	.666
22	1.432	1.621	1.802	1.632	1.836	2.043	1.450
23	1.424	1.465	1.478	.663	.712	.758	.355
24	1.107	1.149	1.183	.881	.924	.949	.402
25	1.2	1.413	1.574	.929	1.01	1.090	.711
26	4.582	5.391	6.225	3.269	3.456	3.631	2.558
27	2.087	2.445	2.811	1.817	2.16	2.529	1.598
28	5.15	6.124	7.113	4.248	4.704	5.177	3.690

TABLE C-IX(Cont'd.)

COMBINED RESULTS FOR LONGITUDINAL STRESS (σ_{yy}) KSI

L/B	.7	.7	.9	.9	.9	1.1	1.1
B/D	3.0	3.0	3.0	3.0	3.0	3.0	3.0
A_f/A_w	3.0	3.5	2.5	3.0	3.5	2.5	3.0
21	.596	.929	.573	.675	.781	.515	.561
22	1.62	1.785	1.33	1.468	1.605	1.237	1.28
23	.361	.366	.202	.198	.189	.136	.116
24	.485	.368	.198	.165	.130	.139	.076
25	.739	.762	.586	.598	.599	.52	.512
26	2.555	2.732	2.122	2.185	2.23	1.861	1.876
27	1.67	2.151	1.407	1.625	1.849	1.245	1.387
28	4.06	4.415	3.25	3.552	3.855	2.903	3.08

TABLE C-IX (Cont'd.)

COMBINED RESULTS FOR LONGITUDINAL STRESS (σ_{yy}) KSI

L/B	1.1	1.3	1.3	1.3	1.3	1.3	1.5
B/D	3.0	2.5	3.0	3.0	3.0	3.5	3.0
A_f/A_w	3.5	3.0	2.5	3.0	3.5	3.0	3.0
21	.639	.449	.469	.532	.602	.522	.440
22	1.475	1.001	1.144	1.25	1.347	1.28	1.063
23	.115	.021	.105	.096	.087	-.0357	-.0302
24	.079	-.291	.138	.105	.081	-.378	-.315
25	.517	.478	.483	.482	.477	.696	.574
26	1.941	1.861	1.702	1.737	1.771	2.481	2.08
27	1.587	1.208	1.109	1.25	1.398	1.404	1.166
28	3.405	2.589	2.606	2.83	3.033	3.286	2.672

TABLE C-IX (Cont'd.)

COMBINED RESULTS FOR LONGITUDINAL STRESS (σ_{yy}) KSI

L/B	.3	.3	.3	.5	.5	.5	.7
B/D	2.5	3.0	3.5	3.0	3.0	3.0	3.0
A_f/A_w	3.0	3.0	3.0	2.5	3.0	3.5	2.5
29	.583	.692	.803	.534	.617	.716	.484
30	1.532	1.830	2.139	1.536	1.693	1.867	1.38
31	.686	.800	.917	.582	.631	.682	.4536
32	1.858	2.212	2.58	1.626	1.745	1.872	1.29
33	.842	.986	1.134	.732	.799	.870	.5884
34	2.377	2.83	3.296	2.094	2.255	2.428	1.69
35	1.005	1.194	1.386	.954	1.113	1.304	.890
36	2.927	3.496	4.074	2.828	3.127	3.453	2.56

TABLE C-IX (Cont'd.)

COMBINED RESULTS FOR LONGITUDINAL STRESS (σ_{yy}) KSI

L/B	.7	.7	.9	.9	.9	1.1	1.1
B/D	3.0	3.0	3.0	3.0	3.0	3.0	3.0
A_f/A_w	3.0	3.5	2.5	3.0	3.5	2.5	3.0
29	.554	.633	.445	.504	.569	.412	.442
30	1.505	1.652	1.251	1.368	1.491	1.148	1.204
31	.484	.511	.372	.3915	.4087	.3245	.3261
32	1.364	1.442	1.079	1.137	1.188	.9565	.966
33	.630	.669	.482	.5085	.5313	.4115	.4159
34	1.796	1.908	1.401	1.483	1.552	1.2135	1.234
35	1.024	1.177	.823	.934	1.061	.758	.830
36	2.815	3.088	2.309	2.532	2.769	2.092	2.21

TABLE C-IX (Cont'd.)

COMBINED RESULTS FOR LONGITUDINAL STRESS (σ_{yy}) KSI

L/B	1.1	1.3	1.3	1.3	1.3	1.3	1.5
B/D	3.0	2.5	3.0	3.0	3.0	3.5	3.0
A_f/A_w	3.5	3.0	2.5	3.0	3.5	3.0	3.0
29	.517	.375	.385	.424	.474	.470	.392
30	1.361	.994	1.058	1.149	1.248	1.284	1.059
31	.3503	.262	.296	.308	.316	.343	.286
32	1.04	.780	.884	.923	.950	1.028	.866
33	.4417	.328	.364	.377	.384	.422	.344
34	1.32	.976	1.091	1.137	1.17	1.284	1.053
35	.957	.692	.695	.776	.868	.864	.716
36	2.489	1.816	1.902	2.071	2.252	2.335	1.911

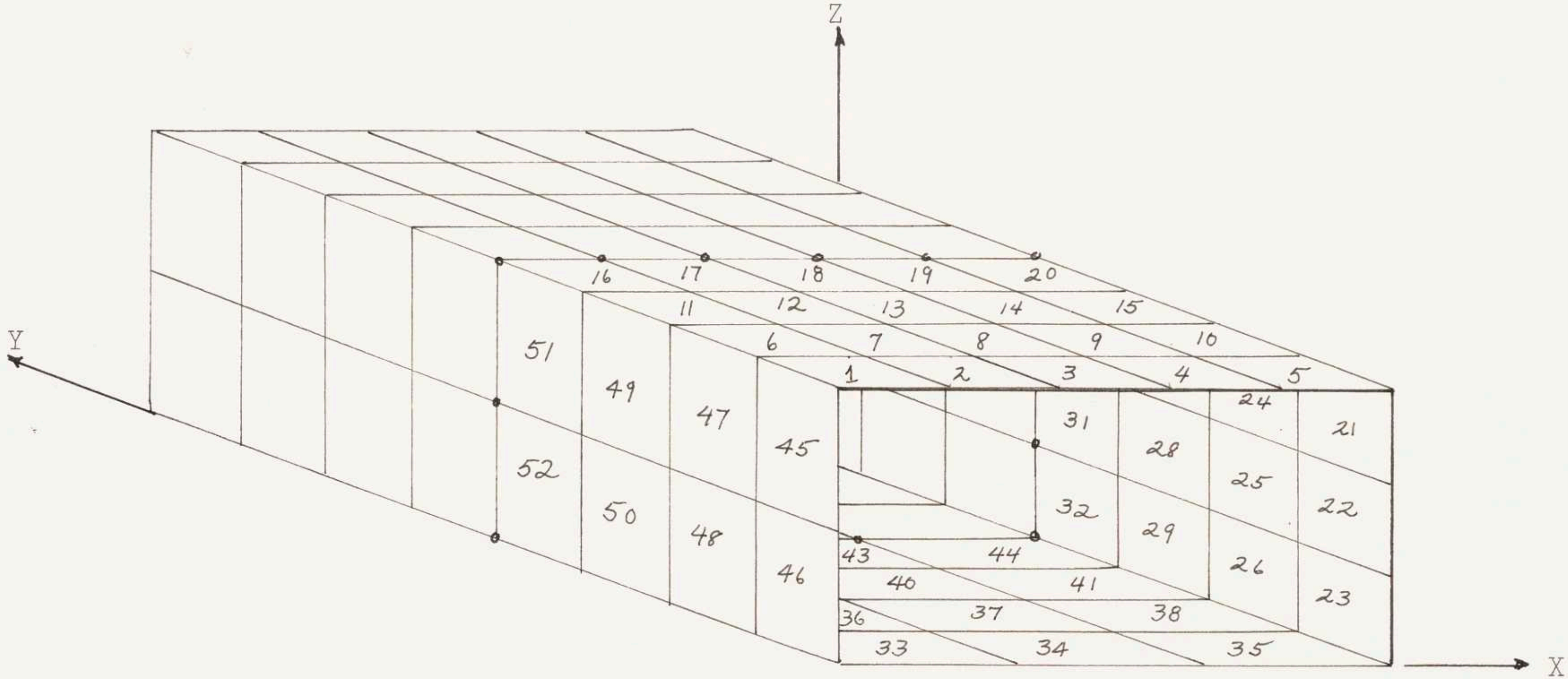

FIGURE C-I
TORSION MODEL ELEMENT NUMBERING SEQUENCE (1/8 STRUCTURE)

TABLE C-X

COMPUTER CALCULATED TORSION RESULTS (FOR 1/8 STRUCTURE)

M_t=1000ft-tons*

GIRTH STRESSES

L/B	.5	1.3	1.3
B/D	3.0	3.0	3.0
A_f/A_w	3.5	3.0	3.5
Element			
1	$-.186\text{x}10^{-7}$	$.157\text{x}10^{-4}$	$.167\text{x}10^{-4}$
2	$-.415\text{x}10^{-5}$	$.495\text{x}10^{-4}$	$.54\text{x}10^{-4}$
3	$.588\text{x}10^{-4}$	$.126\text{x}10^{-3}$	$.135\text{x}10^{-3}$
4	$-.126\text{x}10^{-4}$	$.482\text{x}10^{-4}$	$.517\text{x}10^{-4}$
5	$.413\text{x}10^{-5}$	$.187\text{x}10^{-3}$	$.2\text{x}10^{-3}$
6	$.18\text{x}10^{-3}$	$.376\text{x}10^{-3}$	$.4\text{x}10^{-3}$
7	$-.98\text{x}10^{-5}$	$.745\text{x}10^{-4}$	$.798\text{x}10^{-4}$
8	$.663\text{x}10^{-6}$	$.264\text{x}10^{-3}$	$.284\text{x}10^{-3}$
9	$.314\text{x}10^{-3}$	$.635\text{x}10^{-3}$	$.68\text{x}10^{-3}$
10	$-.62\text{x}10^{-5}$	$-.239\text{x}10^{-5}$	$.146\text{x}10^{-5}$
11	$-.156\text{x}10^{-4}$	$-.525\text{x}10^{-5}$	$-.238\text{x}10^{-5}$
12	$-.108\text{x}10^{-4}$	$-.55\text{x}10^{-5}$	$-.295\text{x}10^{-5}$
13	$-.758\text{x}10^{-5}$	$-.221\text{x}10^{-4}$	$-.264\text{x}10^{-4}$
14	$.164\text{x}10^{-4}$	$-.686\text{x}10^{-5}$	$-.95\text{x}10^{-5}$
15	$.984\text{x}10^{-5}$	$-.11\text{x}10^{-5}$	$-.114\text{x}10^{-5}$

*See Figure C-1 for Element Numbering Sequence.

TABLE C-X (Cont'd.)

COMPUTER CALCULATED TORSION RESULTS (FOR 1/8 STRUCTURE)

M_t=1000ft-tons*

GIRTH STRESSES

L/B	.5	1.3	1.3
B/D	3.0	3.0	3.0
A_f/A_w	3.5	3.0	3.5
Element			
16	$.645 \times 10^{-4}$	$.102 \times 10^{-4}$	$+. 11 \times 10^{-3}$
17	$.455 \times 10^{-4}$	$.614 \times 10^{-4}$	$+.657 \times 10^{-4}$
18	$. 18 \times 10^{-4}$	$.204 \times 10^{-4}$	$.219 \times 10^{-4}$
19	0	0	0
20			
21			
22			
23			
24			
25			
26			
27			
28			
29			
30			

*See Figure C-1 for Element Numbering Sequence.

TABLE C-X (Cont'd.)

COMPUTER CALCULATED TORSION RESULTS (FOR 1/8 STRUCTURE)

M_t-1000ft-tons*

LONGITUDINAL STRESSES

L/B	.5	1.3	1.3
B/D	3.0	3.0	3.0
A_f/A_w	3.5	3.0	3.5
Element			
1	$-.101\times10^{-5}$	$-.377\times10^{-4}$	$-.405\times10^{-4}$
2	$-.\ 8\times10^{-4}$	$-.985\times10^{-4}$	$-.107\times10^{-4}$
3	$-.753\times10^{-4}$	$-.646\times10^{-4}$	$-.692\times10^{-4}$
4	$-.688\times10^{-5}$	$.145\times10^{-4}$	$.157\times10^{-4}$
5	$.437\times10^{-5}$	$.384\times10^{-4}$	$.406\times10^{-4}$
6	$.787\times10^{-5}$	$.\ 94\times10^{-5}$	$.\ 91\times10^{-5}$
7	$-.125\times10^{-5}$	$.271\times10^{-4}$	$.\ 29\times10^{-4}$
8	$.159\times10^{-4}$	$.764\times10^{-3}$	$.814\times10^{-4}$
9	$.727\times10^{-4}$	$.115\times10^{-3}$	$.123\times10^{-3}$
10	$.975\times10^{-4}$	$.148\times10^{-3}$	$.159\times10^{-3}$
11	$.484\times10^{-4}$	$.826\times10^{-4}$	$.886\times10^{-4}$
12	$.151\times10^{-4}$	$.263\times10^{-4}$	$.287\times10^{-4}$
13	$.266\times10^{-3}$	$.407\times10^{-3}$	$.433\times10^{-3}$
14	$.151\times10^{-3}$	$.257\times10^{-3}$	$.273\times10^{-3}$
15	$.454\times10^{-4}$	$.867\times10^{-4}$	$.926\times10^{-4}$

*See Figure C-1 for Element Numbering Sequence.

TABLE C-X (Cont'd.)

COMPUTER CALCULATED TORSION RESULTS (FOR 1/8 STRUCTURE)

M_t=1000ft-tons*

LONGITUDINAL STRESSES

L/B	.5	1.3	1.3
B/D	3.0	3.0	3.0
A_f/A_w	3.5	3.0	3.5
Element			
16	$.442\times10^{-3}$	$.716\times10^{-3}$	$.767\times10^{-3}$
17	$.204\times10^{-3}$	$.405\times10^{-3}$	$.434\times10^{-3}$
18	$.616\times10^{-4}$	$.131\times10^{-3}$	$.141\times10^{-3}$
19	0	0	0
20			
21			
22			
23			
24			
25			
26			
27			
28			
29			
30			

*See Figure C-1 for Element Numbering Sequence.

TABLE C-X (Cont'd.)

COMPUTER CALCULATED TORSION RESULTS (FOR 1/8 STRUCTURE)

M_t=1000ft-tons*

SHEAR STRESSES

L/B	.5	1.3	1.3
B/D	3.0	3.0	3.0
A_f/A_w	3.5	3.0	3.5
Element			
1	-.263	-.263	-.263
2	↓	↓	↓
3	↓	↓	↓
4	↓	↓	↓
5	↓	↓	↓
6	↓	↓	↓
7	↓	↓	↓
8	↓	↓	↓
9	↓	↓	↓
10	-.3125	-.263	-.3125
11	↓	↓	↓
12	↓	↓	↓
13	↓	↓	↓
14	↓	↓	↓
15	↓	↓	↓

*See Figure C-1 for Element Numbering Sequence.

TABLE C-X (Cont'd.)

COMPUTER CALCULATED TORSION RESULTS (FOR 1/8 STRUCTURE)

M_t=1000ft-tons*

SHEAR STRESSES

L/B	.5	1.3	1.3
B/D	3.0	3.0	3.0
A_f/A_w	3.5	3.0	3.5
Element			
16	-.3125	-.263	-.3125
17	↓	↓	↓
18	↓	↓	↓
19	0	0	0
20	↓	↓	↓
21	↓	↓	↓
22	↓	↓	↓
23	↓	↓	↓
24	↓	↓	↓
25	↓	↓	↓
26	↓	↓	↓
27	↓	↓	↓
28	↓	↓	↓
29	↓	↓	↓
30	↓	↓	↓

*See Figure C-1 for Element Numbering Sequence.

TABLE C-XI

CALCULATED SHEAR STRESSES (M_t=1000ft-tons) FOR TORSION CASE*

δ_{ij}	B/D=3.0 A_f/A_w=2.5	B/D=3.0 A_f/A_w=3.0	B/D=3.0 A_f/A_w=3.5	B/D=2.5 A_f/A_w=3.0	B/D=3.5 A_f/A_w=3.0	After Struc.	Fwd. Struc.
δ_{11}	$\frac{1}{G}(2024)$	$\frac{1}{G}(2106)$	$\frac{1}{G}(2206)$	$\frac{1}{G}(2212)$	$\frac{1}{G}(2032)$	$\frac{1}{G}(1973)$	$\frac{1}{G}(1856)$
$\delta_{21}=\delta_{12}$	$-\frac{1}{G}(222)$	$-\frac{1}{G}(264)$	$-\frac{1}{G}(313)$	$-\frac{1}{G}(263)$	$-\frac{1}{G}(226)$	$-\frac{1}{G}(288)$	$-\frac{1}{G}(288)$
$\delta_{31}=\delta_{13}$	$-\frac{1}{G}(789)$	$-\frac{1}{G}(789)$	$-\frac{1}{G}(789)$	$-\frac{1}{G}(789)$	$-\frac{1}{G}(789)$	$-\frac{1}{G}(896)$	$-\frac{1}{G}(768)$
$\delta_{41}=\delta_{14}$	0	0	0	0	0	0	0
δ_{22}	$\frac{1}{G}(2024)$	$\frac{1}{G}(2106)$	$\frac{1}{G}(2206)$	$\frac{1}{G}(2212)$	$\frac{1}{G}(2032)$	$\frac{1}{G}(1856)$	$\frac{1}{G}(1784)$
$\delta_{32}=\delta_{23}$	0	0	0	0	0	0	0
$\delta_{42}=\delta_{24}$	$-\frac{1}{G}(789)$	$-\frac{1}{G}(789)$	$-\frac{1}{G}(789)$	$-\frac{1}{G}(789)$	$-\frac{1}{G}(789)$	$-\frac{1}{G}(768)$	$-\frac{1}{G}(768)$
δ_{33}	$\frac{1}{G}(2024)$	$\frac{1}{G}(2106)$	$\frac{1}{G}(2206)$	$\frac{1}{G}(2212)$	$\frac{1}{G}(2032)$	$\frac{1}{G}(2451)$	$\frac{1}{G}(2266)$
$\delta_{43}=\delta_{34}$	$-\frac{1}{G}(222)$	$-\frac{1}{G}(264)$	$-\frac{1}{G}(313)$	$-\frac{1}{G}(263)$	$-\frac{1}{G}(226)$	$-\frac{1}{G}(288)$	$-\frac{1}{G}(288)$
δ_{44}	$\frac{1}{G}(2024)$	$\frac{1}{G}(2106)$	$\frac{1}{G}(2206)$	$\frac{1}{G}(2212)$	$+\frac{1}{G}(2032)$	$\frac{1}{G}(2266)$	$\frac{1}{G}(2757$
A_1 (ft.^{2})	208.325	208.325	208.325	250	178.75	252	216
A_2	↓	↓	↓	↓	↓	216	216

*For details See Appendix A.

TABLE C-XI (Cont'd.)

CALCULATED SHEAR STRESSES (M_t=1000ft-tons) FOR TORSION CASE*

	B/D=3.0 A_f/A_w=2.5	B/D=3.0 A_f/A_w=3.0	B/D=3.0 A_f/A_w=3.5	B/D=2.5 A_f/A_w=3.0	B/D=3.5 A_f/A_w=3.0		After Struc.	Fwd. Struc.
A_3	↓	↓	↓	↓	↓		252	216
A_4							216	288
Q_i $\frac{tons}{ft.}$	-.60	-.60	-.60	-.50	-.70		-.602	-.585
							-.552	-.596
							-.509	-.494
							-.467	-.476
Top Plate	-.263	-.263	-.263	-.219	-.307	Left	-.178	-.174
Shear Stress						Rt.	-.164	-.176
KSI								
Left Side	0	0	0	0	0		-.200	-.260
Rt. Side	-.222	-.263	-.3125	-.219	-.307		-.24	-.199
Center							-.0222	+.0049

*For Details See Appendix A.

TABLE C-XII

AVERAGE LONGITUDINAL STRESS $(\sigma yy)_{avg.}$ AND EFFECTIVENESSES

FOR SYMM. B.M. AND ANTISYM. B.M. + SHEAR CASES

L/B	.3	.3	.3	.5	.5	.5	.7
B/D	2.5	3.0	3.5	3.0	3.0	3.0	3.0
A_f/A_w	3.0	3.0	3.0	2.5	3.0	3.5	2.5
ANTISYM. B.M. + SHEAR							
End Elements							
Avg Stress	-.276	-.326	-.374	-.291	-.320	-.337	-.305
ρ_1	.222	.223	.224	.229	.227	.233	.260
ρ_2	.244	.243	.241	.286	.241	.288	.346
Center Elements							
Avg Stress	-.447	-.528	-.609	-.329	-.347	-.374	-.326
ρ_1	.165	.165	.165	.183	.183	.187	.205
ρ_2	.361	.358	.359	.420	.419	.398	.534

TABLE C-XII (Cont'd.)

AVERAGE LONGITUDINAL STRESS (σyy)avg. AND EFFECTIVENESSES

FOR SYMM. B.M. AND ANTISYM. B.M. + SHEAR CASES

L/B	.7	.7	.9	.9	.9	1.1	1.1
B/D	3.0	3.0	3.0	3.0	3.0	3.0	3.0
A_f/A_w	3.0	3.5	2.5	3.0	3.5	2.5	3.0
				ANTISYM. B.M. + SHEAR			
End Elements							
Avg Stress	-.326	-.341	-.314	-.336	-.356	-.319	-.341
ρ_1	.261	.260	.300	.302	.306	.343	.347
ρ_2	.345	.336	.416	.413	.412	.490	.489
Center Elements							
Avg Stress	-.346	-.362	-.324	-.347	-.363	-.328	-.342
ρ_1	.206	.206	.232	.235	.237	.267	.265
ρ_2	.532	.527	.689	.693	.692	.903	.896

TABLE C-XII (Cont'd.)

AVERAGE LONGITUDINAL STRESS (σyy)avg. AND EFFECTIVENESSES

FOR SYMM. B.M. AND ANTISYM. B.M. + SHEAR CASES

L/B	1.1	1.3	1.3	1.3	1.3	1.3	1.5
B/D	3.0	2.5	3.0	3.0	3.0	3.5	3.0
A_f/A_w	3.5	3.0	2.5	3.0	3.5	3.0	3.0
ANTISYM. B.M. + SHEAR							
End Elements							
Avg Stress	-.359	-.336	-.327	-.346	-.364	-.453	-.401
ρ_1	.350	.407	.392	.394	.397	.401	.453
ρ_2	.483	.651	.571	.565	.556	.650	.748
Center Elements							
Avg Stress	-.363	-.432	-.329	-.347	-.362	-.570	-.506
ρ_1	.270	.274	.298	.299	.300	.284	.301
ρ_2	.902	1.216	1.149	1.152	1.151	1.18	1.51

TABLE C-XII

AVERAGE LONGITUDINAL STRESS $(\sigma yy)_{avg.}$ AND EFFECTIVENESSES
FOR SYMM. B.M. AND ANTISYM. B.M. + SHEAR CASES

L/B	.3	.3	.3	.5	.5	.5	.7
B/D	2.5	3.0	3.5	3.0	3.0	3.0	3.0
A_f/A_w	3.0	3.0	3.0	2.5	3.0	3.5	2.5
SYMM. BEND. MOM.							
End Elements							
Avg Stress	.877	1.058	1.244	1.02	1.092	1.13	1.045
ρ_1	.233	.232	.232	.267	.273	.272	.315
ρ_2	.258	.260	.260	.304	.304	.297	.354
Center Elements							
Avg Stress	.901	1.0958	1.295	1.11	1.18	1.24	1.185
ρ_1	.276	.274	.273	.412	.418	.425	.595
ρ_2	.305	.307	.308	.437	.434	.428	.611

TABLE C-XII (Cont'd.)

AVERAGE LONGITUDINAL STRESS (σyy)avg. AND EFFECTIVENESSES

FOR SYMM. B.M. AND ANTISYM. B.M. + SHEAR CASES

L/B	.7	.7	.9	.9	.9	1.1	1.1
B/D	3.0	3.0	3.0	3.0	3.0	3.0	3.0
A_f/A_w	3.0	3.5	2.5	3.0	3.5	2.5	3.0
				SYMM. BEND. MOM.			
End Elements							
Avg Stress	1.115	1.19	1.04	1.17	1.165	1.07	1.13
ρ_1	.321	.329	.355	.380	.364	.406	.409
ρ_2	.354	.347	.398	.418	.392	.458	.452
Center Elements							
Avg Stress	1.24	1.24	1.215	1.27	1.31	1.235	1.282
ρ_1	.584	.563	.735	.731	.717	.857	.852
ρ_2	.620	.607	.788	.809	.821	.920	.940

TABLE C-XII (Cont'd.)

AVERAGE LONGITUDINAL STRESS (σyy)avg. AND EFFECTIVENESSES

FOR SYMM. B.M. AND ANTISYM. B.M. + SHEAR CASES

L/B	1.1	1.3	1.3	1.3	1.3	1.3	1.5
B/D	3.0	2.5	3.0	3.0	3.0	3.5	3.0
A_f/A_w	3.5	3.0	2.5	3.0	3.5	3.0	3.0
SYMM. BEND. MOM.							
End Elements							
Avg Stress	1.191	.953	1.065	1.122	1.175	1.288	1.117
ρ_1	.415	.449	.446	.447	.449	.444	.484
ρ_2	.448	.492	.505	.498	.490	.502	.542
Center Elements							
Avg Stress	1.33	1.079	1.230	1.278	1.315	1.469	1.265
ρ_1	.838	.932	.941	.936	.930	.940	.993
ρ_2	.961	1.02	.993	1.011	1.029	1.002	1.049

TABLE C-XIII

COMBINED RESULTS OF AVERAGE LONGITUDINAL STRESSES (KSI) AND EFFECTIVENESS

L/B	.3	.3	.3	.5	.5	.5	.7
B/D	2.5	3.0	3.5	3.0	3.0	3.0	3.0
A_f/A_w	3.0	3.0	3.0	2.5	3.0	3.5	2.5
Plane $Y={}^{L}/_{8}$ Avg Stress	.601	.731	.870	.733	.769	.652	.740
ρ_1	.238	.237	.235	.289	.293	.254	.347
ρ_2	.266	.268	.270	.312	.308	.346	.361
Plane $Y={}^{3L}/_{8}$ Avg Stress	.455	.566	.685	.789	.835	.832	.856
ρ_1	.265	.270	.274	.448	.436	.419	.6212
ρ_2	.802	.714	.648	.874	.909	1.121	2.4747
Plane $Y={}^{5L}/_{8}$ Avg Stress	1.348	1.625	1.905	1.446	1.517	1.601	1.508
ρ_1	.226	.226	.226	.321	.322	.326	.428
ρ_2	.322	.322	.323	.436	.433	.424	.580
Plane $Y={}^{7L}/_{8}$ Avg Stress	1.152	1.384	1.619	1.323	1.427	1.626	1.361
ρ_1	.230	.230	.230	.261	.261	.283	.304
ρ_2	.255	.255	.256	.301	.303	.284	.353

TABLE C-XIII (Cont'd.)

COMBINED RESULTS OF AVERAGE LONGITUDINAL STRESSES (KSI) AND EFFECTIVENESS

L/B	.7	.7	.9	.9	.9	1.1	1.1
B/D	3.0	3.0	3.0	3.0	3.0	3.0	3.0
A_f/A_w	3.0	3.5	2.5	3.0	3.5	2.5	3.0
Plane $Y=L/8$ Avg Stress	.802	.815	.748	.788	.820	.745	.782
ρ_1	.348	.347	.398	.398	.389	.439	.434
ρ_2	.357	.353	.402	.401	.402	.442	.441
Plane $Y=3L/8$ Avg Stress	.896	.923	.891	.924	.949	.904	.931
ρ_1	.603	.597	.759	.743	.734	.837	.829
ρ_2	2.776	3.18	6.268	8.697	16.967	7.882	13.521
Plane $Y=5L/8$ Avg Stress	1.576	1.648	1.544	1.6156	1.672	1.557	1.622
ρ_1	.432	.434	.526	.530	.536	.606	.611
ρ_2	.574	.566	.731	.721	.715	.864	.858
Plane $Y=7L/8$ Avg Stress	1.419	1.509	1.378	1.458	1.528	1.388	1.466
ρ_1	.301	.305	.347	.348	.350	.39	.392
ρ_2	.354	.346	.408	.404	.398	.465	.458

TABLE C-XIII (Cont'd.)

COMBINED RESULTS OF AVERAGE LONGITUDINAL STRESSES (KSI) AND EFFECTIVENESS

L/B	1.1	1.3	1.3	1.3	1.3	1.3	1.5
B/D	3.0	2.5	3.0	3.0	3.0	3.5	3.0
A_f/A_w	3.5	3.0	2.5	3.0	3.5	3.0	3.0
Plane $Y=^L/_8$ Avg Stress	.820	.602	.737	.777	.807	.835	.716
ρ_1	.428	.447	.475	.472	.469	.446	.470
ρ_2	.441	.470	.480	.477	.476	.471	.503
Plane $Y=^{3L}/_8$ Avg Stress	.958	.647	.901	.930	.957	.99128	.759
ρ_1	.817	.802	.892	.878	.880	.640	.808
ρ_2	29.257	-1.26	7.539	9.263	14.128	-2.195	-1.605
Plane $Y=^{5L}/_8$ Avg Stress	1.679	1.511	1.560	1.624	1.676	1.992	1.77
ρ_1	.616	.573	.669	.670	.669	.586	.614
ρ_2	.850	.999	.984	.978	.963	1.003	1.099
Plane $Y=^{7L}/_8$ Avg Stress	1.538	1.289	1.391	1.468	1.543	1.726	1.537
ρ_1	.393	.437	.432	.434	.436	.431	.468
ρ_2	.451	.525	.519	.511	.502	.532	.588

TABLE C-XIV

EXTRAPOLATED & AVERAGE STRESS VALUES & PLATING EFFECTIVENESS FOR THE ACTUAL STRUCTURES

	Top Plate (Right)		Top Plate (Left)	
	Forward Cross Structure	After Cross Structure	Forward Cross Structure	After Cross Structure
		SYMM. BEND. MOM.		
Extrapolated Left y=L/8	1.170	1.149	1.190	1.1465
Extrapolated Right y=L/8	1.026	1.0504	1.1246	1.033
Average Stress	.3746	.3780	.3946	.343
ρ_1	.3203	.329	.332	.2988
ρ_2	.3652	.360	.351	.3316
Extrapolated Left y=3L/8	.6742	.6824	.6770	.6959
Extrapolated Right y-3L/8	.68205	.7331	.7752	.7511
Average Stress	.4192	.4345	.4453	.3791
ρ_1	.6146	.5927	.5745	.5047
ρ_2	.6217	.6368	.6581	.545

TABLE C-XIV(Cont'd.)

EXTRAPOLATED & AVERAGE STRESS VALUES & PLATING EFFECTIVENESS FOR THE ACTUAL STRUCTURES

	Bottom Plate (Right)		Bottom Plate (Left)	
	Forward Cross Structure	After Cross Structure	Forward Cross Structure	After Cross Structure
	SYMM. BEND. MOM.			
Extrapolated Left y=L/8	-1.750	-1.774	-1.7201	-1.756
Extrapolated Right y=L/8	-1.548	-1.497	-1.407	-1.421
Average Stress	-.484	-.5611	-.5401	-.4989
ρ_1	.277	.316	.314	.284
ρ_2	.313	.375	.384	.351
Extrapolated Left y=3L/8	-1.0866	-1.035	-1.0424	-1.051
Extrapolated Right y=3L/8	-1.1298	-.973	-.9219	-.946
Average Stress	-.5108	-.6280	-.6133	-.535
ρ_1	.4521	.6065	.588	.509
ρ_2	.4701	.6452	.665	.565

TABLE C-XIV (Cont'd.)

EXTRAPOLATED & AVERAGE STRESS VALUES & PLATING EFFECTIVENESS FOR THE ACTUAL STRUCTURES

	Top Plate (Right)		Top Plate (Left)	
	Forward Cross Structure	After Cross Structure	Forward Cross Structure	After Cross Structure
	ANTISYMM. B.M. + SHEAR			
Extrapolated Left y=L/8	-.4640	-.4496	-.4714	-.3962
Extrapolated Right y=L/8	-.4006	-.4028	-.4408	-.342
Average Stress	-.1389	-.142	-.1461	-.140
ρ_1	.2994	.316	.310	.353
ρ_2	.347	.353	.332	.408
Extrapolated Left y=3L/8	-.6694	-.5841	-.6843	-.665
Extrapolated Right y=3L/8	-.6132	-.5571	-.6759	-.622
Average Stress	-.1925	-.2122	-.2036	-.179
ρ_1	.288	.363	.297	.269
ρ_2	.314	.381	.301	.288

TABLE C-XIV (Cont'd.)

EXTRAPOLATED & AVERAGE STRESS VALUES & PLATING EFFECTIVENESS FOR THE ACTUAL STRUCTURES

	Bottom Plate (Right)		Bottom Plate (Left)	
	Forward Cross Structure	After Cross Structure	Forward Cross Structure	After Cross Structure
	ANTISYMM. B.M. + SHEAR			
Extrapolated Left y=L/8	.699	.6939	.6782	.6864
Extrapolated Right y=L/8	.664	.5731	.5462	.543
Average Stress	.1881	.203	.1961	.181
ρ_1	.269	.292	.289	.2635
ρ_2	.283	.354	.359	.333
Extrapolated Left y=3L/8	1.0068	.9375	.9308	.928
Extrapolated Right y=3L/8	1.076	.839	.8182	.7898
Average Stress	.274	.268	.264	.2410
ρ_1	.255	.286	.283	.2598
ρ_2	.272	.320	.322	.3052

TABLE C-XIV (Cont'd.)

EXTRAPOLATED & AVERAGE STRESS VALUES & PLATING EFFECTIVENESS FOR THE ACTUAL STRUCTURES

	Top Plate (Right)		Top Plate (Left)	
	Forward Cross Structure	After Cross Structure	Forward Cross Structure	After Cross Structure
	COMBINED LOAD			
Extrapolated Left y=L/8	.7055	.6888	.7181	.6865
Extrapolated Right y=L/8	.6251	.6381	.6837	.6271
Average Stress	.2357	.238	.2484	.2152
ρ_1	.3341	.346	.346	.313
ρ_2	.377	.372	.363	.343
Extrapolated Left y=3L/8	.00321	.015	-.00764	.029
Extrapolated Right y=3L/8	.06846	.093	.0993	.128
Average Stress	.2264	.2388	.2418	.1995
ρ_1	.706	.719	.712	.767
ρ_2	----	----	----	----

TABLE C-XIV (Cont'd.)

EXTRAPOLATED & AVERAGE STRESS VALUES & PLATING EFFECTIVENESS FOR THE ACTUAL STRUCTURES

	Bottom Plate (Right)		Bottom Plate (Left)	
	Forward Cross Structure	After Cross Structure	Forward Cross Structure	After Cross Structure
		COMBINED LOAD		
Extrapolated Left y=L/8	-1.0515	-1.080	-1.0419	-1.0686
Extrapolated Right y=L/8	-.8839	-.924	-.8612	-.8779
Average Stress	-.2962	-.359	-.3439	-.3182
ρ_1	.282	-.332	.330	.298
ρ_2	.335	.388	.399	.362
Extrapolated Left y=3L/8	-.8842	-.0971	-.1128	-.121
Extrapolated Right y=3L/8	-.8583	-.133	-.105	-.155
Average Stress	-.239	-.360	-.349	-.293
ρ_1	.745	.745	.744	.79
ρ_2	----	----	----	----

TABLE C-XIV(Cont'd.)

EXTRAPOLATED & AVERAGE STRESS VALUES & PLATING EFFECTIVENESS FOR THE ACTUAL STRUCTURES

	Top Plate (Right)		Top Plate (Left)	
	Forward Cross Structure	After Cross Structure	Forward Cross Structure	After Cross Structure
COMBINED LOAD				
Extrapolated Left y=5L/8	1.634	1.350	1.662	1.362
Extrapolated Right y=5L/8	1.426	1.374	1.565	1.373
Average Stress	.514	.631	.541	.5585
ρ_1	.314	.4589	.3255	.4068
ρ_2	.360	.467	.3455	.4099
Extrapolated Left y=7L/8	1.3419	1.609	1.361	1.6058
Extrapolated Right y=7L/8	1.295	1.464	1.451	1.439
Average Stress	.6113	.518	.6489	.4701
ρ_1	.4556	.322	.447	.293
ρ_2	.4721	.3541	.477	.327

TABLE C-XIV (Cont'd.)

EXTRAPOLATED & AVERAGE STRESS VALUES & PLATING EFFECTIVENESS FOR THE ACTUAL STRUCTURES

	Bottom Plate (Right)		Bottom Plate (Left)	
	Forward Cross Structure	After Cross Structure	Forward Cross Structure	After Cross Structure
	COMBINED LOAD			
Extrapolated Left y=5L/8	-2.4489	-1.973	-2.398	-1.979
Extrapolated Right y=5L/8	-2.211	-1.813	-1.954	-1.74
Average Stress	-.6724	-.896	-.7362	-.776
ρ_1	.2746	.454	.307	.391
ρ_2	.304	.494	.377	.447
Extrapolated Left y=7L/8	-2.0933	-2.47	-1.974	-2.442
Extrapolated Right y=7L/8	-2.206	-2.072	-1.741	-1.9647
Average Stress	-.785	-.764	-.8767	-.6797
ρ_1	.356	.3096	.444	.278
ρ_2	.375	.369	.503	.346

APPENDIX D

REFERENCES

(1) Meier, H.A., "Preliminary Design of a Catamaran Rescue Ship," Marine Technology, Vol. 5, No. 1, Jan. 1968.

(2) Christensen, J.F. et al., "The New Catamaran Submarine Rescue Ships: ASR-21 Class," Marine Technology, Vol. 7, No. 3, July 1970.

(3) Lankford, B.W., Jr., "The Structural Design of the ASR Catamaran Cross Structure," The Naval Engineers Journal, Vol. 79, No. 4, August 1967.

(4) Dinsenbacher, A.L., "A Method for Estimating Loads on the Catamaran Cross Structure," Marine Technology, Vol. 7, No. 4, October, 1970.

(5) Dinsenbacher, A.L., et al, "Model Test Determinations of Sea Loads on Catamaran Cross Structures," Naval Ship Research and Development Center Report #2378, May 1967.

(6) Wahab, R. et al, "On the Behavior of the ASR Catamaran in Waves," Marine Technology, Vol. 8, No. 3, July 1971.

(7) Schade, H.A. "Feasibility Study of Ocean Going Catamarans" Prepared for the Crowley Launch and Tugboat Co., California, June, 1965.

(8) Mandel, P. "A Comparative Evaluation of Novel Ship Types" Transactions SNAME, Vol. 70, 1962.

APPENDIX D (Cont'd.)

REFERENCES

(9) Logcher, R.D. et al., ICES STRUDL-II - The Structural Design Language Engineering User's Manual, Volumes I and II, Structures Division and Civil Engineering Systems Laboratory, Department of Civil Engineering, Massachusetts Institute of Technology, Cambridge, Massachusetts, First Edition, 1969.

(10) Mehrotra, B.L. et al., "Analysis of 3 Dimensional Thin Walled Structures," Journal of the Structural Division Proceedings of the American Society of Civil Engineers, December 1969.

(11) Mansour, A., "Effective Flange Breadth of Stiffened Plates Under Axial Tensile Load or Uniform Bending Moment," The Journal of Ship Research, March 1970.

(12) Schade, H.A., "The Effective Breadth of Stiffened Plating Under Bending Loads," Transactions of the Society of Naval Architects and Marine Engineers, Vol. 59, 1951.

(13) Schade, H.A., "The Effective Breadth Concept in Ship Structural Design," Transactions of the Society of Naval Architects and Marine Engineers, Vol. 61, 1953.

(14) Benscoter, S.U., "A Theory of Torsion Bending for Multi-cell Beams," Journal of Applied Mechanics, March 1954.

APPENDIX D (Cont'd.)

REFERENCES

(15) Ebner, H., "Torsional Stresses in Box Beams with Cross Sections Partially Restrained Against Warping," NACA-TM 744, 1934.

(16) Goodier, J.N., "A Theorem on the Shearing Stress in Beams with Applications to Multicellular Sections," Journal of the Aeronautical Sciences, Vol. II, No. 3, July 1944.

(17) Baron, F.M. "Torsion of Multiconnected Thin Walled Cylinders," Journal of Applied Mechanics, Vol. 9 #2, June 1942.

(18) Benscoter, S.U., "Numerical Transformation Procedures for Shear Flow Calculations," Journal of the Aeronautical Sciences, Vol. 13, No. 8, August 1946.

(19) Den Hartog, J.P., Advanced Strength of Materials, McGraw-Hill Book Co., New York, 1952.

(20) Oden, J.T., Mechanics of Elastic Structures, McGraw-Hill Book Co., New York, 1967.

(21) Vlasov, V.Z., "Thin Walled Elastic Beams," Translated from Russian Published for the National Science Foundation, Washington and The Department of Commerce by Scientific Translations, Jerusalem, 1961.

APPENDIX D (Cont'd.)

REFERENCES

(22) Venkatraman, B. and S.A. Patel, Structural Mechanics With Introduction to Elasticity and Plasticity, McGraw-Hill Book Co., New York, 1970.

(23) Reissner, E., "Least Work Solutions of Shear Lag Problems," Journal of the Aeronautical Sciences, May 1941.

(24) Reissner, E., "A Method for Solving Shear Lag Problems," Aviation, May 1941.

(25) Kuhn, P., "A Procedure for the Shear Lag Analysis of Box Beams," NACA WRL-401 ARR January 1943.

(26) Kuhn, P., "Stress Analysis of Beams with Shear Deformation of the Flanges," NACA, Report #608.

(27) Kuhn, P. and P.T. Chiarito, "Shear Lag in Box Beams - Methods of Analysis and Experimental Investigations," NACA Report #739, 1942.

(28) Hildebrand, F.B. and E. Reissner, "Least Work Analysis of the Problem of Shear Lag in Box Beams," NACA TN 893, May 1943.

(29) Hildebrand, F.B., "The Exact Solution of Shear Lag Problems in Flat Plates and Box Beams Assumed Rigid in the Transverse Direction," NACA TN 894, June 1943.

APPENDIX D (Cont'd.)

REFERENCES

(30) Maniar, W.M. and W.P. Chiang, "Catamarans - Technological Limits to Size and Appraisal of Structural Design Information and Procedures," SSC-222, U.S. Coast Guard, Headquarters, Washington, D.C., 1971.

(31) Wah, T. Editor, A Guide for the Analysis of Ship Structures, U. S. Department of Commerce, Office of Technical Service, Washington, D.C., 1960.

(32) Yuille, I.M., "Shear Lag in Stiffened Plating," Transactions of the Institute of Naval Architects, Vol. 97, 1955.

(33) Smith, C.S., "Bending, Buckling and Vibration of Orthotropic Plate-Beam Structures," Journal of Ship Research, Vol. 12, No. 4, December 1968.

(34) Smith, C.S., "Elastic Analysis of Stiffened Plating Under Lateral Loading," Quarterly Transactions of the Royal Institution of Naval Architects, Vol. 108, No. 2, April 1966.

(35) Winter, G., "Stress Distribution in and Equivalent Width of Flanges of Wide, Thin-Wall Steel Beams". NACA TN 784, 1940.